9-5-2013

Development of Novel Reaction-based Fluorescent Probes

Weimin xuan

Weimin Xuan

Candidate

Department of Chemistry and Chemical Biology

Department

This dissertation is approved, and it is acceptable in quality and form for publication:

Approved by the Dissertation Committee:

Prof. Wei Wang   , Chairperson

Prof. Yang Qin

Prof. Charles E. Melançon III

Prof. Changjian Feng

DEVELOPMENT OF NOVEL REACTION-BASED
FLUORESCENT PROBES

by

WEIMIN XUAN

B.S., Pharmaceutical Science, Tianjin University, 2007

DISSERTATION

Submitted in Partial Fulfillment of the
Requirements for the Degree of

Doctor of Philosophy
Chemistry

The University of New Mexico
Albuquerque, New Mexico

July, 2013

To my time in B50 clark hall

ACKNOWLEDGEMENTS

DEVELOPMENT OF NOVEL REACTION-BASED FLUORESCENT PROBES

By

Weimin Xuan

B.S., Pharmaceutical Science, Tianjin University, 2007

Ph.D., Chemistry, University of New Mexico, 2013

ABSTRACT

Fluorescent probes have been proved to be very valuable tools in chemical and biological applications, and extensive exploration has been made. Recently, reaction-based fluorescent probes became a new design trend and displayed great potential with remarkable implementation to the conventional design method. However, this field is still underdeveloped, and a lot of problems remain to be solved.

As part of our group's research interest, my Ph. D. study centered on the development of new reaction-based fluorescent probes. Firstly, our previous research on Hg^{2+} was continued. In this work, we developed a novel ratiometric fluorescent probe for Hg^{2+} with impressive sensitivity, selectivity and imaging property; also, a new fluorescent probe with excellent detection limit was explored. Secondly, the first FRET-based ratiometric fluorescent probe for nerve agent was designed and synthesized, and it exhibited great potential for practical application. Furthermore, a new design strategy for H_2S probe development was discovered, and the new probe displayed excellent sensitivity and specificity. Finally, probes for Fe^{2+} were intensively investigated due to their biological

significance and urgent demand, and the real time and off-on fluorescence detection of

Fe^{2+} was achieved for the first time.

Contents

List of Abbreviations

Ac	acetyl, acetate
AChE	acetylcholinesterase
ATP	adenosine-5'-triphosphate
aq.	aqueous
BHQ	black hole quencher
BODIPY	*boron-dipyrromethene*
CDCl$_3$	deuterated chloroform
CWAs	chemical warfare agents
cys	cysteine
δ	chemical shift
DCM	dichloromethane
DCP	diethyl chlorophosphate
DFO	desferoxamine
DMEM	Dulbecco's Modified Eagle medium
DMF	N,N-dimethylformamide
DMSO	dimethyl sulfoxide
DNA	deoxyribonucleic acid
EDC	1-ethyl-3-(3-dimethylaminopropyl)carbodiimide
EDG	electron-donating group
Em.	emission
equiv.	equivlent
Ex.	excitation
ESI	electrospray ionization
EWG	electron-withdrawing group
FBS	foetal bovine serum
FRET	fluorescence resonance energy transfer

g	gram
GFP	green fluorescent protein
GSH	glutathione
h	hour
HEPES	4-(2-Hydroxyethyl)piperazine-1-ethanesulfonic acid
Hz	hertz
J	coupling constant
ICT	intramolecular charge transfer
λ	wavelength
LAMMA	laser microprobe mass analysis
LIP	labile iron pool
M	molar
mg	milligram
MHz	megahertz
min	minute(s)
mL	milliliter
mmol	millimole
ε	molar absorbtivity
NADH	β-Nicotinamide adenine dinucleotide, reduced disodium salt hydrate
NBD	nitro-benzoxadiazole
NIR	near-infrared
nm	nanometer
nM	nanomolecular
NMR	nuclear magnetic resonance
M	molar
PBS	phosphate buffer solution
ppb	part per billion
PET	photo-induced electron transfer

Φ	quantum yield
RNA	deoxyribonucleic acid
ROS	reactive oxygen species
rt	room temperature
TATP	triacetone triperoxide
TEA	triethylamine
TFA	trifluoroacetic acid
TLC	thin-layer chromatography
μL	microliter

Chapter 1

Introduction

1.1 Background

The development and application of fluorescent imaging techniques in sensing of chemical and biological molecules have been received increasing attention in the past two decades,[1-5] since Roger Y. Tsien reported a fluorescent probe for Ca^{2+} in 1980.[6] The technology offers the unrivalled merits of operational simplicity, high sensitivity and low-cost. Furthermore, the noninvasive feature is particularly attractive for the biological studies in living cells, tissues and animals.

A fluorescent probe/sensor contains an essential fluorophore for signal transduction, which can be protein (such as GFP), quantum dots and small dye molecules. Up to now, small-molecule based probes are most widely used due to their low cytotoxicity, high quantum yield and versatility. A typical chemical probe possesses a small signaling fluorescent molecule. The commonly used dyes include coumarins, xanthene derivatives, such as fluorescein and rhodamine, NBD (nitro-benzoxadiazole), cyanines, and polycyclic aromatic hydrocarbons naphthalene, anthracene and pyrene, etc (Scheme 1.1).

The requirements of a fluorescent probe depend on its application. To detect toxic metals and chemicals in water such as Hg^{2+}, Pb^{2+}, F^- etc, the probes should be able to work in water or at least in a certain percentage of water. Probes designed for biological imaging, such as probes for NO, H_2O_2, Zn^{2+}, Cu^{2+} etc, must satisfy more requirements, besides water soluble. They should be cell permeable, and excited at long excitation wavelength to minimize background fluorescence and cell damage and have low toxicity.

For quantitative analysis, ratiometric fluorescent probe is desired due to its ability of self-calibration. For fast detection of certain toxic or explosive analytes, such as nerve agent and TATP (Triacetone triperoxide), colorimetric probe is in great demand.

Scheme 1.1 Examples of widely used fluorophores

Hydroxycoumarin

NBD core

BODIPY core

fluorescein

rhodamine 123

naphthalene

anthracene

pyrene

aminonaphthalimide

IR-783
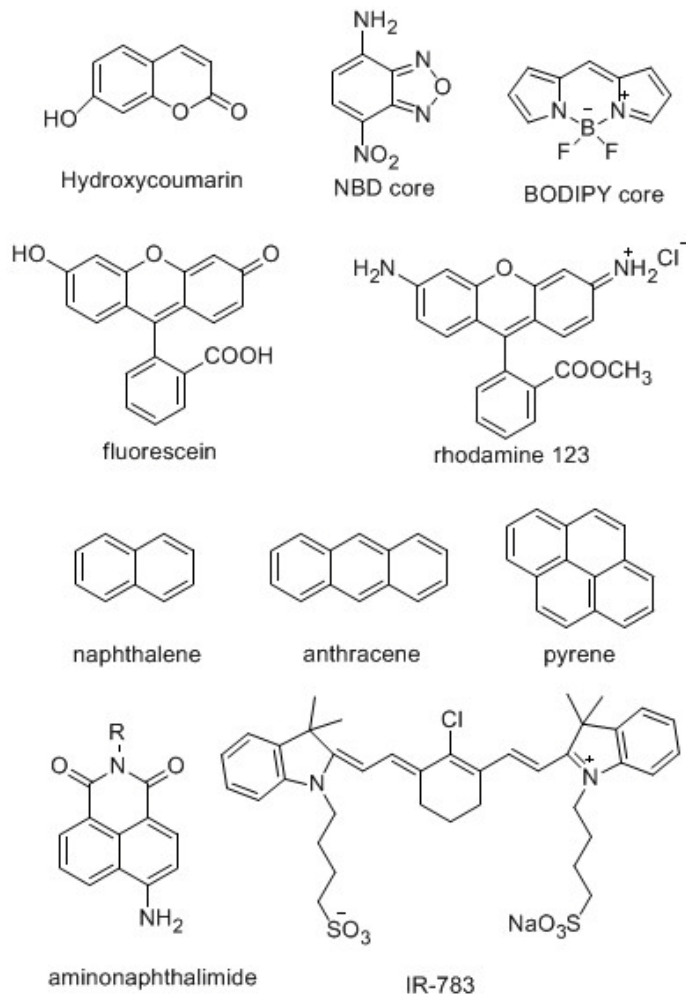
One of the widely used strategies in the development of fluorescent probes rely on non-covalent interactions, such as hydrogen bonding, electrostatic, hydrophobic, hydrophilic, π-π, anion-π and coordination-based interactions.[7,8] The architecture of such

probes usually is composed by a fluorophore and an analyte acceptor connected through an unsaturated linker or a conjugation system (Scheme 1.2).

Scheme 1.2 General strategies in design of fluorescent probes and selected examples

(1) photo-induced electron transfer (PET)

Zn²⁺ probe

Mg²⁺ probe
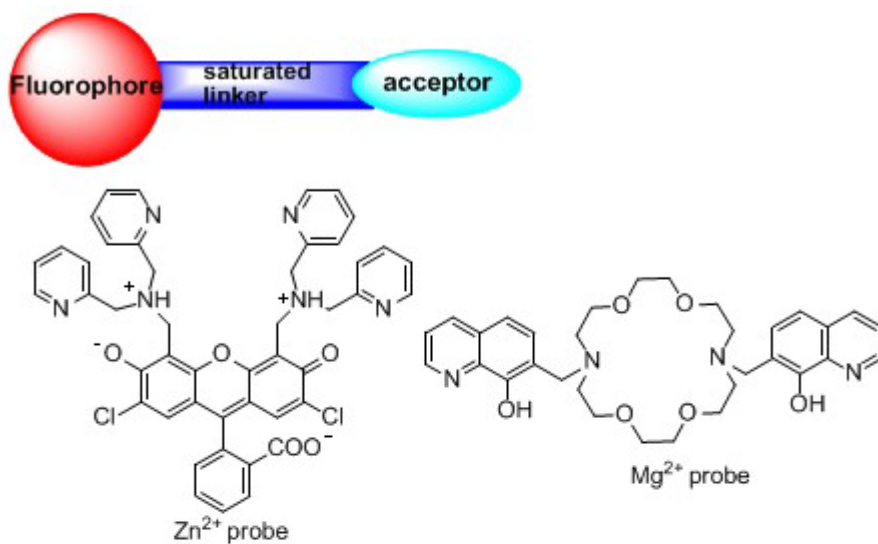
(2) Photoinduced intermolecular charge transfer(ICT)

Cu²⁺ probe

Cd²⁺ probe
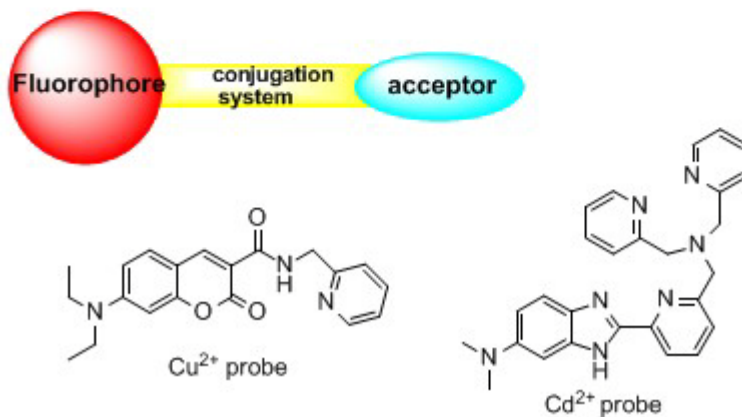
If the linker is a saturated moiety and the fluorophore does not participate in the coordination, the detection mechanism generally undergoes a photoinduced electron transfer (PET), and the fluorescence can be quenched.[9] With the binding of the acceptor

to certain targets, for example metal cations, the PET is switched off, and consequently the fluorescence is restored. The approach has been is widely utilized for probe design through combination of different acceptors to fluorophores, such as probe for Zn^{2+}[10] and Mg^{2+}[11] (Scheme 1.2). If the liker is a conjugated system or the fluorophore directly engage in the target recognition, the fluorescence property of the compound potentially can be altered in various manners via different mechanisms.[9] For example, the Cu^{2+} probe[12] displays a fluorescence on-off due to heavy atom effect; the Cd^{2+} probe[13] showed a desired ratiometric response as a result of the alteration of the ICT (intramolecular charge transfer) process upon Cd^{2+} coordination (Scheme 1.2).

Despite the great success in developing of fluorescent probes using non-covalent interactions between a probe and a target of interest, the drawbacks must be realized. Firstly, coordination-based probes generally suffer from a low selectivity issue as a result of the weak interactions. For example, probes for Zn^{2+} often suffer from interference from the presence of Cd^{2+} due to their similar complexation with ligands.[14,15] Secondly, the heavy atom effect often leads to the fluorescence quenching, giving undesired on-off signal and poor signal to noise ratio. This effect has been observed in fluorescent sensors for heavy metals Cu^{+},[16] Cu^{2+},[12] Fe^{2+}[17,18] and Pb^{2+}.[19] Finally, the design method has a limited scope and it is very challenging to extend it to complicated biological systems when many molecules are present. The specific and weak interactions such as F^{-} through hydrogen bond[20,21] or anion-π interaction,[22] can be interrupted by other species.

To overcome the above limitations, reaction-based fluorescent probes have emerged and significant progress has been made in the past decade.[23-25]

1.2 Reaction-based Small-molecular Fluorescent Probes

Reaction-based small-molecular fluorescent probes are designed based upon a specific reaction of the probe with an analyte. Therefore the reaction triggers the alternation of fluorescent properties. In addition, the reaction should be fast and carried out under mild reaction conditions such as room temperature, air/water tolerance and catalyst-independence.

Compared with conventional non-covalent interaction based fluorescent probes, this reaction-based approach affords several merits. Firstly, due to the immeasurable size of chemical reaction library, the probe design possibility is greatly extended to a much broader range of analytes of interest. One example to illustrate this point is the probes developed for hypoxia. Several reactions have been successfully investigated for hypoxia probe development, such as azo bond cleavage reaction,[26] nitro-reduction reaction[27] and one-electron bio-reduction reaction.[28] However, based on conventional method, the fluorescence analysis of hypoxia is unlikely to be possible. Secondly, through elegant application of a specific chemical reaction, good specificity usually can be expected for reaction-based fluorescent probes. For example, by Cu^+-catalyzed azide-alkyne ligation reaction, Cu^+ probe was developed with good selectivity over all other metal cations,[29] and through well-known ozonolysis reaction, ozone can be exclusively monitored in living cells.[30,31] However, due to the inherent poor specificity of the noncovalent interaction, conventional fluorescent probes often suffer from severe interference from other competitive analytes. For example, coordination-based probes for Cu^{2+} usually fail to differentiate Cu^{2+} from Zn^{2+},[32] [33] Ni^{2+}[34], Mg^{2+}[35] and Hg^{2+},[36] while reaction-based probes for Cu^{2+} can overcome the challenging issue.[37-39]

Finally and importantly, a specific chemical reaction is less likely to be influenced by other moieties of the probe, so the existing reaction-based fluorescent probes usually allow further modification to satisfy biological application needs. For instance, through the selective H_2O_2-mediated transformation of arlboronates to phenols, a series of H_2O_2 fluorescent probes have been successfully reported, as shown in Scheme 1.3. Initially, Chang and co-workers developed a fluorescein-based off-on probe for H_2O_2,[40] by combination of a phosphonium head group, they further developed a mitochondria targetable fluorescent probe to facilitate detailed study of H_2O_2 in cellular microenvironment.[41] Furthermore, two different ratiomertic fluorescent probes for H_2O_2 were also developed through intermolecular charge transfer (ICT)[42] and fluorescence resonance energy transfer (FRET) with the chemistry.[43] D. Shabat et al. extended this method to a NIR fluorophore, and made it a good probe for in vivo imaging.[44] W. Lin et al. came out with a bifunctional fluorescent probe for H_2O_2 and NO based on FRET strategy.[45] However, traditional coordination-based probes usually cannot tolerate intensive structure modification without compromising the probe property.

Reaction-based and noncovalent interaction design strategies have their pros and cons. Reaction-based methods are irreversible while the later is reversible, which can be reused such as Zn^{2+},[3] Ca^{2+},[46-48] Mg^{2+},[49,50] Na^+[51,52] and K^+.[53,54] Therefore, this newly emerging reaction-based design tactic are complementary to the conventional fluorescent probe design, and for different chemical and biological applications, both of them should be taken into consideration.

Scheme 1.3 Arylboronate-based fluorescent probes for H_2O_2

off-on probe

mitochondria-targetable probe

ICT-based ratiometric probe

FRET-based ratiometric probe

NIR fluorescence probe

bifunctional probe
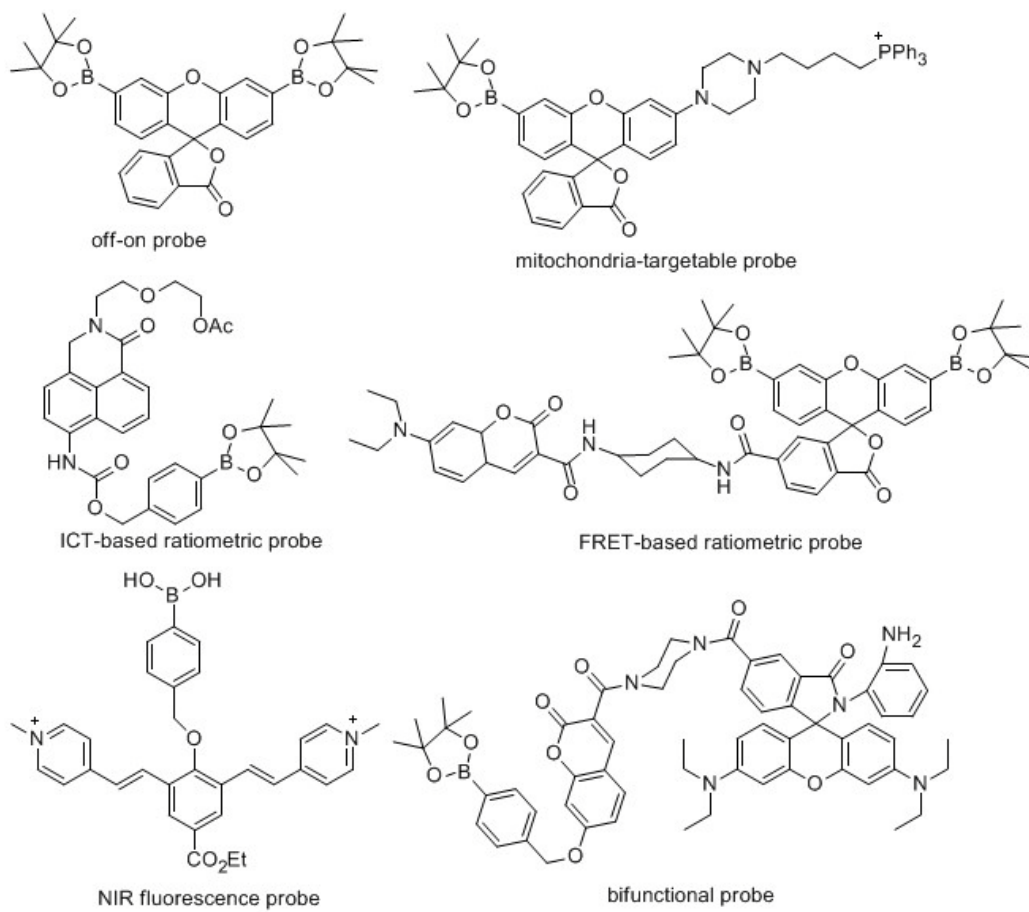
1.3 Basic Design Strategies of Reaction-based Small-molecular Fluorescent Probes

A nice feature of reaction-based fluorescent probes is versatile. A variety of fluorescent mechanisms such as ICT, PET and FRET can be incorporated into the strategy. For example, our group has developed 2 probes for thiolphenols based on ICT and PET mechanism respectively. As shown in Scheme 1.4, the ICT-based probe is non-fluorescent due to the masking of electron-donating amine by dinitrobenzenesulfonyl group, which blocks the ICT process;[55] the PET-based probe is turned off because of the dinitrobenzenesulfonyl group induced PET process.[56] Thiolphenols can selectively remove the dinitrobenzenesulfonyl group, then the ICT will be recovered, and the PET will be blocked, accordingly in both cases, the fluorescence of the two fluorophores is restored.

Scheme 1.4 Fluorescent probes for thiolphenols

ICT probe for thiolphenol   PET probe for thiolphenol
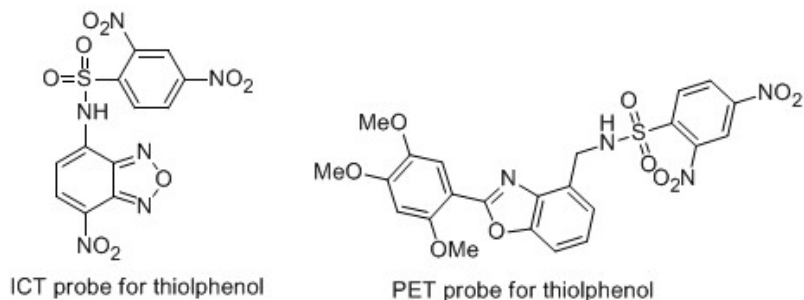
An effective FRET process requires three essential elements: 1) a FRET donor and a FRET acceptor, which are usually two different fluorophores; 2) the distance of a FRET donor and an acceptor within a 10 nm; 3) an overlap between donor emission and acceptor absorption. In the process of bond cleavage or formation, the donor/acceptor distance can be changed and the emission/absorption overlap can be altered. As shown in Scheme 1.5, Zhang et al. reported a fluorescent probe system for phosgene in which the

Scheme1.5 FRET-based fluorescent probes

1) A FRET-based probe for phosgene
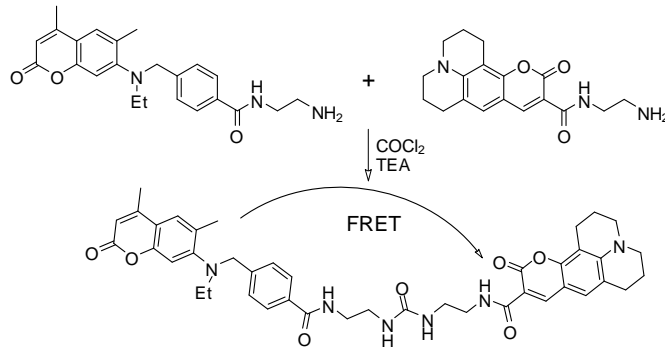
2) A FRET-based probe for thiol-containing amino acids

fluorescent

nonfluorescent
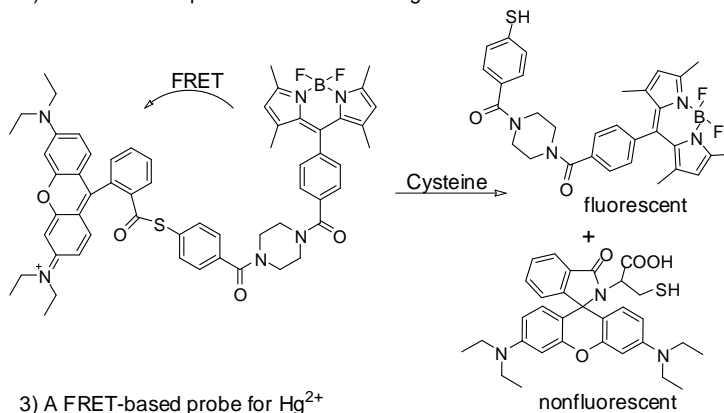
3) A FRET-based probe for Hg^{2+}
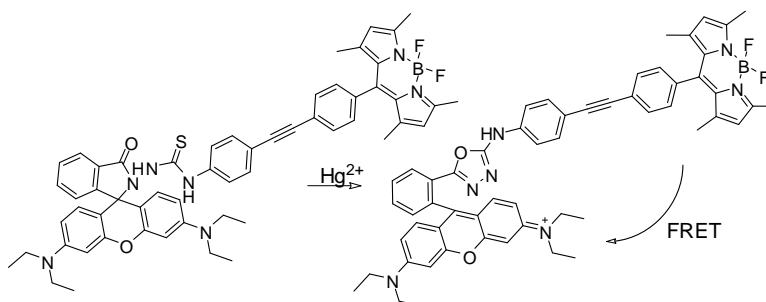
4) A FRET-based probe for hypoxia

nonfluorescent

fluorescent
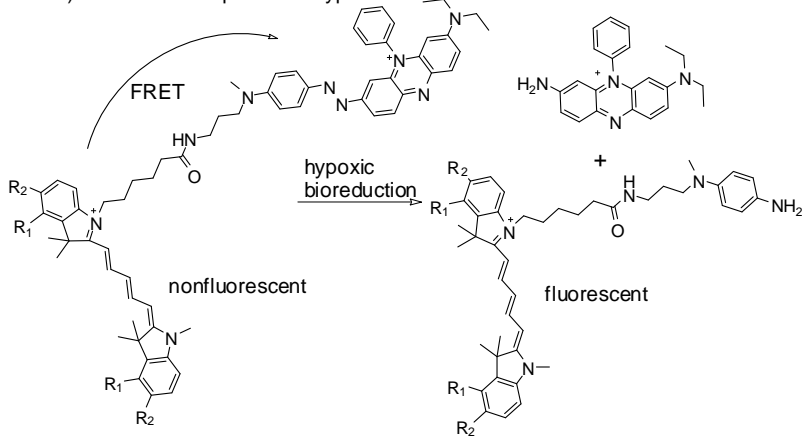
FRET process can be switched on through the connection of FRET donor and acceptor by a phosgene-mediated reaction.[57] Lin et al. developed a RRET-based ratiometric probe for thiol-containing amino acid by a thiol-induced cleavage reaction.[58] Qian et al. combined a bodipy fluorophore (donor) and a rhodamine fluorophore (acceptor) together, and through Hg^{2+} promoted rhodamine conjugation recovery, the FRET will be turned on with a notable emission shift from 514 nm to 589 nm.[59] Besides fluorophores, black hole quencher (BHQ) has been adopted to turn off the fluorescence when it serves as FRET acceptor, one probe based on this method is a hypoxia-sensitive fluorescent probe reported by Nagano et al.[26] In this probe, BHQ can effectively quench the cyanine dye fluorescence. However, hypoxic bioreduction of the azo bond results in the cleavage of the quencher. Therefore the FRET-based quenching effect is eliminated with concurrent observation of a desired off-on response.

Besides ICT, PET and FRET fluorescent mechanisms, a specific reaction is also very critical in the design of reaction-based fluorescent probes.[25] First, a certain chemical structure offers a unique reaction for the design of a series of fluorescent probes. Spirolactam ring-opening of rhodamines provides an excellent example to illustrate this point. Rhodamine derivatives are widely used in probe design due to their excellent stability, high quantum yield, long emission wavelength and expectable color change. As shown in Scheme 1.6, when rhodamine is in the spirolactam ring closing form, it is nonfluorescent and colorless. Through elaborate design and manipulation of the structure and reactivity, an analyte of interest can selectively open the spirolactam ring, thus generating high fluorescence signal and obvious color change. Probes based on this strategy have recently been reviewed.[60,61] Due to the attractive properties of these probes,

other spiro-ring systems based on rhodamine structure have also been extensively investigated, such as probes developed for HOCl,[62] Hg^{2+}/Ag^{+}[63] and nerve agents.[64,65]

Scheme 1.6 Illustration of rhodamine spirolactam ring based probe design system
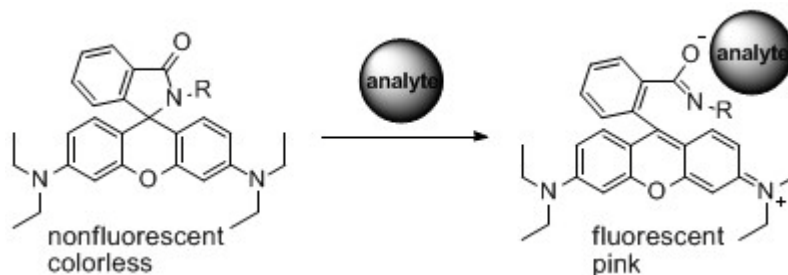
Another general design approach is to alter the fluorophore conjugation through a reaction, and in this process fluorescence signal can be manipulated in the desired manner. As shown in Scheme 1.7, a reactive oxygen species (ROS) probe has been designed through oxidation of a cyanine dye precursor.[66] A Cu^{2+} probe was developed via the recovery of a rhodamine conjugation by Cu^{2+} mediated oxidation.[67] A ratiometric probe for hydroxyl radical (HO•) was successfully obtained through HO• oxidation induced conjugation elongation.[68] It is noted that conjugation system extension is usually formed by oxidation, while conjugation shrinking usually arises from nucleophilic addition. A series of probes based on nucleophilic addition induced conjugation shrinking have been reported, such as probe for thiol,[69] CN^-,[70] and H_2S.[71] For these probes, expectable blue shifted emissions are observed.

Scheme 1.7 Fluorescent probes based on manipulation of fluorophore conjugation

1) oxidation induced fluorophore recovery and alteration

ROS probe   Cu^{2+} probe   HO· probe

2) nucleophilic addition induced conjugation shrinking

thiol probe   CN$^-$ probe   H$_2$S probe
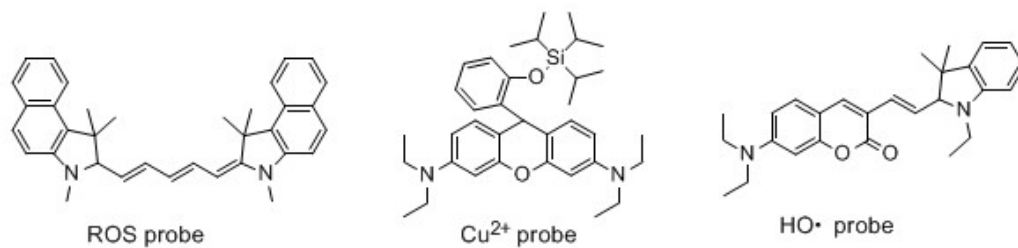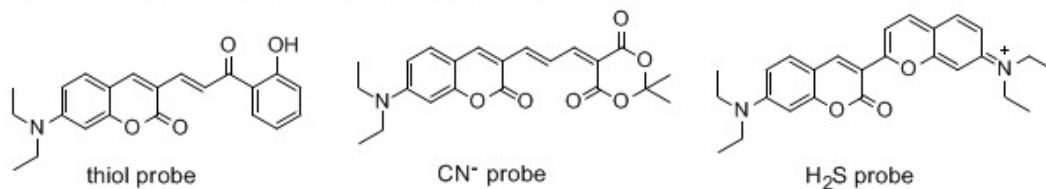
It also has been proved to be a very effective design strategy through masking of a fluorophore by an analyte-reactive moiety. By caging the phenol moiety with a 4-aminophenol group, a probe that can respond to highly reactive oxygen species has been developed.[72] Converting the 7-amine of coumarin to azide leads to a H$_2$S probe (Scheme 1.8).[73]

Scheme 1.8 Design of fluorescent probes through masking of fluorophores

nonfluorescent   fluorescent

nonfluorescent   fluorescent
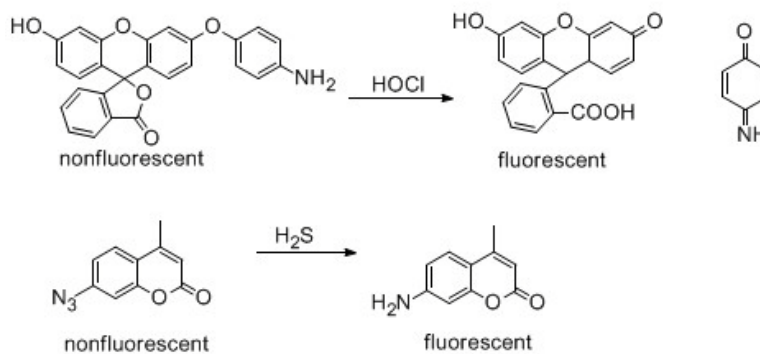
Analytes induced cascade reactions have also been explored in the development of fluorescent probes. Such an example is a Hg^{2+} probe reported by our group (Scheme 1.9).[74] In this study, Hg^{2+} promotes a desulfurization reaction with the generation of 2-hydroxycoumarinic acid, and this highly reactive intermediate undergoes a spontaneous lactonization reaction with the formation of strongly fluorescent coumarin fluorophore.

Scheme 1.9 A probe for Hg^{2+} based on a cascade reaction
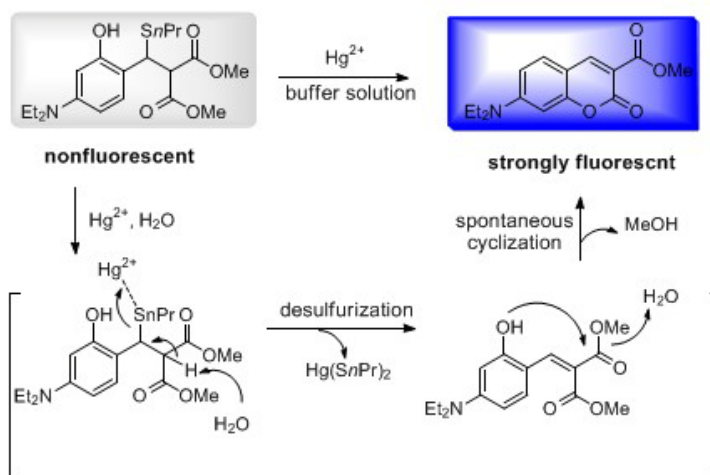
Finally, some researchers take advantage of the catalytic properties of certain analytes to design fluorescent probes. Generally it is expected that such probes display high sensitivity. Transition metals have been widely used in catalysis for reaction development, and these reactions have been applied in sensor development. For example (Scheme 1.10), a fluorescence sensor for Pd was designed by Pd catalyzed the allylic oxidative cleavage reaction.[75] Au(III) probe was designed through a selective Au(III)-

mediated hydroarylation reaction,[76] and a fluorogenic probe for the copper(I)-catalyzed azide-alkyne ligation reaction was reported.[29]

Scheme 1.10 Probes designed based on analyte's catalytic properties
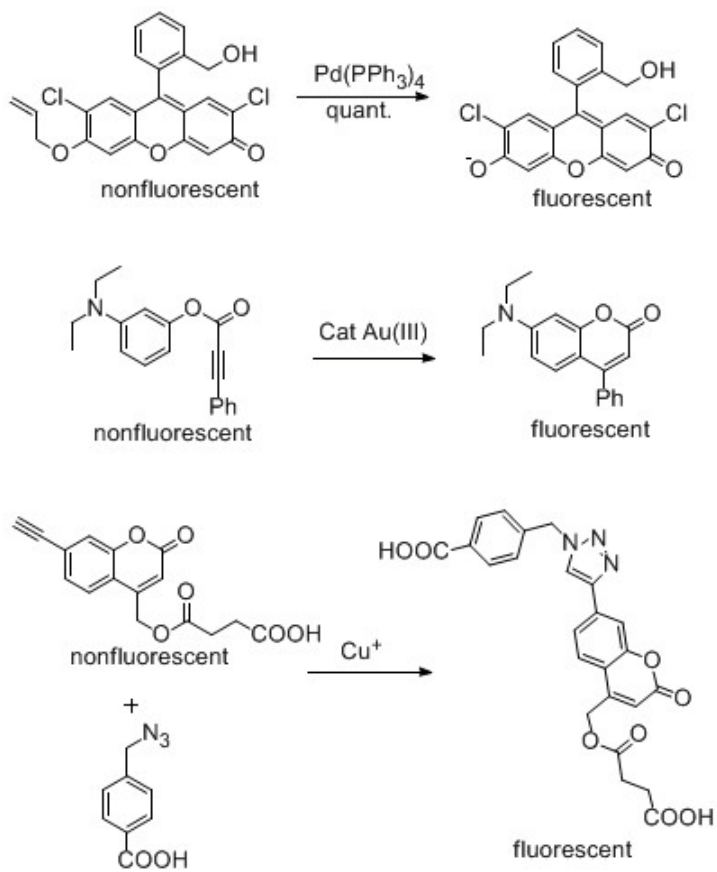
1.4 Summary of Thesis Research

Although much progress has been made in the development of the reaction-based fluorescent probes in the past decade, there is still significant room for improvement and innovation. On one hand, better probes are needed to meet the strict practical applications, especially for biological systems. On the other hand, for some analytes, the probes for their fluorescence detection are not available. With these challenges in mind, I have been focusing on the design and development of new fluorescent probes during my Ph.D study period. In the following chapters, I will detail the effort towards the development of novel fluorescent probes for Hg^{2+}, nerve agent, H_2S and Fe^{2+}.

1.5 References

(1) Yang, Y.; Zhao, Q.; Feng, W.; Li, F. *Chem. Rev.* **2012**, *113*, 192.

(2) Peng, H.; Chen, W.; Cheng, Y.; Hakuna, L.; Strongin, R.; Wang, B. *Sensors* **2012**, *12*, 15907.

(3) Que, E. L.; Domaille, D. W.; Chang, C. J. *Chem. Rev.* **2008**, *108*, 1517.

(4) Beija, M.; Afonso, C. A. M.; Martinho, J. M. G. *Chem. Soc. Rev.* **2009**, *38*, 2410.

(5) Kim, H. N.; Ren, W. X.; Kim, J. S.; Yoon, J. *Chem. Soc. Rev.* **2012**, *41*, 3210.

(6) Tsien, R. Y. *Biochemistry* **1980**, *19*, 2396.

(7) Beer, P. D.; Gale, P. A. *Angew. Chem. Int. Ed.* **2001**, *40*, 486.

(8) Valeur, B.; Leray, I. *Coordination Chemistry Reviews* **2000**, *205*, 3.

(9) de Silva, A. P.; Gunaratne, H. Q. N.; Gunnlaugsson, T.; Huxley, A. J. M.; McCoy, C. P.; Rademacher, J. T.; Rice, T. E. *Chem. Rev.* **1997**, *97*, 1515.

(10) Walkup, G. K.; Burdette, S. C.; Lippard, S. J.; Tsien, R. Y. *J. Am. Chem. Soc.* **2000**, *122*, 5644.

(11) Farruggia, G.; Iotti, S.; Prodi, L.; Montalti, M.; Zaccheroni, N.; Savage, P. B.; Trapani, V.; Sale, P.; Wolf, F. I. *J. Am. Chem. Soc.* **2005**, *128*, 344.

(12) Jung, H. S.; Kwon, P. S.; Lee, J. W.; Kim, J. I.; Hong, C. S.; Kim, J. W.; Yan, S.; Lee, J. Y.; Lee, J. H.; Joo, T.; Kim, J. S. *J. Am. Chem. Soc.* **2009**, *131*, 2008.

(13) Liu, Z.; Zhang, C.; He, W.; Yang, Z.; Gao, X.; Guo, Z. *Chem. Commun.* **2010**, *46*, 6138.

(14) Xu, Z.; Baek, K.-H.; Kim, H. N.; Cui, J.; Qian, X.; Spring, D. R.; Shin, I.; Yoon, J. *J. Am. Chem. Soc.* **2009**, *132*, 601.

(15) Taki, M.; Wolford, J. L.; O'Halloran, T. V. *J. Am. Chem. Soc.* **2003**, *126*, 712.

(16) Qi, J. J.; Han, M. S.; Tung, C. H. *Bioorg. Med. Chem. Lett.* **2012**, *22*, 1747.

(17) Kursunlu, A. N.; Guler, E.; Ucan, H. I.; Boyle, R. W. *Dyes Pigment.* **2012**, *94*, 496.

(18) Li, P.; Fang, L. B.; Zhou, H.; Zhang, W.; Wang, X.; Li, N.; Zhong, H. B.; Tang, B. *Chem. Eur. J.* **2011**, *17*, 10519.

(19) Roussakis, E.; Pergantis, S. A.; Katerinopoulos, H. E. *Chem. Commun.* **2008**, 6221.

(20) Kim, S. K.; Bok, J. H.; Bartsch, R. A.; Lee, J. Y.; Kim, J. S. *Org. Lett.* **2005**, *7*, 4839.

(21) Wang, Q.; Xie, Y.; Ding, Y.; Li, X.; Zhu, W. *Chem. Commun.* **2010**, *46*, 3669.

(22) Guha, S.; Saha, S. *J. Am. Chem. Soc.* **2010**, *132*, 17674.

(23) Cho, D.-G.; Sessler, J. L. *Chem. Soc. Rev.* **2009**, *38*, 1647.

(24) Eun Jun, M.; Roy, B.; Han Ahn, K. *Chem. Commun.* **2011**, *47*, 7583.

(25) Chan, J.; Dodani, S. C.; Chang, C. J. *Nat. Chem.* **2012**, *4*, 973.

(26) Kiyose, K.; Hanaoka, K.; Oushiki, D.; Nakamura, T.; Kajimura, M.; Suematsu, M.; Nishimatsu, H.; Yamane, T.; Terai, T.; Hirata, Y.; Nagano, T. *J. Am. Chem. Soc.* **2010**, *132*, 15846.

(27) Cui, L.; Zhong, Y.; Zhu, W.; Xu, Y.; Du, Q.; Wang, X.; Qian, X.; Xiao, Y. *Org. Lett.* **2011**, *13*, 928.

(28) Takahashi, S.; Piao, W.; Matsumura, Y.; Komatsu, T.; Ueno, T.; Terai, T.; Kamachi, T.; Kohno, M.; Nagano, T.; Hanaoka, K. *J. Am. Chem. Soc.* **2012**, *134*, 19588.

(29) Zhou, Z.; Fahrni, C. J. *J. Am. Chem. Soc.* **2004**, *126*, 8862.

(30) Garner, A. L.; St Croix, C. M.; Pitt, B. R.; Leikauf, G. D.; Ando, S.; Koide, K. *Nat. Chem.* **2009**, *1*, 316.

(31) Xu, K. H.; Sun, S. X.; Li, J.; Li, L.; Qiang, M. M.; Tang, B. *Chem. Commun.* **2012**, *48*, 684.

(32) Yu, M.-M.; Li, Z.-X.; Wei, L.-H.; Wei, D.-H.; Tang, M.-S. *Org. Lett.* **2008**, *10*, 5115.

(33) Jiang, J.; Jiang, H.; Tang, X.; Yang, L.; Dou, W.; Liu, W.; Fang, R.; Liu, W. *Dalton Trans.* **2011**, *40*, 6367.

(34) Bodenant, B.; Weil, T.; Businelli-Pourcel, M.; Fages, F.; Barbe, B.; Pianet, I.; Laguerre, M. *J. Org. Chem.* **1999**, *64*, 7034.

(35) Chandrasekhar, V.; Pandey, M. D.; Bag, P.; Pandey, S. *Tetrahedron* **2009**, *65*, 4540.

(36) Suresh, M.; Ghosh, A.; Das, A. *Chem. Commun.* **2008**, *0*, 3906.

(37) Kim, M. H.; Jang, H. H.; Yi, S.; Chang, S.-K.; Han, M. S. *Chem. Commun.* **2009**, *0*, 4838.

(38) Kumar, M.; Kumar, N.; Bhalla, V.; Sharma, P. R.; Kaur, T. *Org. Lett.* **2011**, *14*, 406.

(39) Zhao, Y.; Zhang, X.-B.; Han, Z.-X.; Qiao, L.; Li, C.-Y.; Jian, L.-X.; Shen, G.-L.; Yu, R.-Q. *Anal. Chem.* **2009**, *81*, 7022.

(40) Chang, M. C. Y.; Pralle, A.; Isacoff, E. Y.; Chang, C. J. *J. Am. Chem. Soc.* **2004**, *126*, 15392.

(41) Dickinson, B. C.; Chang, C. J. *J. Am. Chem. Soc.* **2008**, *130*, 9638.

(42) Srikun, D.; Miller, E. W.; Domaille, D. W.; Chang, C. J. *J. Am. Chem. Soc.* **2008**, *130*, 4596.

(43) Albers, A. E.; Okreglak, V. S.; Chang, C. J. *J. Am. Chem. Soc.* **2006**, *128*, 9640.

(44) Karton-Lifshin, N.; Albertazzi, L.; Bendikov, M.; Baran, P. S.; Shabat, D. *J. Am. Chem. Soc.* **2012**, *134*, 20412.

(45) Yuan, L.; Lin, W.; Xie, Y.; Chen, B.; Zhu, S. *J. Am. Chem. Soc.* **2011**, *134*, 1305.

(46) Kim, H. J.; Han, J. H.; Kim, M. K.; Lim, C. S.; Kim, H. M.; Cho, B. R. *Angew. Chem. Int. Ed.* **2010**, *49*, 6786.

(47) Collot, M.; Loukou, C.; Yakovlev, A. V.; Wilms, C. D.; Li, D.; Evrard, A.; Zamaleeva, A.; Bourdieu, L.; Léger, J.-F.; Ropert, N.; Eilers, J.; Oheim, M.; Feltz, A.; Mallet, J.-M. *J. Am. Chem. Soc.* **2012**, *134*, 14923.

(48) Egawa, T.; Hirabayashi, K.; Koide, Y.; Kobayashi, C.; Takahashi, N.; Mineno, T.; Terai, T.; Ueno, T.; Komatsu, T.; Ikegaya, Y.; Matsuki, N.; Nagano, T.; Hanaoka, K. *Angew. Chem. Int. Ed.* **2013**, *125*, 3966.

(49) Komatsu, H.; Iwasawa, N.; Citterio, D.; Suzuki, Y.; Kubota, T.; Tokuno, K.; Kitamura, Y.; Oka, K.; Suzuki, K. *J. Am. Chem. Soc.* **2004**, *126*, 16353.

(50) Dong, Y.; Mao, X.; Jiang, X.; Hou, J.; Cheng, Y.; Zhu, C. *Chem. Commun.* **2011**, *47*, 9450.

(51) Yamada, K.; Nomura, Y.; Citterio, D.; Iwasawa, N.; Suzuki, K. *J. Am. Chem. Soc.* **2005**, *127*, 6956.

(52) Kim, M. K.; Lim, C. S.; Hong, J. T.; Han, J. H.; Jang, H.-Y.; Kim, H. M.; Cho, B. R. *Angew. Chem. Int. Ed.* **2010**, *49*, 364.

(53) Hirata, T.; Terai, T.; Komatsu, T.; Hanaoka, K.; Nagano, T. *Bioorg. Med. Chem. Lett.* **2011**, *21*, 6090.

(54) Baruah, M.; Qin, W.; Vallée, R. A. L.; Beljonne, D.; Rohand, T.; Dehaen, W.; Boens, N. *Org. Lett.* **2005**, *7*, 4377.

(55) Jiang, W.; Fu, Q.; Fan, H.; Ho, J.; Wang, W. *Angew. Chem. Int. Ed.* **2007**, *119*, 8597.

(56) Jiang, W.; Cao, Y.; Liu, Y.; Wang, W. *Chem. Commun.* **2010**, *46*, 1944.

(57) Zhang, H.; Rudkevich, D. M. *Chem. Commun.* **2007**, *0*, 1238.

(58) Long, L.; Lin, W.; Chen, B.; Gao, W.; Yuan, L. *Chem. Commun.* **2011**, *47*, 893.

(59) Zhang, X.; Xiao, Y.; Qian, X. *Angew. Chem. Int. Ed.* **2008**, *47*, 8025.

(60) Chen, X.; Pradhan, T.; Wang, F.; Kim, J. S.; Yoon, J. *Chem. Rev.* **2011**, *112*, 1910.

(61) Kim, H. N.; Lee, M. H.; Kim, H. J.; Kim, J. S.; Yoon, J. *Chem. Soc. Rev.* **2008**, *37*, 1465.

(62) Kenmoku, S.; Urano, Y.; Kojima, H.; Nagano, T. *J. Am. Chem. Soc.* **2007**, *129*, 7313.

(63) Shi, W.; Sun, S.; Li, X.; Ma, H. *Inorg. Chem.* **2009**, *49*, 1206.

(64) Wu, Z.; Wu, X.; Yang, Y.; Wen, T.-b.; Han, S. *Bioorg. Med. Chem. Lett.* **2012**, *22*, 6358.

(65) Wu, X.; Wu, Z.; Han, S. *Chem. Commun.* **2011**, *47*, 11468.

(66) Kundu, K.; Knight, S. F.; Willett, N.; Lee, S.; Taylor, W. R.; Murthy, N. *Angew. Chem. Int. Ed.* **2009**, *48*, 299.

(67) Lin, W.; Long, L.; Chen, B.; Tan, W.; Gao, W. *Chem. Commun.* **2010**, *46*, 1311.

(68) Yuan, L.; Lin, W.; Song, J. *Chem. Commun.* **2010**, *46*, 7930.

(69) Kim, G.-J.; Lee, K.; Kwon, H.; Kim, H.-J. *Org. Lett.* **2011**, *13*, 2799.

(70) Li, H.; Wen, Z.; Jin, L.; Kan, Y.; Yin, B. *Chem. Commun.* **2012**, *48*, 11659.

(71) Liu, J.; Sun, Y.-Q.; Zhang, J.; Yang, T.; Cao, J.; Zhang, L.; Guo, W. *Chem. Eur. J.* **2013**, *19*, 4717.

(72) Setsukinai, K.; Urano, Y.; Kakinuma, K.; Majima, H. J.; Nagano, T. *J. Biol. Chem.* **2003**, *278*, 3170.

(73) Chen, B. F.; Li, W.; Lv, C.; Zhao, M. M.; Jin, H. W.; Jin, H. F.; Du, J. B.; Zhang, L. R.; Tang, X. J. *Analyst* **2013**, *138*, 946.

(74) Jiang, W.; Wang, W. *Chem. Commun.* **2009**, *0*, 3913.

(75) Song, F.; Garner, A. L.; Koide, K. *J. Am. Chem. Soc.* **2007**, *129*, 12354.

(76) Do, J. H.; Kim, H. N.; Yoon, J.; Kim, J. S.; Kim, H.-J. *Org. Lett.* **2010**, *12*, 932.

Chapter 2

The Development of Novel Fluorescent Probes for Hg^{2+}

2.1 Background and Significance

The demand of facile, sensitive, selective and cost-effective detection techniques for mercury ion (Hg^{2+}) has been growing dramatically recently as results of its high toxicity[1-4] and the facts of growing and broad contamination and pollution.[5,6] Among the distinct detection methods, the use of fluorescence technique for Hg^{2+} has been much appreciated owning to its high sensitivity, selectivity and simple operation procedures.[7,8] For quantification of an analyst, especially in a complicated analysis system, a ratiometric fluorescent sensing is highly desirable. However, the development of such probes for Hg^{2+} has proven quite challenging, and only a handful of examples of the fluorescent probes displayed ratiometric response to Hg^{2+}.[9-21] Nevertheless they are far from ideal. To our knowledge, nearly all ratiometric chemosensors are interfered by Ag(I), Cu(II), Fe(II) and low sensitivity.[10,15-18] Some of them required a high proportion of organic solvent as media for analysis,[19-21] and the one that can work in 100% aqueous solution was very rare.[22] Moreover, in general, they have undistinguishable ratiometric fluorescent intensity change and significant overlap due to an unsatisfactory emission shift.

The general strategy in design of a fluorescent sensor/probe involves an incorporation of recognition moiety into a fluorophore.[23,24] The analyte (e.g., an ion) binding to the probe by perturbing either ground state or excited state properties of the fluorophore yields a detectable signal. In many cases, a shift in the absorbance spectra or changes in the fluorescent emission characteristics such as intensity and/or emission wavelength are typically observed. Nevertheless, other fluorophore characteristics such

as a significant emission shift are usually difficult to modulate. Furthermore, while the convenient strategy in the development of ratiometric sensors is the employment of FRET sensing mechanism,[25] the examples using ICT ratiometric sensors for Hg^{2+} are very rare,[10,16,21] and significant overlap between two relatively broad emission spectra usually makes it difficult to accurately determine the ratio of the two emission signals. Therefore, a large shift of the maxima emission wavelengths between the probe and probe formed product is required in order to overcome the problem.

On the other hand, a probe that can respond to ppb level of Hg^{2+} is very desired due to its lethal toxicity, but still rare.[26] Due to all these concerns, we have developed 1) a ratiometric Hg^{2+} probe with remarkable emission shift, and 2) a Hg^{2+} probe with impressive detection limit at ppb level.

**2.2 A Ratiometric Fluorescent Probe with Large Emission Shift for the Facile Detection of Hg^{2+} (Probe-1)**

2.2.1 Probe Design Strategy

Previously our group developed a Hg^{2+} probe based on Hg^{2+}-induced elimination-cyclization reaction, and this probe displayed excellent sensitivity and specificity.[27] Inspired by this work, we conceived that the new double bond generated by Hg^{2+}-induced elimination could serve as a conjugation extending, then a red shifted ratiometric response could be expected.

With the insight in mind, we envisioned that the incorporation of the recognition moiety into a fluorophore could produce an Hg^{2+} selective probe. The critical challenge remains the selection of a fluorophore, which should display a ratiometric response to Hg^{2+}, while requiring a noticeable ratiometric fluorescent intensity alternation and a large emission shift. These features could be realized if Hg^{2+} facilitates a desulfur elimination of a fluorophore through a tethered saturated carbonyl to form an α,β-unsaturated system. The newly formed unsaturated system should be part of the conjugated fluorophore, and therefore a large and red emission shifted fluorescence response can be expected. We were interested in the widely used coumarin as choice of fluorophore due to its favorable physical and optical properties and stability (Probe-1, Scheme 2.1). Crucially positioning the thioether recognition moiety on the coumarin fluorophore significantly affects the fluorescent properties. In coumarin system, in general, electron-donating groups (EDGs) at positions 7 and/or 6 can increase the fluorescence quantum yield and render longer excitation and emission wavelength since ICT efficiency is enhanced from these EDGs to the electron-withdrawing moiety lactone. Therefore it is conceivable to incorporate the

23

thioether functionality at position 3 of the coumarin framework. The Hg^{2+} catalyzed elimination leads to an EWG (electron-withdrawing group) α,β-unsaturated ketone, thus extending the coumarin conjugate system. It is expected that the fluorescence emission will be red-shifted and a ratiometric response will occur. It should also be noted that unlike most of the desulfurization-based probes which usually require at least 1 equiv. of Hg^{2+} to reach the maximum fluorescence enhancement,[28,29] probe-1 only needs 0.5 equiv. of Hg^{2+} to get the maximum fluorescence due to the alkylated sulfur. In this way, the sensitivity can be further improved to some extent.

Scheme 2.1 Rational design of a selective ratiometric fluorescent probe for Hg(II)
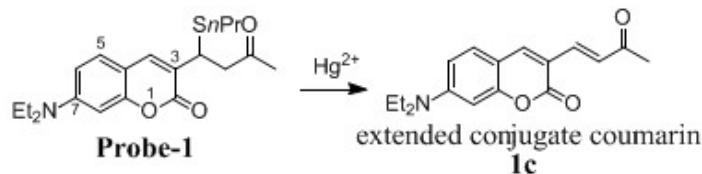
2.2.2 Preparation of Probe-1

The preparation of probe-1 involved a facile four-step synthesis form commercially available starting materials (Scheme 2.2). 7-Diethylaminocoumarin (**1a**) was synthesized from 4-diethylaminosalicylaldehyde in 68% total yield. Incorporation of an aldehyde moiety at position 3 (**1b**) was realized by reaction of **1a** with DMF and $POCl_3$. An aldol condensation reaction with acetone gave the conjugation-extended coumarin (**1c**). Finally a facile Michael addition reaction with propanethiol in the presence of pyrrolidine led to the probe-**1**. It was fully characterized by NMR and mass spectroscopy.

Scheme 2.2 Synthesis of probe-**1**
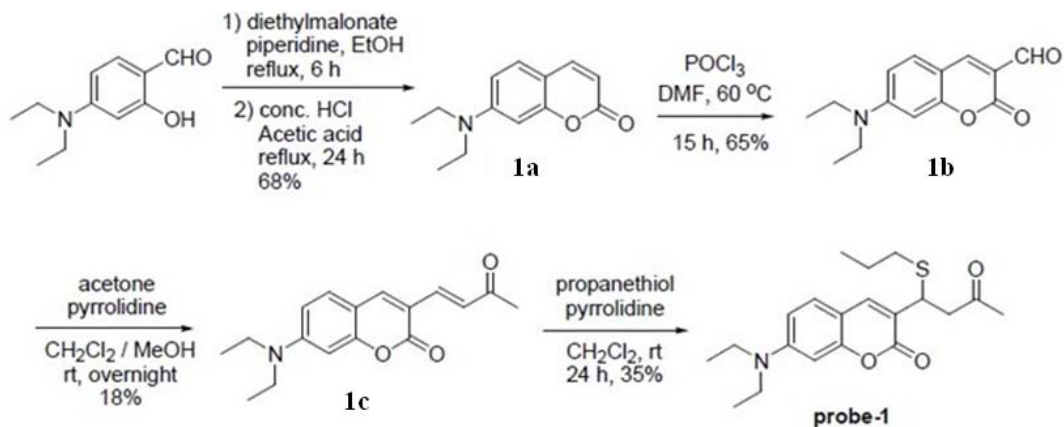
2.2.3 Probe-1 Evaluation in Buffer Solution

With the probe-**1** in hand, we firstly investigated its response to Hg^{2+} in the aspect of both emission and absorption. Notably, the probe is water soluble; a phosphate buffer solution using only 0.5% acetonitrile is sufficient. In the absence of Hg^{2+}, the probe at a concentration of 5.0 µM displayed an emission at 488 nm when excited at 435 nm. When addition of 2.0 equiv. of Hg^{2+}, a new emission peak appeared at 560 nm instantly, meanwhile the emission at 488 nm disappeared, indicative of a ratiometric response (Figure 2.1a). The maximum absorbance was switched from 400 nm to 460 nm (Figure 2.1b) due to the elongation of the fluorescent system by formation of enone. Furthermore, the probe response to Hg^{2+} was facile; the whole process took place within 1 min. In addition, an obvious color change was observed under both daylight and UV light, making it possible to detect Hg^{2+} with naked eyes (Figure 2.1c).
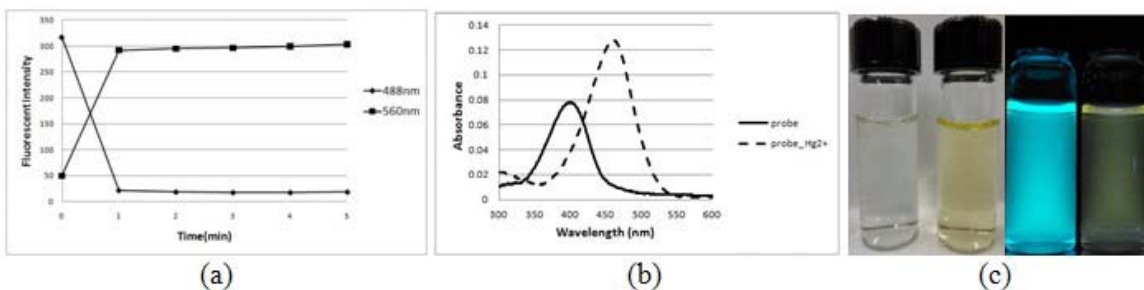
Figure 2.1 (a) Emission of 5µM probe-1 at 488 nm and 560 nm after addition of 10 µM Hg^{2+}. $\lambda_{ex}= 435$ nm. Data were recorded every minute; (b) UV/Vis spectra of 5µM probe-1 (solid line) and 5µM probe-1 with 10µM Hg^{2+} (dashed line); (c) Color change under daylight and UV light. All experiments were carried out in 0.1M phosphate buffer solution containing 0.5% acetonitrile (pH = 7.4).
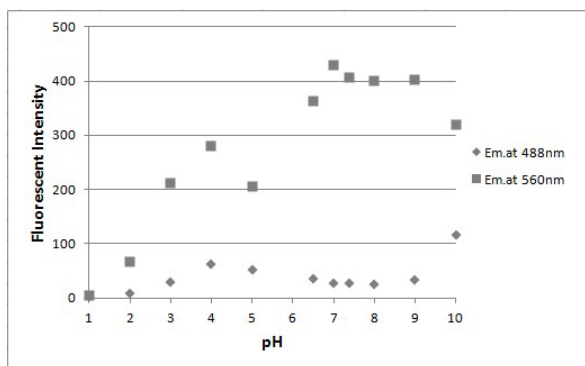
Figure 2.2 The response of 5µM probe-1 to 10µM Hg^{2+} was investigated at different pH.

Also, we investigated the probe at different pH, and it turned out that probe-1 can respond to Hg^{2+} at acidic condition (pH > 1), and displayed a similar result at pH 6.5 -9 (Figure 2.2).

Next fluorescence titration experiments with Hg^{2+} ions were conducted (Figure 2.3). To a 5.0 µM probe-1 buffer solution was added Hg^{2+} at concentration in a range of 0.0-3.5 µM. It was found that the emission at 560 nm gradually increased while the emission at 488 nm decreased. The emission shift was as large as 72 nm to a longer (Figure 2.3a). As predicted, when more than 0.5 equiv. of Hg^{2+} (2.5 µM) was used, the

emission spectra remained unchanged, and the ratio of the emission intensities at 560 nm and 488 nm became constant (Figure 2.3b), demonstrating that the reaction stoichiometry was 2:1 (probe-1/Hg^{2+}). Furthermore, a pronounced fluorescent signal change was observed even when Hg^{2+} was as low as 2×10^{-8} M (Figure 2.3c).

(a)　　　　　　　　　(b)　　　　　　　　　(c)

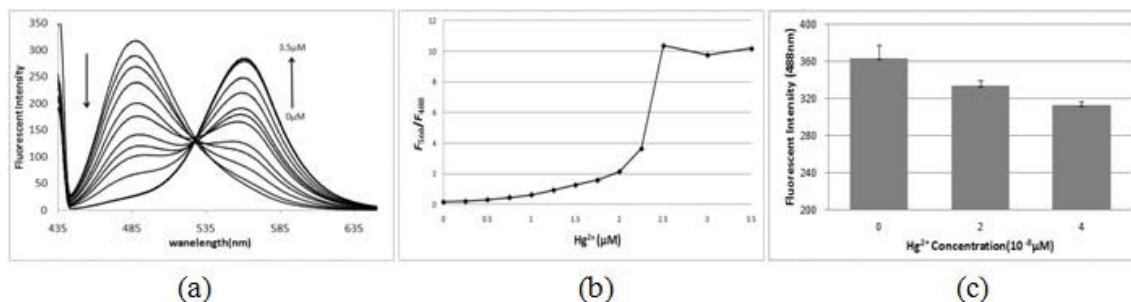**Figure 2.3** a) Fluorescence titration spectra of 5µM probe-1 in 0.1M (containing 0.5% acetonitrile) at pH 7.4 upon addition of 0, 0.25, 0.5, 0.75, 1.0, 1.25, 1.5, 1.75, 2.0, 2.25, 2.5, 3.0, 3.5µM Hg^{2+} ions; b) Fluorescence intensity ratio changes (F_{560}/F_{488}) of 5µM probe-1 upon addition of different concentration of Hg^{2+} ions. 3) The fluorescence at 488nm was recorded when 2×10^{-8} or 4×10^{-8} µM Hg^{2+} was added. λ_{ex}= 435 nm.

The novel ratiometric probe-**1** possessed an excellent selectivity toward Hg^{2+} over other metal cations. As shown (Figure 2.4), only Hg^{2+} induced significant ratiometric fluorescence change, while the addition of even 2.0 equiv. of other metal cations, such as alkali Li^+, K^+ and Cs^+, alkaline-earth Mg^{2+}, Ca^{2+} and Ba^{2+}, and transition and heavy metal ions Ag^+, Mn^{2+}, Fe^{2+}, Fe^{3+}, Co^{2+}, Ni^{2+}, Cu^{2+}, Cu^+, Zn^{2+}, Cd^{2+} and Pb^{2+} could not induce obvious fluorescence alternation. Moreover, in the presence of all above cations (each at 10.0 µM while Hg^{2+} at 2.5 µM), probe-**1** still exhibited a similar fluorescence profile. These studies clearly indicate that the probe can be utilized for selective detection of Hg^{2+} without interference from other metal ions. These acclaimed features make this probe

promising for practical application. It is noteworthy that compared with many reported desulfurization-based probes,[28,29] the excellent selectivity of probe-**1** is attributed to the unique chemoreactivity between thioether and Hg^{2+}. It implies that the desulfurization of thioether serves as a general approach for design of Hg^{2+} fluorescent probes with high selectivity and sensitivity, but examples based on this strategy are still scarce.[30]
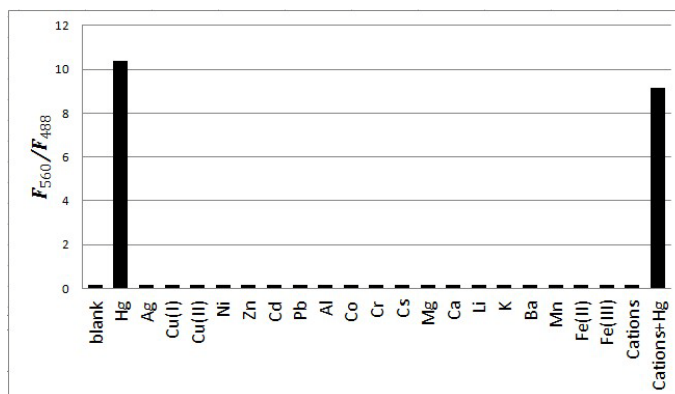
Figure 2.4 To probe-1 (5.0 μM) in a 0.1 M phosphate buffer solution (pH = 7.4, containing 0.5% acetonitrile) was added a series of metal cations. Hg^{2+} was at 2.5 μM, and all other cations were at 10.0 μM. Cations and Hg^{2+}: all above metal cations, each with 10 μM while Hg^{2+} at 2.5 μM.

2.2.4 Live Cell Imaging

To test the feasibility of the probe-**1** for cellular imaging, fluorescence images of C8D1A cells were carried out using a confocal microscope (Figure 2.5). Firstly, C8D1A cells were incubated with 5.0 μM probe-**1** in PBS for 30 min, and only a bright blue intracellular fluorescence was observed, suggesting that the probe was cell-permeable. Furthermore, in the imaging process, the probe didn't show obvious toxicity to the cells. Then, C8D1A cells were incubated with 5.0 μM Hg^{2+} for 30 min followed by 5.0 μM probe-**1** for another 30 min. An obvious decrease in blue fluorescence was observed,

while a new yellow fluorescence appeared. The double-channel fluorescence images were observed at 475 – 525 nm and 530 – 600 nm respectively (Figure 2.5). When C8D1A cells were incubated firstly with this probe (5.0 µM), then with Hg^{2+} at 5.0 µM (1.0 equiv.), very similar results were obtained. These studies demonstrated that probe-1 can detect intracellular Hg^{2+} with a ratiometric response.
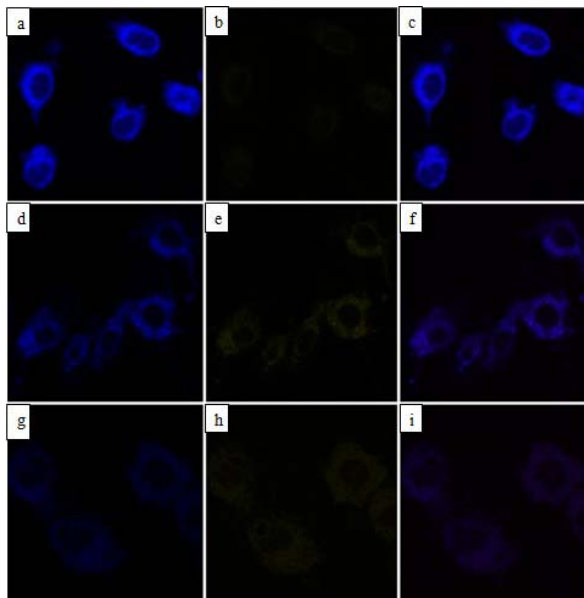
Figure 2.5 Confocal fluorescence images of C8D1A cells (a mouse astrocyte cell line), λ_{ex} = 405 nm, Zeiss LSM510 META Confocal Microscope with a 63 × objective. Top row: C8D1A cells incubated with probe-1 (5.0 µM) at 37 °C. Middle row: C8D1A cells incubated with 5.0 µM Hg^{2+} for 30 min, then further with probe-1 at 5.0 µM for 30 min at 37 °C. Bottom row: C8D1A cells incubated with probe-1 (5.0 µM) for 30 min, then further with Hg^{2+} (5.0 µM) for 30 min at 37 °C. Panels a, d, and g represent the emissions at 475 – 525 nm; panels b, e, and h represent the emissions at 530 – 600 nm; panels c, f, and i represent merged images of a and b, d and e and g and h, respectively.

2.2.5 Summary

In conclusion, we have successfully developed a novel ratiometric and colorimetric fluorescent probe for Hg^{2+} using chemoselective Hg^{2+} promoted

desulfurization of a thioether to form an extended conjugated fluorescent system. As demonstrated, the probe displays excellent sensitivity and selectivity toward Hg^{2+} in aqueous buffer solutions. Notably, significant ratiometric fluorescent response coupling with a large emission red shift allows for convenient detection and quantification of the toxic metal ion in a complicated system. Moreover, colorimetric change makes it possible to detect Hg^{2+} by naked eyes. The intracellular fluorescent imaging renders it a promising tool to study Hg^{2+} in living cells. Taken together, the studies have demonstrated probe-1 as a useful tool for detection and imaging of Hg^{2+}.

2.3 A Novel Fluorescent Probe for Hg^{2+} with Impressive Detection Limit (Probe-2)

2.3.1 Probe Design

Scheme 2.3 Rational design of a highly sensitive fluorescent probe for Hg(II)
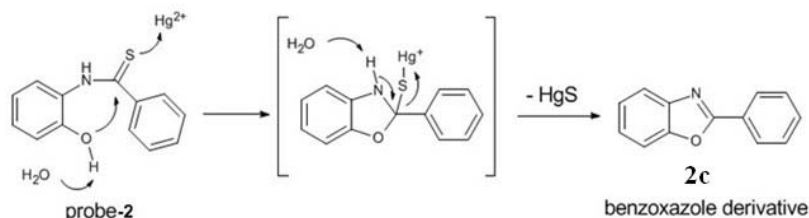
In this design (Scheme 2.3), probe-**2** was a benzoxazole precursor with a thioamide group, and it was completely nonfluorescent. In the presence of Hg^{2+}, the adjacent phenol would spontaneously attack the thioamide carbon trigged by the coordination of the thioamide with Hg^{2+} followed by an elimination reaction, then a highly fluorescent benzoxazole derivative was formed while a molecule of HgS was released.

2.3.2 Probe-2 Preparation

The synthesis commenced with a commercially available compound N-(2-methoxyphenyl)benzamide. The requisite benzothioamide derivative (**2a**) was facilely synthesized in 99% yield, then the amide bond was converted to thiolamide by Lawesson's reagent in 94% yield (**2b**). Finally a AlCl$_3$ induced demethylation reaction give rise to probe-**2** in an overall yield of 43.7%.

Scheme 2.4 Synthesis of probe-**2**
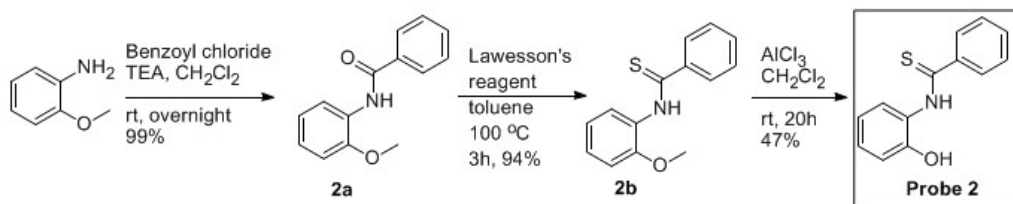
2.3.3 Probe-2 Evaluation in Buffer Solution

With this probe in hand, we firstly investigated its stability in buffer solution. At neutral buffer solution (pH = 7.4), the fluorescence at 360nm (λ_{ex} = 290 nm) increased very fast (Figure 2.6). This instability is presumably attributed to the formation of phenoxide at pH 7.4, which is a strong nucleophile, and thus accelerating the formation of benzoxazole derivative. To avoid the problem, we reasoned that, if the pH was lowered, there would be less reactive neutral phenol. As was expected, at pH 6.5 the fluorescence increased in a much slower pace, and at pH 5.0, no obvious fluorescence increase was observed in a time scale of 10 minutes. So, we decided to perform the studies in a buffer solution at pH 5.
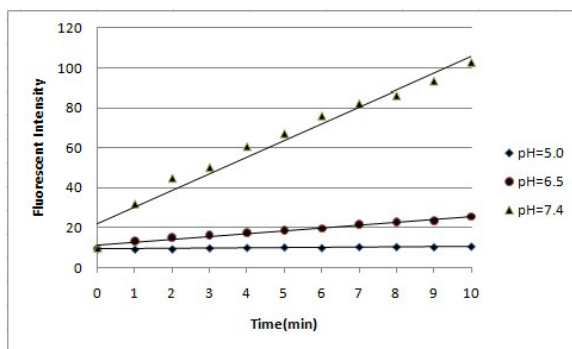
Figure 2.6 Fluorescent intensities of 1μM probe in 0.1M phosphate buffer (containing 1% CH$_3$CN) at different pH were recorded in a time scale of 10 minutes. λ_{ex} = 290 nm, and λ_{em} = 360 nm.

With the optimized detection condition, we evaluated its sensitivity to Hg^{2+}. To 1 μM probe-**2** in 0.1 M phosphate buffer solution was added 10μM Hg^{2+}. The fluorescence increased instantly, and a plateau was reached in 3 minutes (Figure 2.7a). A similar result was also observed for Ag$^+$, and excessive amount of Hg^{2+} or Ag$^+$ can lead 1μM probe to fluorescence at the same intensity level which was consistent with the mechanism we

proposed. In the whole process, the fluorescent intensity was enhanced by 98 folds for Hg^{2+} and 95 folds for Ag^+. Also, after addition of Hg^{2+}, there was a strong absorbance at 266nm in the UV/Vis spectra (Figure 2.7b).

(a)   (b)

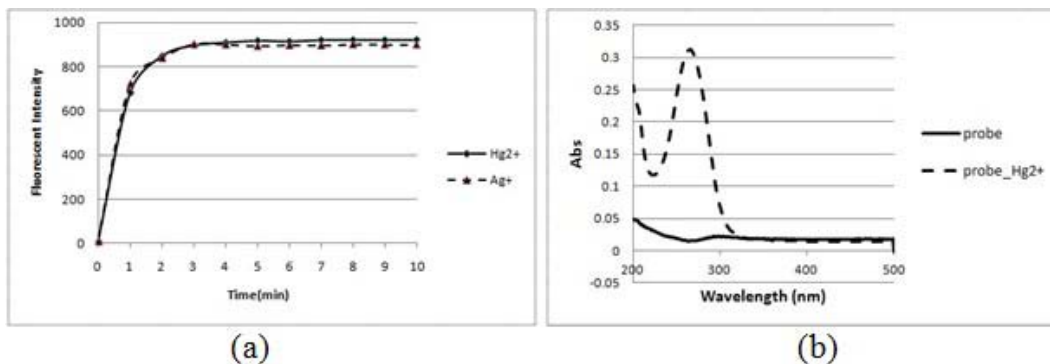**Figure 2.7** a) Fluorometric traces for the reaction Hg^{2+} or Ag^+ (10 μM) with 1 μM probe. All measurements were taken in a pH 5.0 phosphate buffer (0.1 M) containing 1% CH_3CN; b) The solid line was absorbance of 1μM probe; the dashed line was the absorbance of 1μM probe after addition of 10μM Hg^{2+}. All measurements were taken in a pH 5.0 phosphate buffer (0.1 M) containing 1% CH_3CN. $\lambda_{ex} = 290$ nm, and $\lambda_{em} = 360$ nm.

Then, we examined its response to Hg^{2+} and Ag^+ at different concentration. To 1 μM probe-**2** was added Hg^{2+} ranging from 0 to 1.2 equiv. A highest fluorescence was obtained when 1 equiv of Hg^{2+} was used while no further fluorescence enhancement was observed when more Hg^{2+} was added (Figure 2.8a). This demonstrated that the reaction stoichiometry was 1:1. From 0 to 1 equiv of Hg^{2+}, there is a good linear relationship between the Hg^{2+} concentration and fluorescent intensity (Figure 2.8b), indicating that this probe was suitable for Hg^{2+} quantitative analysis. More importantly, this probe can respond well to Hg^{2+} at ppb level (Figure 2.8c), and the detection limit was determined to be 2ppb at a signal to background ratio of 2, which can meet the requirement of US EPA

for drinking water. For Ag$^+$, there was a very similar result (Figure 2.9). The reaction stoichiometry was determined to 1:2 (probe-2/Ag$^+$) with a good leaner relationship, and the detection limit was 2.2 ppb (20 nM) at a signal to noise ratio of 2.
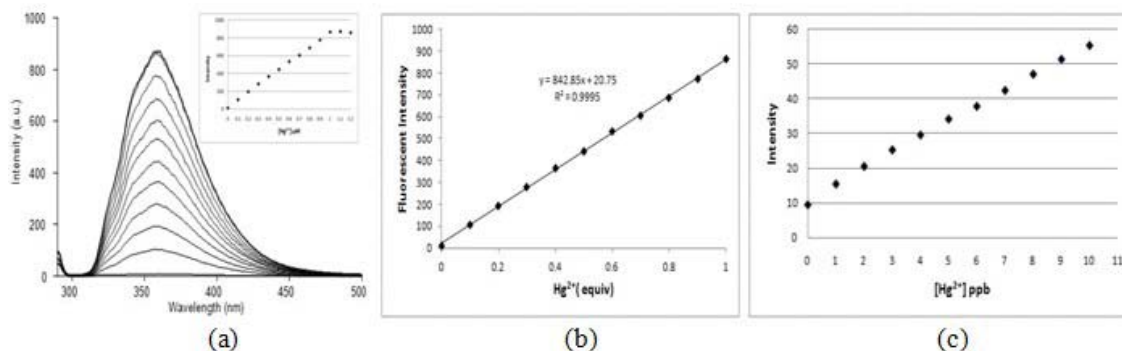

(a)   (b)   (c)

Figure 2.8 (a) A plot of the fluorescence intensity obtained from the reaction of 1 µM probe-2 with Hg^{2+} as a function of equiv. of Hg^{2+}; (b) The linear relationship between the fluorescent intensity and Hg^{2+} concentration; (c) A plot of the fluorescence intensity obtained from the reaction of 1 µM probe-2 with Hg^{2+} as a function of concentration of Hg^{2+} at ppb level. All measurements were taken in a pH 5.0 phosphate buffer (0.1 M) containing 1% CH$_3$CN. λ_{ex} = 290 nm, and λ_{em} = 360 nm.

(a)   (b)   (c)

Figure 2.9 (a) A plot of the fluorescence intensity obtained from the reaction of 1 µM probe-2 with Ag$^+$ as a function of equiv. of Ag$^+$; (b) The linear relationship between the concentration of Hg^{2+} and the fluorescent intensity; (c) A plot of the fluorescence intensity obtained from the reaction of 1 µM probe-2 with Ag$^+$ as a function of concentration of Ag$^+$ at submicromolar level. All measurements were taken in a pH 5.0 phosphate buffer (0.1 M) containing 1% CH$_3$CN. λ_{ex} = 290 nm, and λ_{em} = 360 nm.

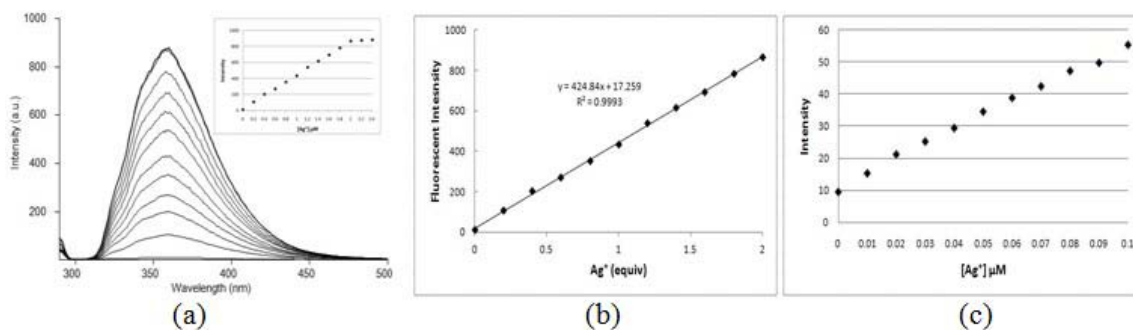To prove that this probe was likely to work in complicated environment, we investigated its selectivity over other metal cations. To 50 equiv of all other metal cations, such as Mg^{2+}, Cu^{2+}, Pb^{2+} and Cd^{2+}, there was no obvious fluorescence enhancement, and only Hg^{2+} and Ag^+ can lead to fluorescence enhancement (Figure 2.10). Also, even in the presence of all above cations in 10 μM respectively, this probe can respond to Hg^{2+} and Ag^+ in a similar way with very limited interference. This exclusive selectivity towards Hg^{2+} and Ag^+ made it very promising to detect Hg^{2+} and Ag^+ in practical application.
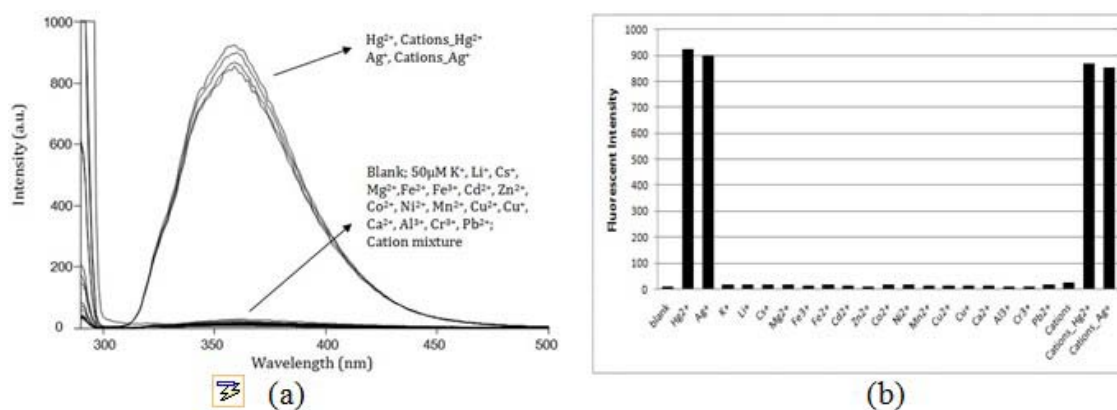
Figure 2.10 Effects of metal ions on the fluorescence. All measurements were taken in a pH 5.0 phosphate buffer (0.1 M) containing 1% CH_3CN. Hg^{2+} and Ag^+ is at 10μM, all other metal cations are at 50 μM. Cations: all mentioned cations in 10μM respectively except Hg^{2+} and Ag^+. λ_{ex} = 290 nm, and λ_{em} = 360 nm.

To prove the reaction mechanism, the proposed benzoxazole derivative (**2c**) was synthesized and probed for Hg^{2+}. The emission spectra of 1 μM benzoxazole derivative and 1μM probe-**2** after addition of Hg^{2+} almost 100% overlapped (Figure 2.11). Undoubtedly, the studies supported our design strategy
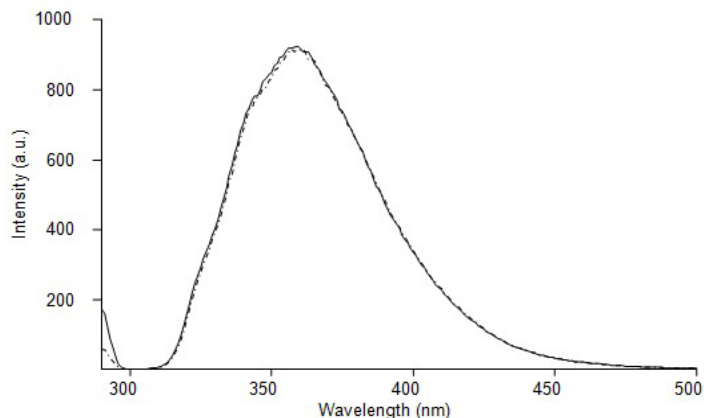
Figure 2.11 The solid line was the emission of 1μM probe-2 treated with 10μM Hg^{2+}, the dashed line was the emission of 1μM benzoxazole product. All measurements were taken in a pH 5.0 phosphate buffer (0.1 M) containing 1% CH$_3$CN. λ_{ex} = 290 nm, and λ_{em} = 360 nm.

To make it a useful tool for Hg^{2+} analysis, it is necessary for probe-**2** to be capable of differentiating Hg^{2+} from Ag$^+$. It's well known that Cl$^-$ has a strong affinity to Ag$^+$ with the formation of AgCl precipitation; however HgCl$_2$ is soluble. So we surmised that modifying buffer solution with Cl$^-$ containing salt such as NaCl may offer method for the selective detection of Hg^{2+}. Indeed, we found that in the presence of 1 M NaCl, the probe couldn't respond to 10 μM Ag^{2+}; when upon addition of 10 μM Hg^{2+}, the fluorescence can be greatly enhanced with limited decrease of reaction rate and fluorescent intensity (Figure 2.12). Therefore, with this further modified buffer condition (pH = 5, and 1 M NaCl), probe-**2** can serve as a detection tool for Hg^{2+}.
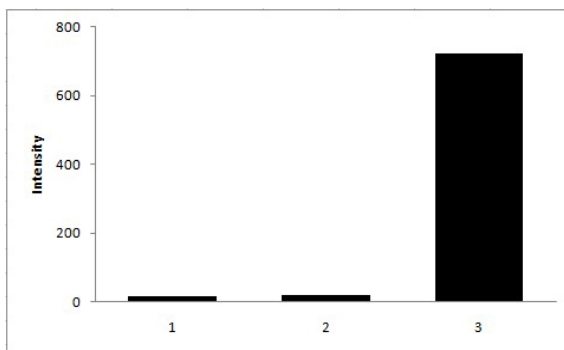
Figure 2.12 1. 1µM probe-**2** with 1M NaCl; 2. To a solution of 1 was added 10µM Ag$^+$; 3. To a solution of 2 was added 10µM Hg^{2+}.

2.3.4 Summary

In this work, we have designed and synthesized a novel fluorescent probe for Hg^{2+}. It displayed excellent sensitivity and selectivity with ppb level detection limit in a buffer solution at pH 5 with 1 M NaCl. Good linear performance made it suitable for quantitative analysis. The studies made it very promising to be put into practical application.

2.4 Experiment Section

2.4.1 Experiment Data for Probe-1

General Information: Commercial reagents were used as received, unless otherwise stated. Merck 60 silica gel was used for chromatography, and Whatman silica gel plates with fluorescence F_{254} were used for thin-layer chromatography (TLC) analysis. ^{1}H and ^{13}C NMR spectra were recorded on Bruker tardis (sb300). Data for ^{1}H are reported as follows: chemical shift (ppm), and multiplicity (s = singlet, d = doublet, t = triplet, q = quartet, m = multiplet). Data for ^{13}C NMR are reported as ppm.

Spectroscopic materials and methods: Millipore water was used to prepare all aqueous solutions. The pH was recorded by a Beckman Φ^{TM} 240 pH me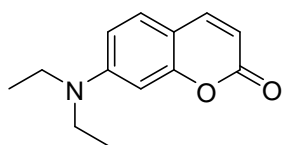ter. UV absorption spectra were recorded on a Shimadzu UV-2410PC UV-Vis spectrophotometer. Fluorescence emission spectra were obtained on a SHIMADZU spectrofluorophotometer RF-5301pc. Cell imaging experiments were carried out by Zeiss LSM510 META Confocal Microscope.

**Synthesis of ratiometric Hg^{2+} probe-1**


7-Diethylaminocoumarin (1a)

To a solution of 4-diethylaminosalicylaldehyde (2 g, 10.35 mM) in 30 mL EtOH was added piperidine (1 mL, 10.12 mM) and diethylmalonate (3.1 mL, 20.32 mM), then heated to reflux and stirred for 6 hours. EtOH was evaporated under reduced pressure, then concentrated HCl (20 mL) and acetic acid (30 mL) was added. The mixture was

heated to reflux and stirred for 24 hours. The solution was cooled to room temperature, and adjusted to be basic by 40% aq. NaOH, and large amount of precipitate was formed and filtered. The crude product was further purified by column chromatograph and obtained as a yellow solid (1.54g, 68%). ^{1}H NMR (CDCl$_3$): δ 7.52(d, J = 9.3Hz, 1H), 7.23(d, J = 8.7Hz, 1H), 6.55(dd, J = 8.7Hz, 2.4Hz, 1H), 6.47(d, J = 2.4Hz, 1H), 6.02(d, J = 9.3Hz, 1H), 3.40(q, J = 4.9Hz, 4H), 1.20(t, J = 6.9Hz, 6H). ^{13}C NMR (300MHz, CDCl$_3$): δ 162.27, 156.74, 150.68, 143.69, 128.76, 109.16, 108.65, 108.26, 97.51, 44.78, 12.43.
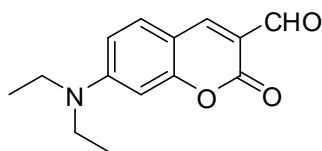
7-(Diethylamino)-2-oxo-2H-chromene-3-carbaldehyde (1b)

DMF (2 mL, 25.83 mM) was added dropwise to POCl$_3$ (2 mL, 21.46 mM) at room temperature, and stirred for 30 min. This solution was combined with a solution of compound 1a (650 mg, 2.99 mM) in 8mL DMF. The mixture was heated to 60°C, and stirred for 15 hours. After cooled to room temperature, the mixture was poured into 50mL ice water, and pH was adjusted to neutral, and large amount of solid was precipitated. The product was filtered, washed with H$_2$O, dried with oil pump, and obtained as a yellow solid (475mg, 64.8%). ^{1}H NMR (CDCl$_3$): δ 10.12(s, 1H), 8.24(s, 1H), 7.40(d, J = 9.0Hz, 1H), 6.63(d, J = 9.0Hz, 1H), 6.48(s, 1H), 3.47(q, J = 7.1Hz, 4H), 1.25(t, J = 7.1Hz, 6H). ^{13}C NMR (300MHz, CDCl$_3$): δ 187.94, 161.88, 158.94, 153.46, 145.36, 132.51, 114.34, 110.17, 108.24, 97.12, 45.28, 12.45.
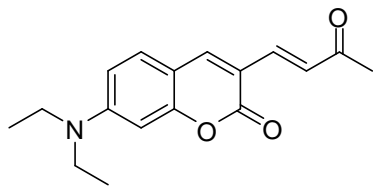
(E)-7-(Diethylamino)-3-(3-oxobut-1-enyl)-2H-chromen-2-one (1c)

To a solution of compound 1b (43 mg, 0.18 mM) in 5mL CH_2Cl_2 (1:1) was added acetone (19 µL, 0.26 mM) and 1 drop of pyrrolidine. The mixture was stirred at room temperature overnight. The product was purified through column chromatograph and obtained as a yellow solid (9 mg, 18%). ^{1}H NMR (CDCl$_3$): δ 7.77(s, 1H), 7.46(d, J = 15.9Hz, 1H), 7.31(d, J = 9.0Hz, 1H), 7.13(d, J = 15.9Hz, 1H), 6.61(d, J = 9.0Hz, 1H), 6.49(s, 1H), 3.44(q, J = 7.1Hz, 4H), 2.35(s, 3H) 1.23(t, J = 6.9Hz, 6H). ^{13}C NMR (300MHz, CDCl$_3$): δ 198.82, 160.46, 156.75, 151.94, 144.11, 137.80, 129.97, 127.12, 114.54, 109.51, 108.76, 97.00, 45.04, 28.36, 12.46.
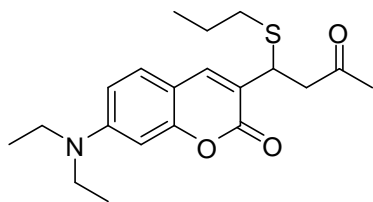
Ratiometric Hg^{2+}Probe-1

To a solution of compound 1c (9 mg, 0.03 mM) in 5 mL CH_2Cl_2 was added propanethiol (12 µL, 0.13 mM) and one drop of pyrrolidine. The mixture was stirred at room temperature for 24 hours. The product was purified through column chromatograph and obtained as a yellow liquid (4 mg, 35%). ^{1}H NMR (CDCl$_3$): δ 7.63(s, 1H), 7.27(d, J = 8.7Hz, 1H), 6.57(dd, J = 8.7Hz, 2.4Hz, 1H), 6.49(d, J = 2.4Hz, 1H), 4.33(t, J = 7.2Hz, 1H), 3.41(q, J = 7.1, 4H), 3.14(dd, J = 16.8Hz, 6.9Hz, 1H), 2.96(dd, J = 16.8Hz, 7.5Hz,

1H), 2.48(m, 2H), 2.17(s, 3H), 1.59(m, 2H), 1.20(t, J = 7.2, 6H), 0.94(t, J = 7.4Hz, 3H). ^{13}C NMR (300MHz, CDCl$_3$): δ 205.80, 161.57, 155.87, 150.43, 140.24, 128.77, 121.01, 108.85, 108.30, 97.16, 48.18, 44.83, 40.55, 34.32, 30.17, 22.66, 13.53, 12.42.

Imaging of C8D1A astrocyte cell line incubated with Probe and Hg^{2+}

a. Cell incubation

C8D1A cells (mouse astrocyte cell line) were seeded on micro cover glasses (VWR, USA) in 6-well plate at a density of 5×10^3 cells per well in DMEM culture media (Invitrogen, USA) with 10% fetal bovine serum (Invitrogen, USA). After 24 h, growth medium was discarded and the cells were washed four times with PBS. Probe was stored as a 1mM stock solution at 4°C.

For control group, C8D1A cells were incubated with 5μM Probe in PBS for 30 min at 37°C, then washed with PBS three times. For Hg^{2+} imaging, cover glasses were incubated with a solution of 5 μM Probe (or 5μM Hg^{2+}) in PBS for 30 min at 37°C. Afterwards, PBS was used to remove the remaining probe (or Hg^{2+}) by washing three times; the cells were further treated with 5μM Hg^{2+} (or 5μM probe) in PBS for 30 min, then washed with PBS three times.

b. Confocal Imaging

The fluorescence measurements of C8D1A cells were performed by live cell confocal imaging by Zeiss LSM510 META Confocal Microscope with a 63× objective. Fluorophores were excited by using a 405 nm laser diode, and emissions were obtained at double channels, 475 – 525nm and 530 – 600 nm. Images were acquired with the Zeiss LSM software.

2.4.2 Experiment Data for Probe-2

General Information: Commercial reagents were used as received, unless otherwise stated. Merck 60 silica gel was used for chromatography, and Whatman silica gel plates with fluorescence F_{254} were used for thin-layer chromatography (TLC) analysis. ^1H and ^{13}C NMR spectra were recorded on Bruker tardis (sb300). Data for ^1H are reported as follows: chemical shift (ppm), and multiplicity (s = singlet, d = doublet, t = triplet, q = quartet, m = multiplet). Data for ^{13}C NMR are reported as ppm.

Spectroscopic materials and methods: Millipore water was used to prepare all aqueous solutions. The pH was recorded by a Beckman Φ^{TM} 240 pH meter. UV absorption spectra were recorded on a Shimadzu UV-2410PC UV-Vis spectrophotometer. Fluorescence emission spectra were obtained on a Varian Eclipse fluorescence spectrophotometer.

Synthesis of probe-2
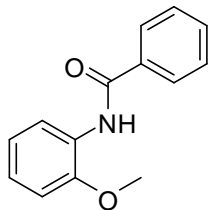
N-(2-Methoxyphenyl)benzamide (2a)

To a solution of o-Anisidine (200 µL, 1.77 mM) in 20mL CH_2Cl_2 was added TEA (300 µL, 2.15 mM) and benzoyl chloride (206 µL, 1.77 mM), then stirred at room temperature overnight. The reaction mixture was washed with H_2O (10 mL × 2) followed by brine (10 mL), then dried over Na_2SO_4. After evaporation of the solvent under reduced pressure, the produ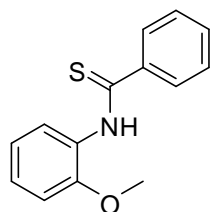ct was obtained as a yellow liquid (400 mg, 99%). ^{1}H NMR (CDCl$_3$): δ 8.54(dd, J = 7.8Hz, 1.8Hz, 2H), 7.92-7.89(m, 2H), 7.56-7.47(m, 3H), 7.10-7.02(m, 2H), 6.93(dd, J = 8.0Hz, 1.8Hz, 1H), 3.93(s, 3H). ^{13}C NMR (300MHz, CDCl$_3$): δ 165.26, 148.13, 135.37, 131.69, 128.76, 127.82, 127.07, 123.86, 121.24, 119.84, 109.92, 55.82.

N-(2-Methoxyphenyl)benzothioamide (2b)

To a solution of compound 2a (380 mg, 1.67 mM) in 10 mL toluene was added Lawesson's reagent (676 mg, 1.67 mM), then heated to 100°C, and stirred for 3 hours. The product was purified through column chromatograph and obtained as a yellow liquid (383mg, 94%). ^{1}H NMR (CDCl$_3$): δ 9.67(s, 1H), 9.17(d, J = 8.1Hz, 1H), 7.87(d, J = 6.9Hz, 2H), 7.53-7.42(m, 3H), 7.26-7.20(m, 1H), 7.09-6.97(m, 2H), 3.92(s, 3H). ^{13}C NMR (300MHz, CDCl$_3$): δ 196.08, 149.89, 144.09, 131.03, 128.66, 126.77, 126.59, 121.51, 120.39, 110.39, 56.00.
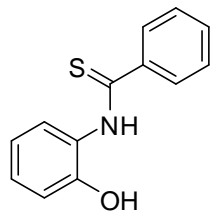
N-(2-Hydroxyphenyl)benzothioamide (probe-2)

To a solution of compound 2b (383 mg, 1.57 mM) in 5mL CH_2Cl_2 was added $AlCl_3$ (420 mg, 3.15 mM), then stirred at room temperature for 20 h. The product was purified through column chromatograph and obtained as a yellow solid (170mg, 47%). ^{1}H NMR ($CDCl_3$): δ 9.33(s, 1H), 7.89(d, J = 7.2Hz, 2H), 7.59-7.43(m, 4H), 7.32-7.26(m, 1H), 7.11-7.01(m, 2H), 6.34(s, 1H). ^{13}C NMR (300MHz, $CDCl_3$): δ 197.13, 149.25, 141.48, 131.93, 129.10, 128.80, 127.47, 127.00, 124.39, 121.62, 120.07.
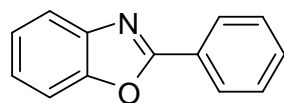
2-Phenylbenzo[d]oxazole (2c)

To a solution of probe-2 (20 mg, 0.09 mM) in MeOH/H_2O (4:1) was added $HgCl_2$ (30 mg, 0.11 mM), then stirred at room temperature for 3 h. The reaction mixture was filtered to remove solid, then concentrated under *vacuo*. The residue was dissolved in 10 mL CH_2Cl_2, and washed with 5mL H_2O, then dried with Na_2SO_4. The solvent was removed under *vacuo*, and the product was further dried with oil pump and obtained as a light yellow solid (16mg, 95%). ^{1}H NMR ($CDCl_3$): δ 8.28-8.25(m, 2H), 7.80-7.77(m, 1H), 7.61-7.51(m, 4H), 7.39-7.34(m, 2H). ^{13}C NMR (300MHz, $CDCl_3$): δ 163.06, 150.77, 142.08, 131.54, 128.92, 127.64, 127.16, 125.13, 124.60, 120.02, 110.61.

2.5 References

(1) Joshi, D.; Mittal, D. K.; Shukla, S. *Toxicol. Lett.* **2011**, *205*, S127.

(2) Khangarot, B. S.; Das, S. *J. Hazard. Mater.* **2009**, *161*, 68.

(3) Arias-Almeida, J. C.; Rico-Martinez, R. *Bull. Environ. Contam. Toxicol.* **2011**, *87*, 138.

(4) Clarkson, T. W.; Magos, L.; Myers, G. J. *N. Engl. J. Med.* **2003**, *349*, 1731.

(5) Renzoni, A.; Zino, F.; Franchi, E. *Environ. Res.* **1998**, *77*, 68.

(6) Harris, H. H.; Pickering, I. J.; George, G. N. *Science* **2003**, *301*, 1203.

(7) Kim, H. N.; Ren, W. X.; Kim, J. S.; Yoon, J. *Chem. Soc. Rev.* **2012**, *41*, 3210.

(8) Nolan, E. M.; Lippard, S. J. *Chem. Rev.* **2008**, *108*, 3443.

(9) Coskun, A.; Akkaya, E. U. *J. Am. Chem. Soc.* **2006**, *128*, 14474.

(10) Nolan, E. M.; Lippard, S. J. *J. Mater. Chem.* **2005**, *15*, 2778.

(11) Kim, J. S.; Choi, M. G.; Song, K. C.; No, K. T.; Ahn, S.; Chang, S. K. *Org. Lett.* **2007**, *9*, 1129.

(12) Atilgan, S.; Ozdemir, T.; Akkaya, E. U. *Org. Lett.* **2010**, *12*, 4792.

(13) Nolan, E. M.; Lippard, S. J. *J. Am. Chem. Soc.* **2007**, *129*, 5910.

(14) Song, K. C.; Kim, J. S.; Park, S. M.; Chung, K. C.; Ahn, S.; Chang, S. K. *Org. Lett.* **2006**, *8*, 3413.

(15) Tian, M. Q.; Ihmels, H. *Chem. Commun.* **2009**, 3175.

(16) Wang, J. B.; Qian, X. H.; Cui, J. N. *J. Org. Chem.* **2006**, *71*, 4308.

(17) Wegner, S. V.; Okesli, A.; Chen, P.; He, C. A. *J. Am. Chem. Soc.* **2007**, *129*, 3474.

(18) Yang, M. H.; Thirupathi, P.; Lee, K. H. *Org. Lett.* **2011**, *13*, 5028.

(19) Zhang, X. L.; Xiao, Y.; Qian, X. H. *Angew. Chem. Int. Ed.* **2008**, *47*, 8025.

(20) Liu, B.; Tian, H. *Chem. Commun.* **2005**, 3156.

(21) Yuan, M. J.; Li, Y. L.; Li, J. B.; Li, C. H.; Liu, X. F.; Lv, J.; Xu, J. L.; Liu, H. B.; Wang, S.; Zhu, D. *Org. Lett.* **2007**, *9*, 2313.

(22) Neupane, L. N.; Kim, J. M.; Lohani, C. R.; Lee, K. H. *J. Mater. Chem.* **2012**, *22*, 4003.

(23) Valeur, B. *Molecular Fluorescence: Principles and Applications*; Wiley-VCH: Weinheim, 2002.

(24) Wang, B.; Anslyn, E. J. *Chemosensors: Principles, Strategies, and Applications*; John Wiley and Sons: New York, 2011.

(25) Jares-Erijman, E. A.; Jovin, T. M. *Nat. Biotech.* **2003**, *21*, 1387.

(26) *EPA, Office of Water: Washington, DC, 2001:The maximum contamination concentration of mercury in drinking water is 2 ppb (10 nM).*

(27) Jiang, W.; Wang, W. *Chem. Commun.* **2009**, *0*, 3913.

(28) Chae, M. Y.; Czarnik, A. W. *J. Am. Chem. Soc.* **1992**, *114*, 9704.

(29) Ko, S.-K.; Yang, Y.-K.; Tae, J.; Shin, I. *J. Am. Chem. Soc.* **2006**, *128*, 14150.

(30) Ros-Lis, J. V.; Marcos, M. D.; Mártinez-Máñez, R.; Rurack, K.; Soto, J. *Angew. Chem. Int. Ed.* **2005**, *44*, 4405.

Chapter 3

A FRET-based Ratiometric Fluorescent Probe for Rapid Detection of Nerve Agent Stimulants

3.1 Background and Significance

Chemical warfare agents (CWAs) have posed a severe threat to public health and homeland security owing to their broad availability, easy operation and lethal toxicity. Among CWAs, organophosphorus-containing nerve agents (Scheme 3.1) are one of the biggest concerns due to their easy production and wide spread devastation ability. The toxicity of nerve agents arises from their ability to inhibit the activity of acetylcholinesterase (AChE), which is critical for the function of central nervous system.[1] The 1995 Tokyo subway Sarin terrorism attack resulting in 12 death and thousands of wounded was one of the recent incident using the highly toxic chemicals as weapons.

Scheme 3.1 Nerve agents and stimulants
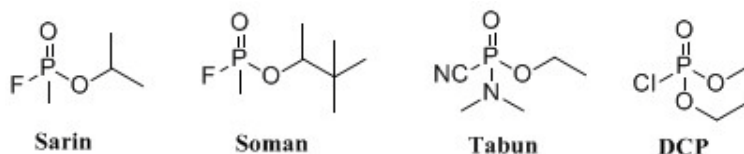
With the increasing concern of public safety and potential terror attack by using chemical weapons, the development of simple detection tactics for nerve agents is of considerable social, economical and scientific importance. Along this line, several methods have been developed for their detection, such as photoacoustics,[2] mass spectrometry,[3,4] capillary electropherograph,[5] electrical sensor,[6] and biosensors.[7] However, these methods usually require expensive instruments, complicated operation,

laborious sample preparation, while suffer from limited portability. These drawbacks make them less practical for easy and fast, and field-oriented detection of nerve agents.

In the past decade, small molecule based fluorescent, luminescent or chromogenic probes have emerged as a powerful tool to monitor nerve agents. To be a practical tool, a probe for nerve agents detection should possess a fast response and low detection limit. A colorimetric response is highly preferred to facilitate the sample analysis. Furthermore, a ratiometric signal pattern can provide a better opportunity for quantitative analysis with less background signal interference. More importantly, a vapor detection capability is in great demand due to the nerve agent vapor induced wide spread devastation. Up to now, many probes for nerve agents have been designed,[8-20] but none of them possess all the above desired merits (Scheme 3.2). To the best of our knowledge, a FRET- based fluorescent probe that can detect nerve agents with a fast, ratiometric, colorimetric and vapor-detective response is still not available.[21] Toward this end, we would like to report the first FRET-based ratiometric fluorescent probe for nerve agents with a fast and naked-eye observable response and excellent nerve agent vapor detection ability.

Scheme 3.2 Examples of some fluorescent/colorimetric probes for nerve agent stimulants
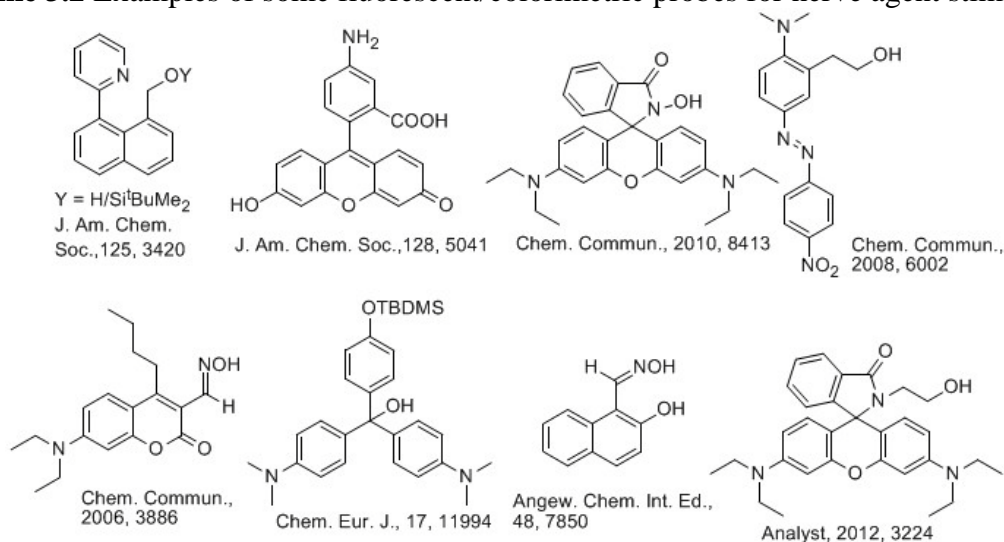
3.2 Probe Design

FRET is a widely used strategy for the design of ratiometric fluorescent probes because of its expectable fluorescence signal manner and broad permission of different design approaches. A new fluorophore called rhodol is designed by a combination of fluorophores of rhodamine and fluorescein (Scheme 3.3).[22] Such structure exist in two different conjugation forms - the fluorescent spirolactone ring opening form, and the nonfluorescent spirolactone ring closing form. We reasoned that, the rhodamine amine moiety can be used as handle to attach a FRET donor. The phenol moiety in fluorescein can serve as a reactive trigger to respond to nerve agents to form a covalent phosphate bond. It is expected that the reaction could result in the formation of spirolacone from the open precursor and thereby inducing both absorption and emission change.

Scheme 3.3 Rhodol and its conjugation structure

spirolactone ring opening
fluorescent

spirolactone ring closed
nonfluorescent
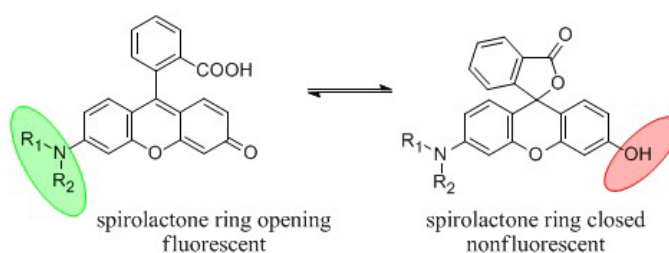
In the design, coumarin was chosen as a FRET donor and connected to rhodol through a rigid piperazine linker (Scheme 3.4). Because of its structure similarity and less toxicity, diethyl chlorophosphate (DCP, scheme 1) has been usually used as the nerve agent stimulant in studies. Without DCP, the rhodol was present in open form. It is expected that the FRET is in play - the energy transfer from coumarin to rhodol by

displaying a rhodol emission (536 nm) with a typical coumarin excitation wavelength (410 nm). However, in the presence of DCP, the phenol group of rhodol is caged, and leads to the formation of a stable spirolactone ring. Such transformation disrupts the rhodol conjugation system. The FRET should be switched off and therefore resulting in a blue shift in fluorescence emission from rhodol (536 nm) to coumarin (460 nm).

Scheme 3.4 Design of the FRET-based ratiometric probe for nerve agent stimulant

probe-3   detection product, 3g
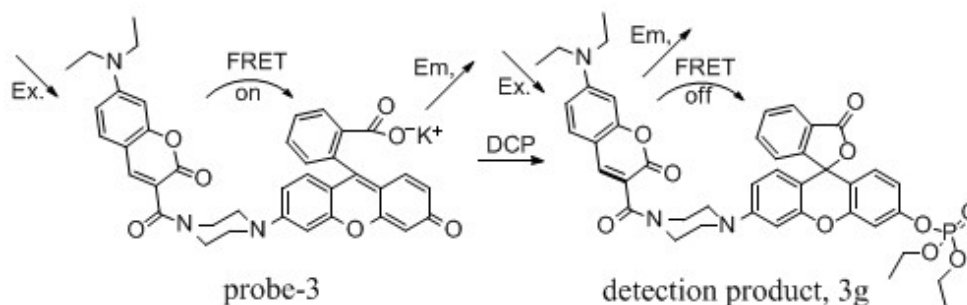
3.3 Synthesis of Probe-3

As shown in Scheme 3.5, coumarin carboxylic acid **3b** was obtained in 2 steps from 2-hydroxy-4-diethylaminebenzaldehyde. Rhodol **3e** was synthesized through two steps involving reaction of 3-hydroxyaniline with di(2-chloroethyl)amine followed by condensation with ketone **3d**. Coupling of 3b with 3d using EDC•HCl as activation agent gave a close spirolactone form **3f**, which is unexpected. However, treatment of **3f** in DMF with K_2CO_3 led to a dramatic emission shift from 460 nm to 536 nm (Figure 3.1). This arises from the formation of probe-**3** with concurrent opening of the lactone.
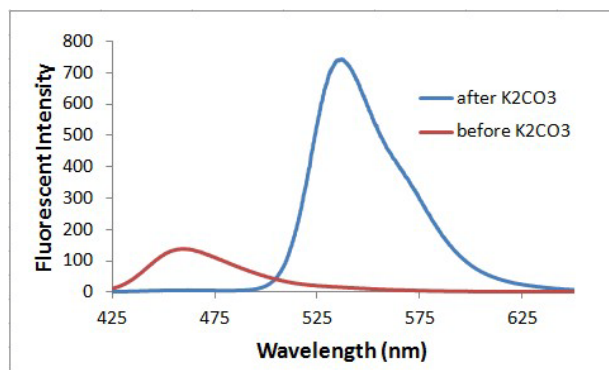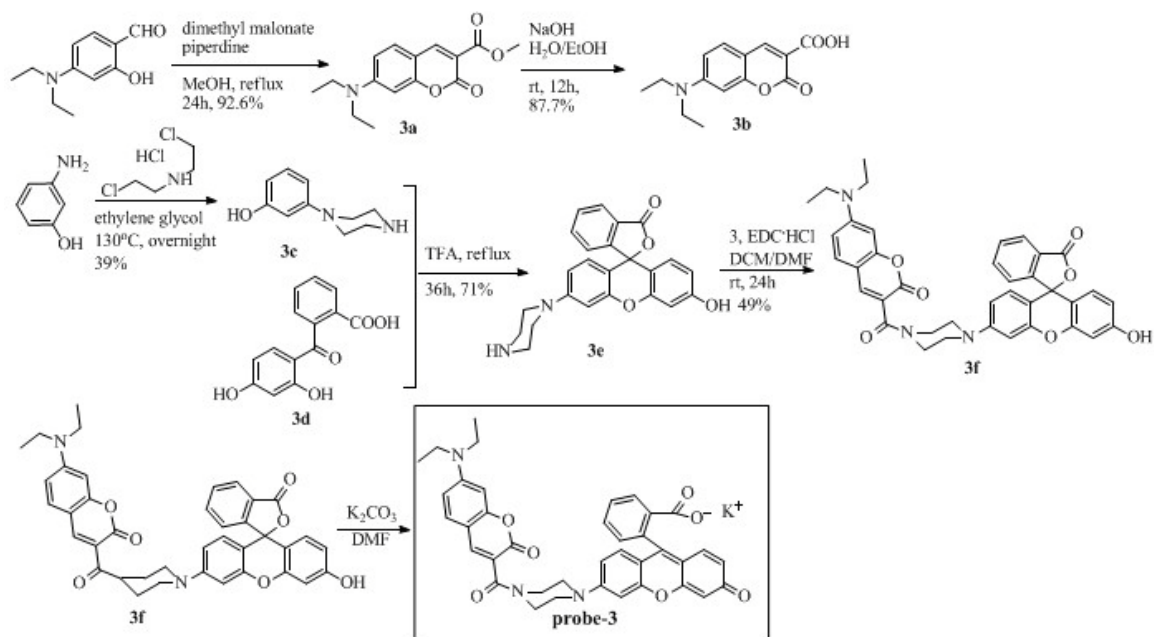
Scheme 3.5 Synthetic route for probe-**3**

Figure 3.1 Emission spectra change of 5 µM compound 3f before and after treatment with K_2CO_3 in DMF. The excitation was set at 410nm with slit/slit 5/1.5.

3.4 Probe-3 Evaluation with DCP in DMF

With the probe **3** in hand, we firstly tested its response to DCP. Upon addition of 100 µM DCP to 5 µM probe-**3** in DMF, an immediate color and fluorescent change was observed (Figure 3.2a). The largest emission wavelength was shifted from 536 nm (bright yellow) to 460 nm (blue), at the same time the solution color was changed from yellow to colorless. Surprisingly, all these occurred in 30s (Figure 3.2b). Obvious UV absorption change was observed (Figure 3.2c). The disappearance of rhodol absorption suggests the caging of the rodol phenol moiety and the loss of FRET energy transfer. The probe showed the absorption peaks of both coumarin and rhodol. However, upon the treatment with DCP, the rhodol absorption peak disappeared as a result of the formation of spirolactone ring. In the absent of DCP, the probe emission spectra stayed the same (Figure 3.3a). To exclude the possible influence from acids, the solution after addition of DCP was further treated with K_2CO_3, and no observable spectra change can be monitored (Figure 3.3b), suggesting the fluorescence change was exclusively and irreversibly caused by DCP. Finally, the formation of the proposed detection product (**3g**) was confirmed by mass spectrometer (M+H, 780.2659). These studies showed that the probe is suitable for fast detection of nerve agents with simple UV light or even naked eyes.
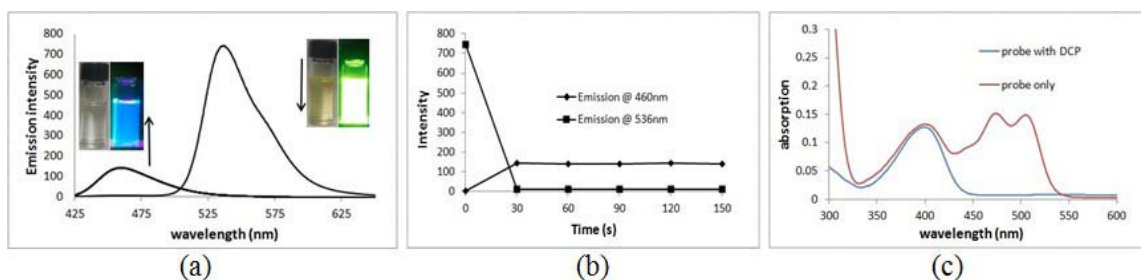

(a)　　　　　　　　　　(b)　　　　　　　　　　(c)

Figure 3.2 (a) To 5 µM probe-3 in DMF was added 100 µM DCP, the emission spectra was recorded every 30s in 150s. The inset picture showed the color change and the fluorescence change under UV lam; (b) The

52

fluorescence intensities at 460 and 536 nm vary in a time range of 150s; (c) The UV absorption of 5 µM probe-3 and 5 µM probe-3 treated with 100 µM DCP. The excitation was set at 410nm with slit/slit 5/1.5.

(a) (b)
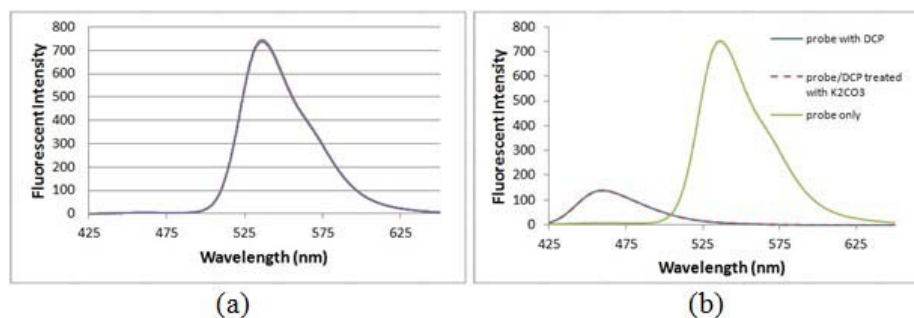
Figure 3.3 (a) The emission spectra of 5 µM probe-3 in DMF was recorded in 3 hours; (b) 5 µM probe-3 treated with 100 µM DCP was further added K_2CO_3.

Next, we investigated the response of this probe to different concentration of DCP in DMF. As shown in Figure 3.4, the response of probe-**3** to DCP is concentration-dependant. When 80 µM DCP was used, the highest fluorescence change was obtained, and the intensity ratio change (F_{460}/F_{536}) reached a plateau with a total enhancement of 1731 folds. According to the fluorescence increase at 460 nm or decrease at 536 nm, the FRET efficiency was calculated to be 96.0% - 98.6%. A clear isoemission point was observed at 504 nm. When as low as 1 µM (0.17 ppm) DCP was used, an obvious emission ratio change can also be detected, demonstrating a high detection limit.

(a) (b)
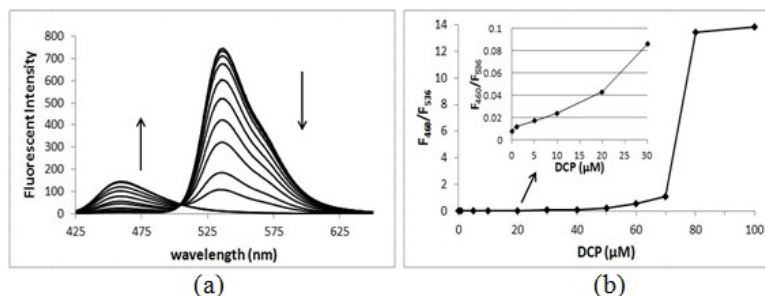
Figure 3.4 (a) To 5 µM probe-3 in DMF was added 0 - 100 µM DCP, the emission spectra was recorded in 1 minute after addition of DCP; (b) Fluorescence intensity ratio changes (F_{460}/F_{536}) of probe-3 at 5.0 µM upon addition of various concentrations of DCP. λ_{ex} = 410nm.

3.5 DCP Vapor Detection
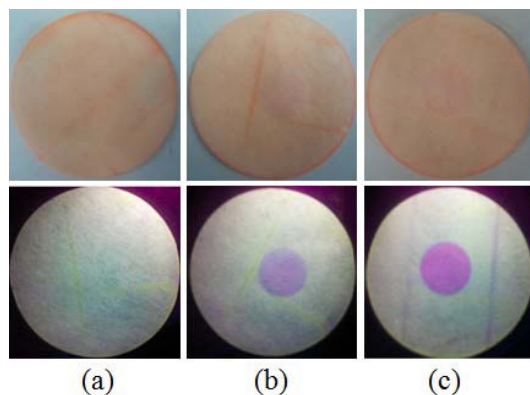
Figure 3.5 (a) Filter paper treated with 0.1 mg/mL probe-3 solution in MeOH in the presence of K_2CO_3; (b) Filter paper exposed to DCP vapor for 1 min; (c) Filter paper exposed to DCP vapor for 5 min. Pictures at the bottom was irradiated at 365 nm with a UV lamp. The FISHERbrand filter paper (09-795A) was used.

We also carried out studies with probe-**3** for detecting DCP in gaseous state. A pH paper was immersed in 0.1 mg/mL probe-**3** solution in MeOH in the presence of K_2CO_3, then dried in the air. The white filter paper became a little pink (Figure 3.5a). The probe-loaded filter paper was put across the top of a vial containing one drop of DCP for a defined exposure time. As shown, an obvious change under a UV hand lamp can be seen in one minute (Figure 3.5b), and an enhanced result can be obtained in a longer exposure time (5 minutes) (Figure 3.5c). Compared with the existing filter paper-based sensing method,[23] the difference induced by DCP in this new filter paper based method was naked eye observable (Figure 3.5c). As control, we also test the fresh filter paper to DCP vapor, and no difference was observed, suggesting the fluorescence/color change is indeed induced by probe-**3**. In short, this probe displayed great potential for the facile detection of nerve agent vapor.

3.6 Summary

In conclusion, the first FRET-based ratiometric fluorescent probe for nerve agent has been developed in this work. Fast response and obvious color change makes it very suitable for real time detection, and the easily made probe-loaded filter paper can be used to detect DCP vapor with a UV hand lamp or even naked eyes. All these together make this probe a very promising tool to detect nerve agents in practice.

3.7 Experimental Section

General Information: Commercial reagents were used as received, unless otherwise stated. Merck 60 silica gel was used for chromatography, and Whatman silica gel plates with fluorescence F_{254} were used for thin-layer chromatography (TLC) analysis. ^{1}H and ^{13}C NMR spectra were recorded on Bruker Avance 500 and Bruker tardis (sb300). Data for ^{1}H are reported as follows: chemical shift (ppm), and multiplicity (s = singlet, d = doublet, t = triplet, q = quartet, m = multiplet, br = broad). Data for ^{13}C NMR are reported as ppm.

Spectroscopic materials and methods: Fluorescence emission spectra were obtained on a SHIMADZU spectrofluorophotometer RF-5301pc. The UV absorption spectra were obtained on a SHIMADZU UV-1800.

Probe synthesis
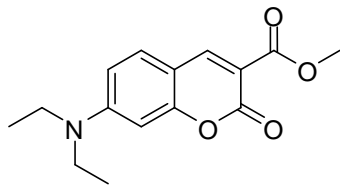
Methyl 7-(diethylamino)-2-oxo-2H-chromene-3-carboxylate (3a)

To a solution of 4-diethylaminosalicyl aldehyde (200 mg, 1.03 mmol) in 20 ml methanol was added dimethyl malonate (356 µL, 3.11 mmol) and piperidine (20 µL) at room temperature. The mixture was heated to reflux, and stirred for 24 hours. The solvent was evaporated under *vacuo.* The crude 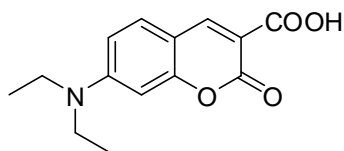product was purified by silica gel chromatography to afford 2 as yellow liquid (264mg, 92.6%). ^{1}H NMR (500MHz, CDCl$_3$): δ8.46(s, 1H), 7.36(d, 1H, J = 9.0Hz), 6.60(d, 1H, J = 8.5Hz), 6.46(s, 1H), 3.91(s, 3H), 3.44 (q, 4H, J = 7.0Hz), 1.23(t, 6H, J = 7.0Hz); ^{13}C NMR (300MHz, CDCl$_3$): δ 165.02, 158.54, 158.33, 152.96, 149.66, 131.11, 109.58, 108.54, 107.72, 96.70, 52.33, 45.12, 12.41.

7-(Diethylamino)-2-oxo-2H-chromene-3-carboxylic acid (3b)

To a solution of 3a (48 mg, 0.17 mmol) in 5 mL ethanol was added 3 mL 0.5 M aqueous NaOH solution. The mixture was stirred at room temperature for 12 hours. The solvent was evaporated in *vacuo.* 5mL H$_2$O was added to dissolve the residue, then pH was adjusted to acidic by 1 M aqueous HCl solution. The mixture was extracted by CH$_2$Cl$_2$ (10mL× 3). The combined layer was dried with sodium sulfate, filtered and evaporated under *vacuo* to afford 3 as orange red solid(40mg, 87.7%). ^{1}H NMR (300 MHz, CDCl$_3$): δ 8.65(s, 1H), 7.45(d, 1H, J = 9.0Hz), 6.70(dd, 1H, J = 1.8Hz, 8.7Hz), 6.52(d, 1H, J = 1.5Hz), 3.49(q, 4H, J = 7.1Hz), 1.26 (t, 6H, J = 7.1Hz); ^{13}C NMR (300 MHz, CDCl$_3$): δ 165.39, 164.30, 157.88, 153.65, 150.05, 131.80, 110.82, 108.37, 105.28, 96.65, 45.22, 12.25.
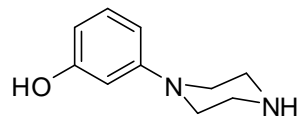
3-(Piperazin-1-yl)phenol (3c)

To a solution of 3-aminophenol (1g, 9.16mM) in 20 mL ethylene glycol was added bis(2-chloroethyl)amine hydrochloride (1.63g, 9.13mM), then the solution was heated to 130°C and stirred under the atmosphere of Ar overnight. After the solution was cooled to room temperature, 40 mL H_2O was added, and the pH was adjusted to 10 by 1 M NaOH. The product was extracted by EtOAc (100 mL × 5), dried over Na_2SO_4. The EtOAc was removed by rotavapor, and the crude product was further washed with 5 mL CH_2Cl_2. The final product was obtained as a white solid (640 mg, 39%). ^{1}H NMR (300 MHz, MeOD): δ 7.03(t, 1H, J = 8.1Hz), 6.45(dd, 1H, J = 1.8Hz, 8.4Hz), 6.39 (t, 1H, J = 2.1Hz), 6.30 (dd, 1H, J = 2.1Hz, 8.4Hz), 3.07(t, 4H, J = 2.7Hz), 2.95 (t, 4H, J = 2.7Hz); ^{13}C NMR (300 MHz, MeOD): δ 159.22, 154.63, 130.75, 109.21, 108.40, 104.69, 51.30, 46.48.
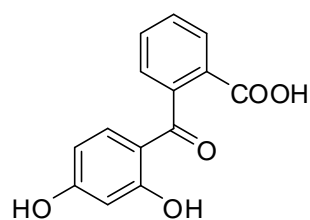
2-(2,4-Dihydroxybenzoyl)benzoic acid (3d) was synthesized according to the reported method.[24]
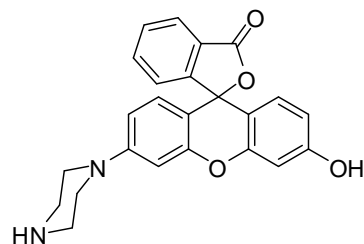
3'-Hydroxy-6'-(piperazin-1-yl)-3H-spiro[isobenzofuran-1,9'-xanthen]-3-one (3e)

To compound 3d (1.74 g, 6.74 mM) in 20 mL TFA was added compound 3c (1 g, 5.61 mM), then heated to reflux and stirred for 36 h. The solvent was removed by rotavapor, and the left residue was dissolved in 30 mL H_2O. The crude product was extracted with EtOAc (40 mL × 3), and dried with Na_2SO_4. The product was further purified by column chromatograph, and obtained as a red solid (1.6g, 71%). ^{1}H NMR (300 MHz, D-acetone): δ 7.97(dd, 1H, J = 1.2, 7.1Hz), 7.77-7.65(m 2H), 7.20 (dd, 1H, J =1.2Hz, 7.5Hz), 6.83-6.73(m, 3H), 6.66-6.61(m, 3H), 3.64-3.60 (m, 4H), 3.49-3.45(m, 4H); ^{13}C NMR (300 MHz, D-acetone): δ 169.65, 161.96, 161.51, 153.65, 153.31, 153.19, 152.75, 135.95, 130.63, 129.87, 129.58, 127.69, 125.32, 124.81, 119.77, 115.88, 113.36, 113.09, 111.26, 111.13, 103.35, 103.21, 84.34, 63.92, 54.86, 45.97, 43.85.
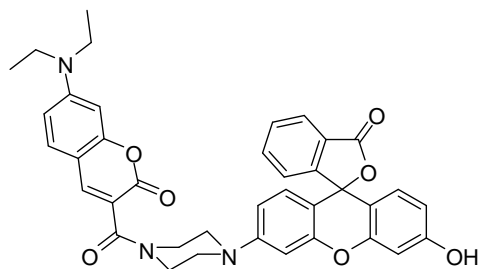
3'-(4-(7-(Diethylamino)-2-oxo-2H-chromene-3-carbonyl)piperazin-1-yl)-6'-

hydroxy-3H-spiro[isobenzofuran-1,9'-xanthen]-3-one (3f)

To a solution of compound 3e (980 mg, 2.45 mM) in 30 mL DCM/DMF (5:1) was added compound 3b (640 mg, 2.45 mM) and EDC•HCl (563 mg, 2.94 mM), then stirred at room temperature for 24 h. The solvent was removed by rotavapor, then the product was purified through column chromatograph and obtain as a red solid (780mg, 49%). ^{1}H NMR (300 MHz, CDCl$_3$): δ 7.97(dd, 1H, J = 1.2, 6.6Hz), 7.88(s, 1H), 7.65-7.54(m, 2H), 7.27 (d, 1H, J = 8.7 Hz), 7.11 (d, 1H, J = 6.9 Hz), 6.74(d, 1H, J = 1.8 Hz),

6.65-6.52(m, 6H), 6.45(d, 1H, 2.1Hz), 3.87(br, 2H), 3.55(br, 2H), 3.41 (q, 4H, J = 7.2Hz), 3.29(br, 4H), 1.2(t, 6H, J = 7.2Hz); ^{13}C NMR (300 MHz, CDCl$_3$): δ 169.95, 165.44, 159.40, 157.36, 152.80, 152.70, 152.54, 151.95, 145.81, 134.80, 130.10, 129.59, 129.24, 128.91, 127.30, 125.10, 124.26, 115.21, 112.87, 112.26, 110.75, 109.97, 109.61, 107.75, 103.16, 102.39, 96.88, 48.47, 48.00, 46.94, 44.99, 42.14, 12.42.
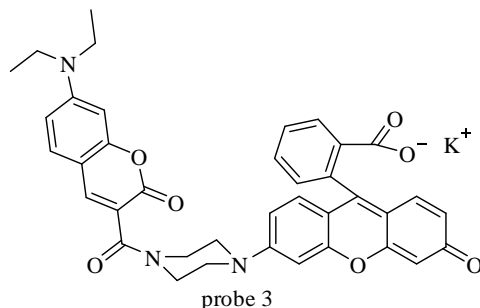
probe 3

Probe-3

The compound of **3f** was dissolved in DMF to make a 5 µM solution, then excessive K$_2$CO$_3$ was added and stirred for 1 h. The conversion was monitored by fluorescence shift and UV absorption change. When the fluorescence and UV spectra stayed the same for a while, the solid K$_2$CO$_3$ was filtered out to afford a 5 µM probe-3 solution in DMF.

3.8 References

(1) Marrs, T. C. *Pharmacology & therapeutics* **1993**, *58*, 51.

(2) Gurton, K. P.; Felton, M.; Tober, R. *Opt. Lett.* **2012**, *37*, 3474.

(3) Bao, Y.; Liu, Q.; Chen, J.; Lin, Y.; Wu, B. D.; Xie, J. W. *J. Chromatogr. A* **2012**, *1229*, 164.

(4) Zydel, F.; Smith, J. R.; Pagnotti, V. S.; Lawrence, R. J.; McEwen, C. N.; Capacio, B. R. *Drug Test. Anal.* **2012**, *4*, 308.

(5) Kuban, P.; Seiman, A.; Makarotseva, N.; Vaher, M.; Kaljurand, M. *J. Chromatogr. A* **2011**, *1218*, 2618.

(6) Simonato, J. P.; Clavaguera, S.; Carella, A.; Delalande, M.; Raoul, N.; Lenfant, S.; Vuillaume, D.; Dubois, E. In *Sensors & Their Applications Xvi*; Kyriacou, P. A., O'Riordan, A., McConnell, G., Eds.; Iop Publishing Ltd: Bristol, 2011; Vol. 307.

(7) Arduini, F.; Amine, A.; Moscone, D.; Palleschi, G. *Microchim. Acta* **2010**, *170*, 193.

(8) Royo, S.; Martinez-Manez, R.; Sancenon, F.; Costero, A. M.; Parra, M.; Gil, S. *Chem. Commun.* **2007**, 4839.

(9) Hewage, H. S.; Wallace, K. J.; Anslyn, E. V. *Chem. Commun.* **2007**, 3909.

(10) Costero, A. M.; Gil, S.; Parra, M.; Mancini, P. M. E.; Martinez-Manez, R.; Sancenon, F.; Royo, S. *Chem. Commun.* **2008**, 6002.

(11) Dale, T. J.; Rebek, J. *Angew. Chem. Int. Ed.* **2009**, *48*, 7850.

(12) Han, S.; Xue, Z.; Wang, Z.; Wen, T. B. *Chem. Commun.* **2010**, *46*, 8413.

(13) Shunmugam, R.; Tew, G. N. *Chem.-Eur. J.* **2008**, *14*, 5409.

(14) Royo, S.; Costero, A. M.; Parra, M.; Gil, S.; Martinez-Manez, R.; Sancenon, F. *Chem.-Eur. J.* **2011**, *17*, 6931.

(15) Nourmohammadian, F.; Wu, T. Q.; Branda, N. R. *Chem. Commun.* **2011**, *47*, 10954.

(16) Wu, X. J.; Wu, Z. S.; Han, S. F. *Chem. Commun.* **2011**, *47*, 11468.

(17) Gotor, R.; Costero, A. M.; Gil, S.; Parra, M.; Martinez-Manez, R.; Sancenon, F. *Chem.-Eur. J.* **2011**, *17*, 11994.

(18) Wu, Z.; Wu, X.; Yang, Y.; Wen, T.-b.; Han, S. *Bioorg. Med. Chem. Lett.* **2012**, *22*, 6358.

(19) Wu, W. H.; Dong, J. J.; Wang, X.; Li, J.; Sui, S. H.; Chen, G. Y.; Liu, J. W.; Zhang, M. *Analyst* **2012**, *137*, 3224.

(20) Sarkar, S.; Mondal, A.; Tiwari, A. K.; Shunmugam, R. *Chem. Commun.* **2012**, *48*, 4223.

(21) Zhang, S.-W.; Swager, T. M. *J. Am. Chem. Soc.* **2003**, *125*, 3420.

(22) Peng, T.; Yang, D. *Org. Lett.* **2010**, *12*, 496.

(23) Dale, T. J.; Rebek, J. *J. Am. Chem. Soc.* **2006**, *128*, 4500.

(24) Inouye, M.; Tsuchiya, K.; Kitao, T. *Angew. Chem. Int. Ed.* **1992**, *31*, 204.

Chapter 4

A New Method for H₂S Fluorescent Probe Design with Improved Sensitivity

4.1 Background and Significance

Despite its unpleasant smell and high toxicity, it cannot be denied the fact that hydrogen sulfide (H_2S) has emerged as the third endogenously produced gaseous signaling molecule besides nitric oxide (NO) and carbon monoxide (CO),[1-4] and it is present in various mammalian tissues.[5] Its biological functions have been gradually recognized in a number of biological and pathological processes, such as cardiovascular protection,[6,7] anti-oxidative effects,[8] cell growth regulation,[9] apoptosis,[10] and mediating O_2 sensing in the carotid body.[11] Recently, a study reveals that H_2S can sustain ATP production in mitochondria under hypoxic conditions.[12] On the other hand, the abnormal production of H_2S has been associated with dilemmas such as chronic kidney disease, liver cirrhosis, and Down's syndrome.[13,14] As a relatively new member of endogenously produced gaseous signaling molecules, there is a strong desire for biologists to fully understand its biological functions.[15-17] Therefore, right tools for its detection and measurement become important.

Traditional methods for H_2S detection including colorimetric,[18-20] electrochemical analysis,[21,22] gas chromatography[23,24] and sulfide precipitation[25] have been reported. As results of the nature of its high activity, volatility and flammability, and fast catabolism, a technique able to spatially and temporally monitor H_2S is more attractive. However, these above methods cannot meet the demand.

Recently several elegantly designed fluorescent imaging probes for H_2S have come into place.[26-36] They are developed by taking advantage of the strong reduction power,[27-29] nucleophilicity[30-33] and binding affinity with metals[34-36] of H_2S (scheme 4.1). For all these probes, the desired "off-on" in fluorescent intensity was obtained. However, their drawbacks have also been realized. The probes based on nucleophilic substitution have the possible interference from thiol-containing amino acids, such as cysteine and homocysteine;[30-33] the probes based on affinity with Cu^{2+} displayed excellent kinetics, but cell permeability and toxicity concern from Cu^{2+} was not negligible.[34-36] Although the probes based on H_2S reductive property are very promising, currently available probes based on azide-reduction exhibit limited sensitivity and/or requires high concentration of the probes (100-200 μM).[27-29] The H_2S concentration in blood is 10-100 μM[37-40] and living cells is in an even lower submicromolar range.[41] Therefore, highly sensitive fluorescent probes are still in demand. Towards this end, we would like to develop new fluorescent probes for H_2S which allows for the detection of H_2S in a submicromolar range and in cellular imaging with improved sensitivity.

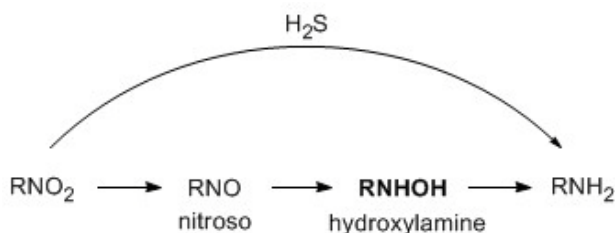**Scheme 4.1** Example of some typical H_2S fluorescent probes

R= tBuO or ⟨morpholine⟩N
J. Am. Chem. Soc., 133, 10078

Angew. Chem. Int. Ed., 50, 9672

Angew. Chem. Int. Ed., 50, 10327

Nat. Commun. 2011, 2.

J. Am. Chem. Soc., 133, 18003

Org. Lett., 2012, 2184
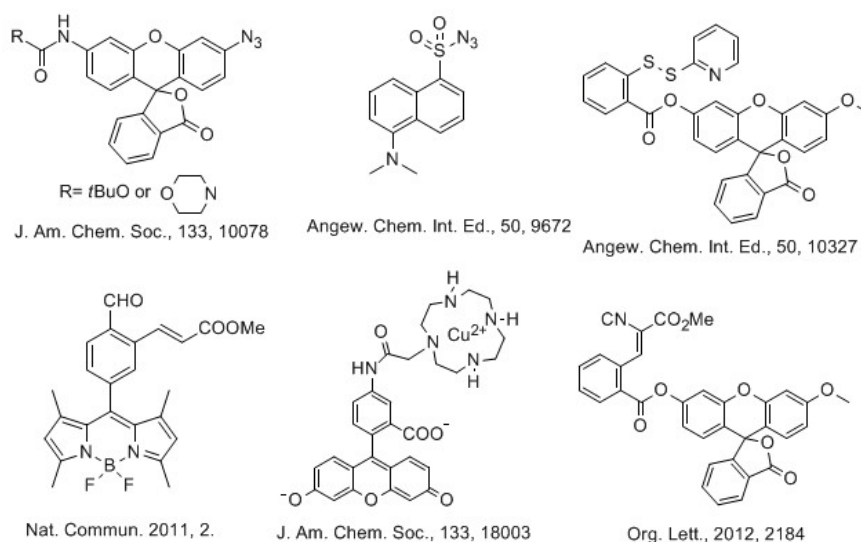
4.2 Probe Design (Probe-4)

A commonly used strategy in the development of fluorescent sensors in emission profile change is the manipulation of electronic features of substituents of a fluorophore through either intramolecular charge transfer (ICT) or photoinduced electron transfer (PET) pathways.[42,43] The PET strategy has been successfully used in the design of PET based fluorescent sensors because of predictable efficiency of the PET process. Nevertheless, the ICT type of fluorescent probes is relatively fewer, but it can afford highly sensitivity since it has a very low intrinsic fluorescence. One typical example is widely used non-fluorescent naphthalimide bearing a electron-withdrawing group (EWG) such as 7-nitro moiety due to two EWGs imide and 7-nitro in a "pull-pull" way, thus blocking the ICT process.[44] However, the conversion of the nitro group to an amine, an electron-donating group (EDG), leads to a dramatic fluorescence increase by changing to a "push-pull" system, hence allowing for the ICT process to restore. Based on the observation, we envisioned that incorporation of an EWG moiety into the naphthalimide fluorophore, which could specifically respond to H_2S to transform the EWG to an EDG, would lead to new fluorescent probe for H_2S. It should be noted that the naphthalimide is relatively non-toxic[45,46] and such favorable property allows it for study of biological systems.

Scheme 4.2 Nitro reduction process

$$RNO_2 \longrightarrow \underset{\text{nitroso}}{RNO} \longrightarrow \underset{\text{hydroxylamine}}{\textbf{RNHOH}} \longrightarrow RNH_2$$

(H₂S above the arc)

Inspired by the reported azide-based probe, we further investigated the reductive property of H_2S. It's known that Na_2S can reduce nitroaromatics to nitroamine.[47,48] However, harsh reaction conditions such as high temperature, organic solvent presence, or even microwave are generally used, suggesting that it may not be feasible for the design of a H_2S probe.[49] It is recognized that in the nitro reduction process, two key intermediates nitroso and hydroxylamine are produced (Scheme 4.2). Therefore, it is conceived that they may be more easily reduced than nitro moiety by H_2S under mild reaction conditions. This shall offer an opportunity to develop a novel sensitive fluorescent probe for H_2S. Considering more labile of nitroso functionality, we envisioned that the incorporation of the stable while electron-withdrawing hydroxylamine moiety into the naphthalimide may lead to a new fluorescent probe for H_2S (probe-**4**, Scheme 4.3). Probe-**4** should be weakly fluorescent due to the interference of ICT process. When treated with H_2S, the hydroxylamine can be easily reduced to an amine (4b), thereby strong fluorescence shall be produced.

Scheme 4.3 Design of H_2S "off-on" fluorescent probe based on reduction of hydroxylamine
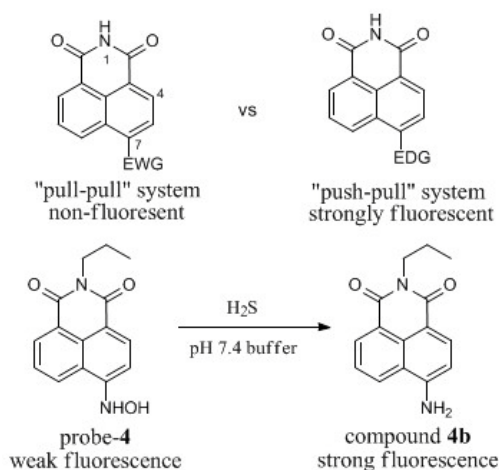
4.3 Preparation of Probe-4

The proposed probe-4 was easily prepared in a two-step synthetic route as shown in Scheme 4.4. From the commercially available 4-nitro-1,8-naphthalic anhydride, we synthesized its naphthalimide derivative (**4a**), then the nitro group was reduced to hydroxylamine by Zn and NH_4Cl at room temperature with a yield of 41%. The probe was characterized by NMR and ESI mass spectroscopy.

Scheme 4.4 Synthetic route of probe-4
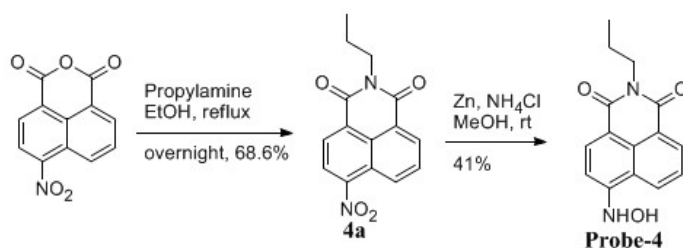
4.4 Probe-4 Evaluation in Buffer Solution

With the probe in hand, we first examined its fluorescence emission intensity. It was found that indeed it displayed weak fluorescence (λ_{max} = 387 nm, ε = 4000 $M^{-1}cm^{-1}$, Φ = 0.0095). Moreover, it is highly stable with a test in 0.1 M phosphate buffer solution at pH 7.4 (Figure 4.1). No decomposition was observed based on fluorescence emission study for at least 120 min. Then its specific response to H_2S was examined (Figure 4.2a). In the experiments, probe-4 at 2.0 µM was treated with 10.0 µM H_2S (Na_2S as supply source), and the emission was recorded over 180 min. To our delight, a remarkable fluorescence increase was observed at 544 nm with a more than 13-fold enhancement. The product 4b (λ_{max} = 435 nm, ε = 14500 $M^{-1}cm^{-1}$, Φ = 0.12) was separated and confirmed by NMR. This result verifies our working hypothesis, and the noticeable

absorbance change suggested the ICT mechanism (Figure 4.2b). The time at 120 min point is selected for the following studies.
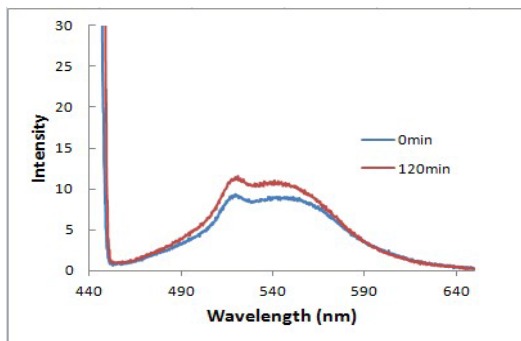
Figure 4.1 Probe-4 (2 µM) was incubated in 100mM pH 7.4 phosphate buffer solution for 120 min. λ_{ex} = 440 nm.
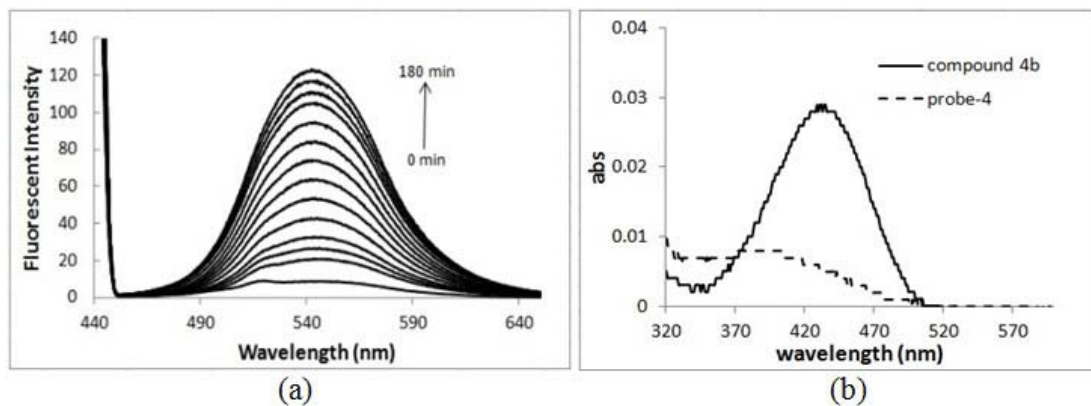
Figure 4.2 (a) Time profile of emission spectra of probe-4 toward Na_2S. To 2.0 µM probe-**4** in 0.1 M pH 7.4 phosphate buffer solution (containing 0.2% DMSO) was added 10.0 µM Na_2S (5.0 equiv.), and the emission was recorded at 0, 10, 20, 30, 45, 60, 75, 90, 105, 120, 135, 150, 165, 180 min, respectively, λ_{ex} = 440 nm; (b) Absorbance of probe-4 and compound 4b (2 µM respectively).
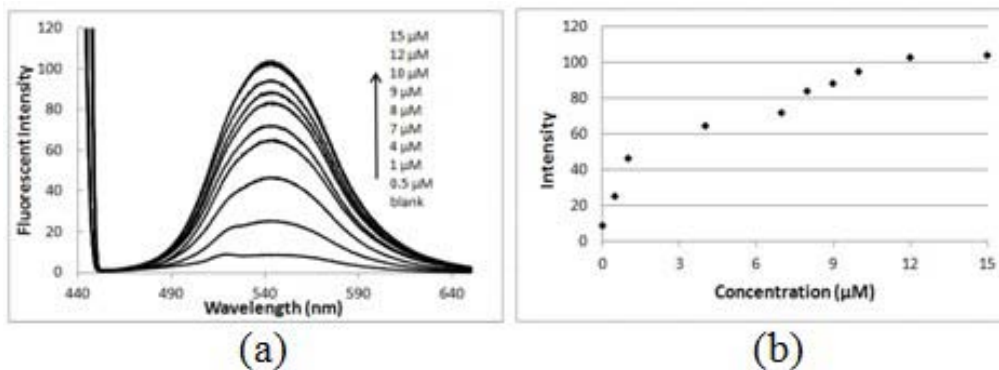
Figure 4.3 Emission spectra of probe-**4** with different concentrations of Na_2S. To 2.0 μM probe-**4** in 0.1 M pH 7.4 phosphate buffer solution (containing 0.2% DMSO) was added different concentrations of Na_2S. Data were recorded after 120 min, λ_{ex} = 440 nm. Fluorescent intensity for Figure b is taken at λ_{em} = 544 nm.

Next, we investigated the sensitivity of probe-**4** toward H_2S and other species. The probe with 2 μM concentration was used to determine the sensitivity of H_2S at different concentrations. As shown in Figure 4.3, the increase in fluorescence intensity is in a concentration dependent manner. With the concentration of H_2S at 10.0 μM (5.0 equiv.), the highest fluorescence is reached without further increase (Figure 4.3b). Compared with the existing fluorescent probes, this probe is impressively sensitive, requiring 5.0 equiv. of H_2S. Furthermore, notably the probe could detect H_2S at a concentration as low as 0.5 μM, while a still pronounced (3 folds) fluorescence enhancement was observed. To our knowledge, few probes are able to detect H_2S at a submicromolar range among available sensors.[29,35,36]
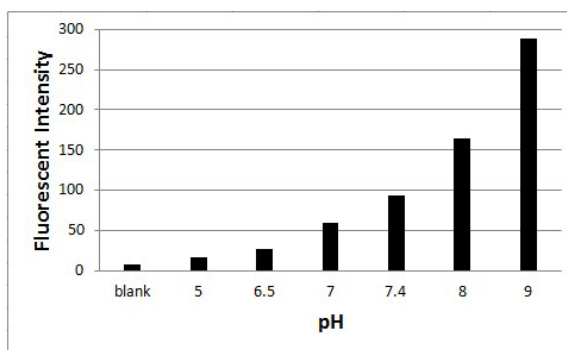
Figure 4.4 The effect of medium pH on probe-**4** toward H_2S. Fluorescence intensity was recorded at 120 min when probe **4** (2.0 μM) reacted with Na_2S (10.0 μM) in 0.1 M phosphate buffer (containing 0.2% DMSO). λ_{ex} = 440 nm, fluorescent intensity is taken at λ_{em} = 544 nm.

The pH effect of the probe was carried out next. As expected, the probe-4 responded to H_2S in a faster pace at a higher pH due to the stronger reducing power of S^{2-} (Figure 4.4). For example, the detection rate at pH 9 is almost two folds faster than that at pH 7.4 within 120 min under the same reaction conditions based on fluorescence intensity signal.

Moreover, we found that probe-4 displayed quicker response than the reported nitro-reduction probe HSN1[49] under the same reaction conditions because the hydroxylamine moiety is more easily reduced than the nitro group (Figure 4.5). This suggests that reduction of hydroxylamine is a better method for probe design using ICT strategy.

Figure 4.5 Probe-**4** (2 µM) or HSN1 was treated with 10 µM Na$_2$S in 100 mM pH 7.4 phosphate buffer solution at room temperature (25 ^{o}C). The fluorescence was recorded at 544nm with an excitation at 440nm.
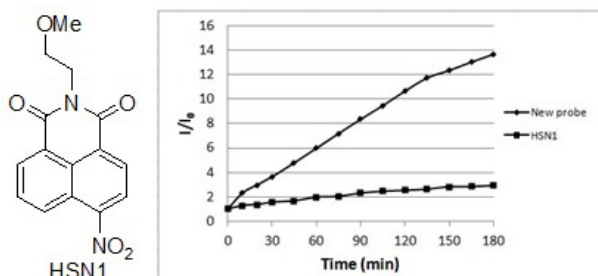
To the best of our knowledge, there is no report on the reduction mechanism of hydroxylamine by hydrogen sulfide, so here a possible mechanism was proposed (Figure 4.6). Based on this hypothesis, HS$^-$ would induce the cleavage of N-O bond in hydroxylamine with the formation of sulphur-substituted hydroxylamine, which should be the rate determining step. The sulfur-substituted hydroxylamine should be very unstable, and will decompose to the desired amine immediately. In this proposed mechanism, only one equiv. of H$_2$S is needed to convert hydroxylamine to amine, providing a good explanation for its excellent sensitivity.
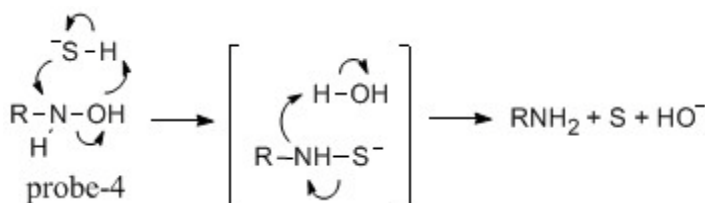
Figure 4.6 A possible mechanism for the reduction of hydroxylamine to amine by H$_2$S.

Another important issue for a sensor is selectivity. Impressively, the probe-4 exhibits high specificity towards H$_2$S (Figure 4.7a). Even 500 equiv. of other biological thiols such as cysteine and glutathione, which could potentially react with the probe-4, cannot induce fluorescence change; 25 equiv. of NADH can only lead to slight fluorescence increase. In addition, biologically related cations in a large excessive amount (50 equiv.) such as Ca^{2+}, Cu^{2+}, Fe^{3+}, Mg^{2+}, Zn^{2+} also failed to enhance fluorescence; reactive oxygen species (ROS), such as H$_2$O$_2$, NaOCl, and O$_2$$^{\bullet-}$ with 100.0

equiv., did not interfere with the detection either. Also, we screened other potential reductants (Figure 4.7b). Although fluorescence enhancement was observed with $Na_2S_2O_3$, sodium ascorbate, and thioacetic acid, they don't pose a severe concern due to their biological absence or obvious fluorescent maximum emission wavelength difference compared to H_2S. Taken together, the probe displayed excellent selectivity over other biological species.

Figure 4.7 (a) The response of 2.0 µM probe-4 to different analytes in 120 min ($\lambda_{ex} = 440$ nm). H_2S at 10.0 µM; cys and GSH at 1.0 mM; NADH at 50 µM; cations at 100.0 µM; reactive oxygen species at 200.0 µM; (b) 2.0 µM probe-4 was treated with 50 µM different compounds above respectively for 2 h.

4.5 Living Cell Imaging

To demonstrate the potential of the biological utility of the probe-4, we performed the studies of detection of H_2S in living cells. Astrocyte cells were incubated with 0, 10, 20 µM Na_2S for 1 h, then further incubated with 2.0 µM probe-4 for another 2.5 h. As shown in Figure 4.8, without Na_2S, as expected, the cell displayed very weak fluorescence (Figure 4.8a). With 10.0 µM Na_2S, notable fluorescence enhancement was observed (Figure 4.8b); while at 20.0 µM Na_2S, obvious fluorescence enhancement was

observed (Figure 4.8c). It is still very rare that a H_2S probe can respond to such low concentration H_2S (≤ 10 µM) in living cells. Also in the experiment process, no obvious cytotoxicity was observed. Therefore, we can conclude that this probe is suitable for H_2S detection in living cells.

Figure 4.8 Fluorescence images of astrocyte cells (a mouse astrocyte cell line) with H_2S using Olympus IX71 fluorescence microscopy. Astrocyte cells were first incubated with (a) 0.0µM Na_2S; (b) 10.0µM Na_2S; (c) 20.0 µM Na_2S for 1 h, then further incubated with 2.0µM probe-4 for 2.5 h respectively.

4.6 Summary

In conclusion, with recognition of the biological significance of emerging endogenously produced gaseous signaling molecule H_2S, we have developed a new highly sensitive and selective fluorescent probe for H_2S. The probe is designed based on the selective reduction of hydroxylamine to amine by H_2S, which subsequently alters the fluorescent emission property in a desired "off-on" fashion through an ICT pathway. Notably, it displays excellent selectivity and sensitivity toward H_2S at submicromolar concentration. Moreover, its impressive ability for detection of H_2S at low concentrations (10-20 µM) in cells renders it an attractive tool for H_2S study in biological system. However, its slow kinetics is also realized. Therefore future endeavor is being made to shorten response time toward H_2S, and the results will be introduced in due course.

4.7 Experimental Section

General Information: Commercial reagents were used as received, unless otherwise stated. Merck 60 silica gel was used for chromatography, and Whatman silica gel plates with fluorescence F_{254} were used for thin-layer chromatography (TLC) analysis. ^1H and ^{13}C NMR spectra were recorded on Bruker tardis (sb300) and Bruker Avance 500. Data for ^1H are reported as follows: chemical shift (ppm), and multiplicity (s = singlet, d = doublet, t = triplet, q = quartet, m = multiplet). Data for ^{13}C NMR are reported as ppm.

Spectroscopic materials and methods: Millipore water was used to prepare all aqueous solutions. The pH was recorded by a Beckman Φ^{TM} 240 pH meter. UV absorption spectra were recorded on a Shimadzu UV-2410PC UV-Vis spectrophotometer. Fluorescence emission spectra were obtained on a SHIMADZU spectrofluorophotometer RF-5301pc. Cell imaging experiments were carried out by Olympus IX71 fluorescence microscopy.
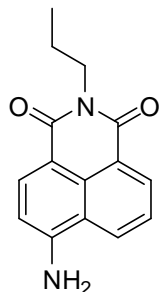
Probe synthesis

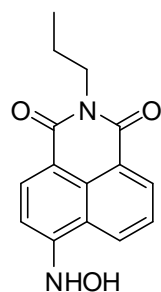### *6-Nitro-2-propyl-1H-benzo[de]isoquinoline-1,3(2H)-dione (4a)*

To 4-nitro-1,8-naphthalic anhydride (300 mg, 1.23 mmol) in 20 mL of EtOH was added propylamine (203 µL, 2.46 mmol), then heated to reflux and stirred overnight. The solvent was removed by rotavapor, then the product was purified through column

chromatograph, and obtained as straw yellow solid (240 mg, 69%). ^{1}H NMR (CDCl$_3$): δ 8.72 (d, J = 8.5 Hz, 1H), 8.63 (d, J = 7.5 Hz, 1H), 8.59 (d, J = 8.0 Hz, 1H), 8.32 (d, J = 8.0 Hz, 1H), 7.91 (t, J = 8.0 Hz, 1H), 4.08 (t, J = 7.5 Hz, 2H), 1.75-1.68 (m, 2H), 0.98 (t, J = 7.5 Hz, 3H),. ^{13}C NMR (500 MHz, CDCl$_3$): δ 156.06, 155.24, 142,29, 125.18, 122.76, 122.58, 122.03, 121.81, 119.80, 116.75, 116.40, 115.82, 35.19, 14.18, 4.38.

6-Amino-2-propyl-1H-benzo[de]isoquinoline-1,3(2H)-dione (4b)

To a solution of compound 4a (240 mg, 0.84 mmol) in 10 mL MeOH was added SnCl$_2$ (960 mg, 5.06 mmol) followed 2 mL conc. HCl. The mixture was stirred at room temperature for 2 hours. The solvent was removed under rotavapor, then 20 mL H$_2$O was added, and the pH was adjust to basic by aq. NaOH (2 M). The product was extracted with DCM (30 mL × 3), dried over Na$_2$SO$_4$, further purified through column chromatograph and obtained as yellow solid (108 mg, 50.3%).^{1}H NMR (CDCl$_3$): δ 8.60 (d, J = 6.9 Hz, 1H), 8.41 (d, J = 8.1 Hz, 1H), 8.10 (d, J = 8.4 Hz, 1H), 7.65 (t, J = 8.4 Hz, 1H), 6.88 (d, J = 8.1 Hz, 1H), 4.95 (s, 2H), 4.13 (t, J = 7.5 Hz, 2H), 1.82-1.69(m, 2H), 1.00 (t, J = 7.4 Hz, 3H),. ^{13}C NMR (500 MHz, CDCl$_3$ with 2 drops of CD$_3$OD): δ.164.70, 164.18, 149.41, 133.83, 131.45, 129.77, 127.01, 124.83, 122.95, 119.96, 111.70, 109.34, 41.69, 21.37, 11.47.

6-(Hydroxyamino)-2-propyl-1H-benzo[de]isoquinoline-1,3(2H)-dione (probe-4)

To a solution of 4a (62 mg, 0.22 mmol) in 10 mL MeOH was added Zinc powder

(32 mg, 0.49 mmol) and NH_4Cl (14 mg, 0.26 mmol), then stirred at room temperature for

1 h. Another 10 mL CH_2Cl_2 and 10 mL of MeOH was added, the solid was removed by

filtration, then the solvent was removed by rotavapor. The product was purified through

column chromatograph, and obtained as yellow solid (24mg, 41%). ^{1}H NMR (DMSO-d_6):

δ 10.46 (s, 1H), 9.31 (s, 1H), 8.43-8.40 (m, 2H), 8.33 (d, J = 8.4 Hz, 1H), 7.68(t, J = 8.0

Hz, 1H), 7.19 (d, J = 8.4 Hz, 1H), 3.96 (t, J = 7.5 Hz, 2H), 1.67-1.55 (m, 2H), 0.98 (t, J =

7.4 Hz, 3H),. ^{13}C NMR (300 MHz, CD_3OD): δ166.13, 165.73, 154.52, 135.38, 132.06,

130.45, 129.05, 125.89, 123.41, 120,11, 112,21, 106.61, 42.62, 22.43, 11.74.   HRMS

(m/z): calcd. for $[M + H]^+$: 271.1083, found, 271.1094.

Quantum yield determination

Fluorescence quantum yields were calculated according to the equation below by

reference to fluorescein in basic ethanol (Φ = 0.97).[50]

$$\Phi_X = \Phi_S * [A_S / A_X] * [F_X / F_S] * [n_X / n_S]^2$$

where, Φ_S is the reported quantum yield of the standard fluorescein. A_S is the

absorbance at the excitation wavelength of the standard. A_X is the absorbance at the

excitation wavelength of the measured compound. F_X is the area under the emission

spectra of the measured compound. F_S is the area under the emission spectra of the srandard. n_X is the refractive index of the solvent used. n_S is the refractive index of the solvent of the standard.

Imaging experiment

a. Primary culture of rat cortical astrocytes

Primary cortical astrocytes were isolated from the cortices of postnatal day 1 rat brains. The cells were harvested from tissue under sterile conditions, placed through one round of enzymatic dissociation and expansion in astrocyte growth medium (85% Dulbecco's Modified Eagle medium containing 4.5 g/L glucose, and 15% Fetal Bovine Serum).

b. Intracellular H_2S detection

Astrocyte cells were plated onto polylysine-coated glass coverslips. Cells were washed with Dulbecco's Modified Eagle medium (DMEM) and incubated with growth medium containing 2.0 µM probe for 1h at 37 ºC. After washing the cells with DMEM, different concentration of Na_2S was added into the growth media of the cells and incubated for 2h at 37 ºC. Following a through wash, the coverslips were placed onto Olympus IX71 fluorescence microscopy and imaged with a GFP dichroic mirror.

4.8 References

(1) Szabo, C. *Rev. Drug Discov.* **2007**, *6*, 917.

(2) Lefer, D. J. *Proc. Natl. Acad. Sci. USA* **2007**, *104*, 17907.

(3) Li, L.; Rose, P.; Moore, P. K. *Annu. Rev. Pharmacol. Toxicol.* **2011**, *51*, 169.

(4) Olson, K. R. *Am. J. Physiol. Regul. Integr. Comp. Physiol.* **2011**, *301*, R297.

(5) Kimura, H. *Amino Acids* **2011**, *41*, 113.

(6) Szabó, G.; Veres, G.; Radovits, T.; Gerő, D.; Módis, K.; Miesel-Gröschel, C.; Horkay, F.; Karck, M.; Szabó, C. *Nitric Oxide* **2011**, *25*, 201.

(7) Sowmya, S.; Swathi, Y.; Yeo, A. L.; Shoon, M. L.; Moore, P. K.; Bhatia, M. *Vascul. Pharmacol.* **2010**, *53*, 138.

(8) Yang, C. T.; Yang, Z. L.; Zhang, M. F.; Dong, Q.; Wang, X. Y.; Lan, A. P.; Zeng, F. Q.; Chen, P. X.; Wang, C. H.; Feng, J. Q. *PLoS One* **2011**, *6*.

(9) Baskar, R.; Bian, J. *Eur. J. Pharmacol.* **2011**, *656*, 5.

(10) Yang, G.; Wu, L. Y.; Wang, R. *FASEB J.* **2006**, *20*, 553.

(11) Peng, Y. J.; Nanduri, J.; Raghuraman, G.; Souvannakitti, D.; Gadalla, M. M.; Kumar, G. K.; Snyder, S. H.; Prabhakar, N. R. *Proc. Natl. Acad. Sci. USA* **2010**, *107*, 10719.

(12) Fu, M.; Zhang, W. H.; Wu, L. Y.; Yang, G. D.; Li, H. Z.; Wang, R. *Proc. Natl. Acad. Sci. USA* **2012**, *109*, 2943.

(13) Perna, A. F.; Ingrosso, D. *Nephrol. Dial. Transplant.* **2012**, *27*, 486.

(14) Kamoun, P.; Belardinelli, M.-C.; Chabli, A.; Lallouchi, K.; Chadefaux-Vekemans, B. *Am. J. Med. Genet. Part A* **2003**, *116A*, 310.

(15) Wang, R. *FASEB J.* **2002**, *16*, 1792.

(16) Moore, P. K.; Bhatia, M.; Moochhala, S. *Trends Pharmacol. Sci.* **2003**, *24*, 609.

(17) Blackstone, E.; Morrison, M.; Roth, M. B. *Science* **2005**, *308*, 518.

(18) Zhao, Y. Z.; Zhu, X. H.; Kan, H.; Wang, W. Z.; Zhu, B. C.; Du, B.; Zhang, X. L. *Analyst* **2012**, *137*, 5576.

(19) Kato, E. T.; Yoshida, C. M. P.; Reis, A. B.; Melo, I. S.; Franco, T. T. *Polym. Int.* **2011**, *60*, 951.

(20) Wallace, K. J.; Cordero, S. R.; Tan, C. P.; Lynch, V. M.; Anslyn, E. V. *Sens. Actuator B-Chem.* **2007**, *120*, 362.

(21) Spilker, B.; Randhahn, J.; Grabow, H.; Beikirch, H.; Jeroschewski, P. *J. Electroanal. Chem.* **2008**, *612*, 121.

(22) Lawrence, N. S.; Deo, R. P.; Wang, J. *Anal. Chim. Acta* **2004**, *517*, 131.

(23) Ubuka, T.; Abe, T.; Kajikawa, R.; Morino, K. *J. Chromatogr. B* **2001**, *757*, 31.

(24) Ramstad, T.; Bates, A. H.; Yellig, T. J.; Borchert, S. J.; Mills, K. A. *Analyst* **1995**, *120*, 2775.

(25) Karbanee, N.; Van Hille, R. P.; Lewis, A. E. *Ind. Eng. Chem. Res.* **2008**, *47*, 1596.

(26) Xuan, W. M.; Sheng, C. Q.; Cao, Y. T.; He, W. H.; Wang, W. *Angew. Chem. Int. Ed.* **2012**, *51*, 2282.

(27) Lippert, A. R.; New, E. J.; Chang, C. J. *J. Am. Chem. Soc.* **2011**, *133*, 10078.

(28) Peng, H. J.; Cheng, Y. F.; Dai, C. F.; King, A. L.; Predmore, B. L.; Lefer, D. J.; Wang, B. H. *Angew. Chem. Int. Ed.* **2011**, *50*, 9672.

(29) Yu, F. B. A.; Li, P.; Song, P.; Wang, B. S.; Zhao, J. Z.; Han, K. L. *Chem. Commun* **2012**, *48*, 2852.

(30) Liu, C. R.; Pan, J.; Li, S.; Zhao, Y.; Wu, L. Y.; Berkman, C. E.; Whorton, A. R.; Xian, M. *Angew. Chem. Int. Ed.* **2011**, *50*, 10327.

(31) Liu, C. R.; Peng, B.; Li, S.; Park, C. M.; Whorton, A. R.; Xian, M. *Org. Lett.* **2012**, *14*, 2184.

(32) Qian, Y.; Karpus, J.; Kabil, O.; Zhang, S. Y.; Zhu, H. L.; Banerjee, R.; Zhao, J.; He, C. *Nat. Commun.* **2011**, *2*.

(33) Qian, Y.; Zhang, L.; Ding, S. T.; Deng, X.; He, C.; Zheng, X. E.; Zhu, H. L.; Zhao, J. *Chem. Sci.* **2012**, *3*, 2920.

(34) Sasakura, K.; Hanaoka, K.; Shibuya, N.; Mikami, Y.; Kimura, Y.; Komatsu, T.; Ueno, T.; Terai, T.; Kimura, H.; Naganot, T. *J. Am. Chem. Soc.* **2011**, *133*, 18003.

(35) Hou, F. P.; Huang, L.; Xi, P. X.; Cheng, J.; Zhao, X. F.; Xie, G. Q.; Shi, Y. J.; Cheng, F. J.; Yao, X. J.; Bai, D. C.; Zeng, Z. Z. *Inorg. Chem.* **2012**, *51*, 2454.

(36) Hou, F. P.; Cheng, J.; Xi, P. X.; Chen, F. J.; Huang, L.; Xie, G. Q.; Shi, Y. J.; Liu, H. Y.; Bai, D. C.; Zeng, Z. Z. *Dalton Trans.* **2012**, *41*, 5799.

(37) Jain, S. K.; Manna, P.; Micinski, D.; Lieblong, B. J.; Kahlon, G.; Morehead, L.; Hoeldtke, R.; Bass, P. F.; Levine, S. N. *Antioxid. Redox Signal.* **2013**, *18*, 1154.

(38) Park, S. J.; Kim, T. H.; Lee, S. H.; Ryu, H. Y.; Hong, K. H.; Jung, J. Y.; Hwang, G. H. *Laryngoscope* **2013**, *123*, 557.

(39) Hyšpler, R. r.; Tichá, A.; Indrová, M.; Zadák, Z.; Hyšplerová, L.; Gasparič, J.; Churáček, J. *J. Chromatogr. B* **2002**, *770*, 255.

(40) Savage, J. C.; Gould, D. H. *J. Chromatogr. Biomed.* **1990**, *526*, 540.

(41) Borman, S. *C. & Eng. News* **2011**, *89(42)*, 60.

(42) de Silva, A. P.; Gunaratne, H. Q. N.; Gunnlaugsson, T.; Huxley, A. J. M.; McCoy, C. P.; Rademacher, J. T.; Rice, T. E. *Chem. Rev.* **1997**, *97*, 1515.

(43) Pu, L. *Chem. Rev.* **2004**, *104*, 1687.

(44) Kucheryavy, P.; Li, G.; Vyas, S.; Hadad, C.; Glusac, K. D. *J. Phy. Chem. A* **2009**, *113*, 6453.

(45) Kilpin, K. J.; Clavel, C. M.; Edafe, F.; Dyson, P. J. *Organometallics* **2012**, *31*, 7031.

(46) Zhang, Y. Y.; Zhou, C. H. *Bioorg. Med. Chem. Lett.* **2011**, *21*, 4349.

(47) Yadav, G. D.; Lande, S. V. *Adv. Synth. Catal.* **2005**, *347*, 1235.

(48) Kanth, S. R.; Reddy, G. V.; Rao, V.; Maitraie, D.; Narsaiah, B.; Rao, P. S. *Synth. Commun.* **2002**, *32*, 2849.

(49) Montoya, L. A.; Pluth, M. D. *Chem. Commun.* **2012**, *48*, 4767.

(50) Seybold, P. G.; Garterman, M.; Callis, J. *Photochem. Photobiol.* **1969**, *9*, 229.

Chapter 5

Fluorescent Probes for Fe^{2+}

5.1 Background and Significance

As the most abundant transition metal in human body, iron plays indispensable roles in sustaining normal biological activities. The iron concentration in neurons can reach as high as 1 mM.[1] The iron presence is responsible for numerous cellular functions, such as oxygen metabolism,[2] haem synthesis,[3] DNA/RNA metabolism,[4,5] and neural activities.[6] On the other hand, irregular iron metabolism has been linked to a series of diseases, such as anemia,[7] cardiovascular disease,[8] kidney disease,[9] and neurological diseases[10] including Alzheimer's disease and Parkinson's disease. Thus, a well-regulated iron metabolism will be critical to keep living system in a healthy state.

The essential role of iron in various biological events depends on redox states, ferrous ion (Fe^{2+}) and ferric ion (Fe^{3+}). A great deal of effort has been devoted to the study of iron homeostasis,[11] but research in this field is still very challenging partially due to the lack of effective detection tools. Traditional iron detection methods such as histochemical staining, isotope labeling and laser microprobe mass analysis (LAMMA), are not suitable for current biological research owing to their limited sensitivity, complicated sample preparation and invasive detection nature.[6] Therefore, traditional detection approaches are unlikely to fulfill the strict requirements for iron-related biological studies.

Fluorescent probe has been proved to be a powerful tool for intracellular studies, and fluorescent probes designed for Fe^{3+} [6,12,13] are much more than that for Fe^{2+},[6,14] indicating an inherent difficulty for Fe^{2+} probe design. Actually, Fe^{2+} plays most of

functional role of iron in living cells. For example, hemoglobin with Fe^{2+} can bind oxygen, but methemoglobin with Fe^{3+} can't. Also, Fe^{2+} can catalyze Fenton reaction in which H_2O_2 is degraded to highly reactive and biologically toxic hydroxyl radical (·OH). Therefore, there is an increasing need to carry out research on specific redox state of iron to reveal its complicated functions in biological activities.

To address the above issue, some efforts have been made to develop specific imaging tools for Fe^{2+}, but up to now, no breakthrough has been achieved. Most of the existing Fe^{2+} probes suffer from a fluorescence quenching because of the paramagnetic quenching nature of Fe^{2+}; a few off-on probe for Fe^{2+} is far from the satisfaction of biological study due to the harsh detection condition.[15] Recently an off-on Fe^{2+} probe was reported with an off-on biological imaging ability, but the fluorescence response depended on a long incubation time and relatively high concentration of Fe^{2+},[16] making it less likely to aid biological study (Scheme 5.1). So, despite promising progress in this field, new fluorescent probes for Fe^{2+} with improved sensing properties remain in great demand.

**Scheme 5.1** Reported Fe^{2+} probes
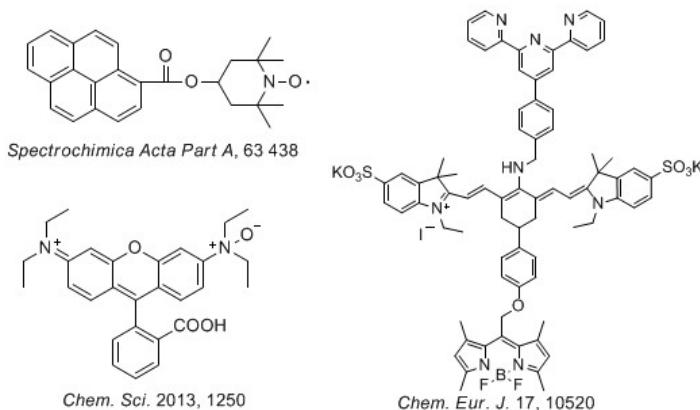
To be a useful tool for Fe^{2+} study, an off-on fluorescence signal is very desired due to its rareness and high S/N ratio; the capability of responding to Fe^{2+} under physiological condition is necessary to meet the requirement for biological study; the ability to differentiate Fe^{2+} from Fe^{3+} will be very valuable for specific iron homeostasis investigation. More importantly, a fast response time will lead to an improved temporary resolution, which will favor the detailed iron cellular study with more accuracy. In this chapter, I would like to introduce our efforts in the exploration of novel reaction-based fluorescent probes for Fe^{2+}, which have afforded valuable tools for Fe^{2+} biological study and provided significant insight into Fe^{2+} probe design.

5.2 A New Turn-on Fluorescent Probe for Fe^{2+} Detection and Cellular Imaging (Probe-5)

5.2.1 Probe Design

The structure of probe-**5** is a rhodamine derivative with an appended hydroxylamine as the fluorescence trigger (scheme 5.2). The probe-**5** is expected to favor the spirolactone ring closing form, so it tends to be weakly fluorescent. However when the hydroxylamine is reduced to amine, the resultant rhodmaine derivative will favor a spirolactone ring opening form, then an enhanced fluorescence can be expected.

Scheme 5.2 Probe-**5** and its detection mechanism
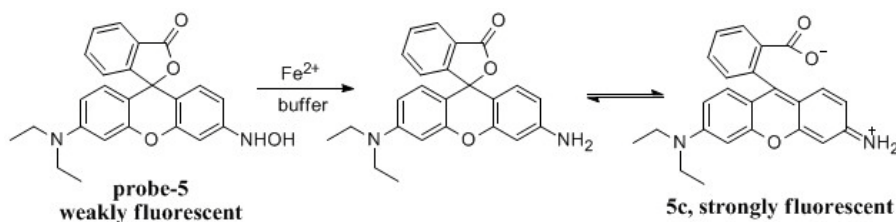
5.2.2 Synthesis of Probe-5

The probe **5** was synthesized in three steps with a total yield of 24% (Scheme 5.3). Ketone 5a was prepared from 3-diethylaminophenol and phthalic anhydride through a Friedel-Crafts reaction in good yield. The rhodamine scaffold **5b** was assembled by reacting **5a** with 3-nitrophenol. Finally reduction of the nitro group with Zn to hydroamine afforded probe **5**. In addition, we synthesized compound **5c** bearing amino group for comparison studies.

Scheme 5.3 Synthetic route of probe-5 and the detection product
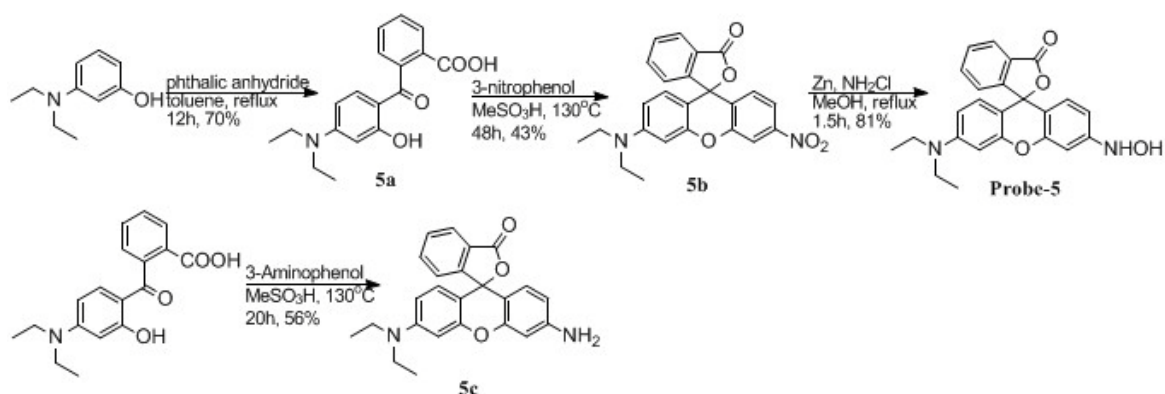
5.2.3 Evaluation of Probe-5 in Buffer Solution

With the probe **5** in hand, we firstly tested its response to Fe^{2+} under physiological condition. To 5 μM probe-**5** in 20 mM HEPES buffer solution was added 30 μM Fe^{2+}, and the fluorescence change was monitored every 5 min. The probe displayed weak fluorescence (Table 1). With addition of Fe^{2+}, the largest emission wavelength was shifted from 542 nm to 556 nm, and in around 30 min, the highest fluorescence intensity was achieved. Meanwhile, the solution color was changed from colorless to pink.

Without Fe^{2+}, no obvious fluorescence change can be observed in 1 h study (Figure 5.2), demonstrating excellent probe stability under physiological conditions.

Table 5.1 Photoabsorption and fluorescence properties of compounds **5** and **5c** in buffer solution

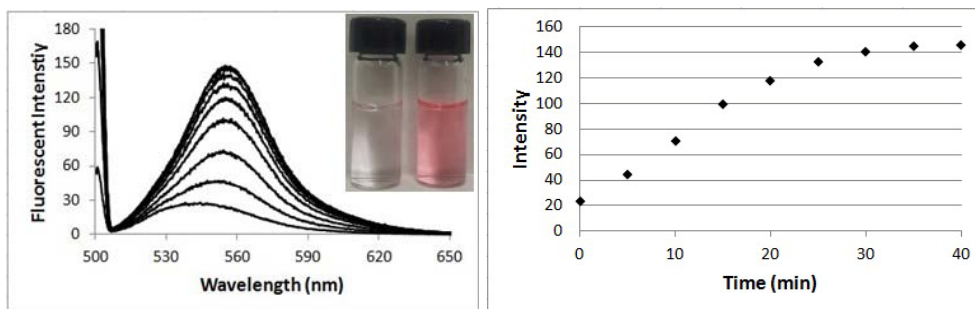| Compound	$\lambda_{max,abs}$ [nm]	ε (M^{-1}cm^{-1})	$\lambda_{max,em}$ [nm]	Φ_{fl}
Probe-5	529	4800	556	0.046
5c	529	55400	542	0.040

Figure 5.1 To 5 µM probe-**5** in 20 mM pH 7.4 HEPES (containing 0.5% DMSO) was added 30 µM Fe^{2+} at 25 ^{o}C. Left: the spectra change and solution color change. Right: the emission intensity change at 556 nm in a time range of 40 min. λ_{ex} = 500 nm.
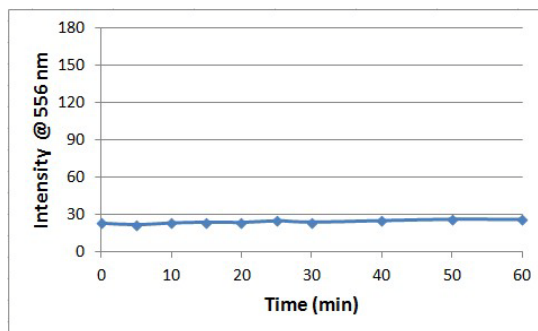

Figure 5.2 The emission of 5 µM probe-5 in 20 mM pH 7.4 HEPES buffer solution (containing 0.5% DMSO) at 556 nm was recorded every 5 min in 1 hour. λ_{ex} = 500 nm.

Besides fluorescence change, remarkable absorption enhancement was also observed. After addition of Fe^{2+}, a great absorption increase at 529 nm was observed, indicative of the recovery of rhodamine conjugation system. In addition, this absorption spectra displayed a good overlap with that of 5 µM compound **5c** (Table 1 and Figure 5.3). Finally, the formation of compound **5c** was confirmed by mass spectra ([M+H]$^+$, 387.1711).
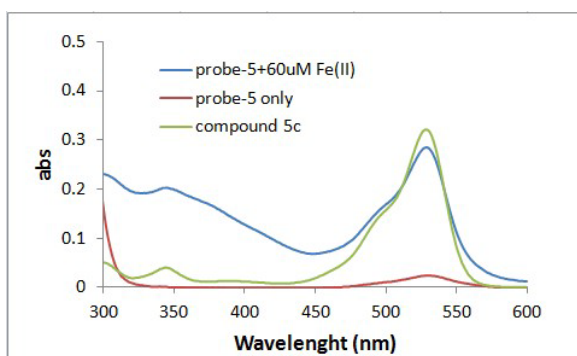

Figure 5.3 The aborption spectra of 5 µM probe-5, 5 µM probe-5 with 30 µM Fe^{2+} and 5 µM compound 5c in 20 mM pH 7.4 buffer solution.

Next, we tested the sensitivity of the probe. As shown in Figure 5.4, the fluorescence response was Fe^{2+} concentration dependant. When around 50 µM Fe^{2+} was added, the highest fluorescence intensity can be reached with a fluorescence enhancement of 7.8 folds. Also, we found that this probe can respond to Fe^{2+} at a concentration as low as 1 µM, and to 2 µM Fe^{2+}, the fluorescence was doubled, suggesting an impressive detection limit.
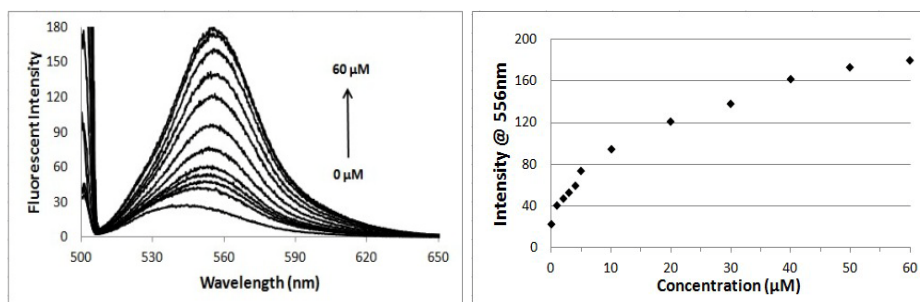
Figure 5.4 To 5 µM probe-**5** in 20 mM pH 7.4 HEPES (containing 0.5% DMSO) was added Fe^{2+} at 0, 1, 2, 3, 4, 5, 10, 20, 30, 40, 50, 60 µM 25 °C. Left: the emission spectra change with addition different concentration of Fe^{2+}. Right: the emission intensity change at 556 nm when 0-60 µM Fe^{2+} was added. $\lambda_{ex} = 500$ nm.

In addition, we conducted a study to see if the conversion of probe-**5** to compound **5c** was exclusive without severe interference from possible side reactions. To evaluate this, we carried out a comparison investigation of the emission intensity of probe-**5** with Fe^{2+} and compound **5c**. It turned out that the two spectra were very similar, and the conversion of probe-**5** to compound **5c** was calculated to be as high as 96% (Figure 5.5). This result suggested that the Fe^{2+}-induced reduction of hydroxylamine to amine was highly efficient in this rhodamine-based probe.
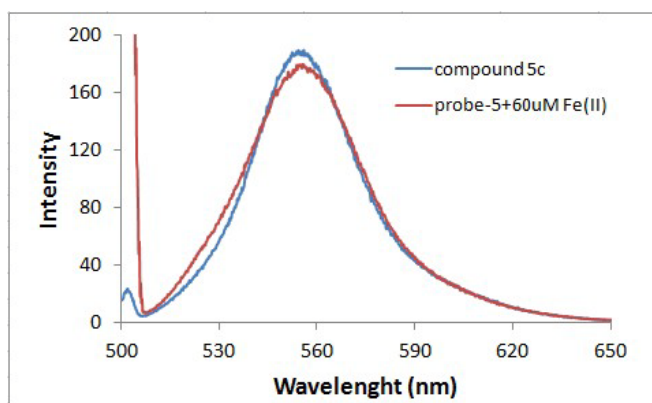

Figure 5.5 The emission spectra of 5 µM compound **5c** and 5 µM probe-**5** treated with 60 µM Fe^{2+}.

Next, we examined the selectivity of this probe over other biologically concerned species (Figure 5.6). It was found that other reductive species in biological system, such as Cys, GSH, NADH, and ascorbate, did not induce noticeable response. Moreover, reactive oxygen species such as H_2O_2 and NaOCl did not have action either. It should be noted that recently we reported a H_2S probe based on reduction of hydroxylamine to amine,[17] but in this case H_2S (Na_2S as source) failed to induce comparable fluorescence increase along with other sulfur-containing salts, such as Na_2SO_3 and $Na_2S_2O_3$. Also, this probe didn't respond to other biologically important cations, including Cu^{2+}, Zn^{2+}, Ca^{2+}, and Fe^{3+}. It's noteworthy that this probe responded to Cu^+ at 50 µM, but to 10 µM Cu^+ with weaker fluorescence intensity increase than that caused by 1 µM Fe^{2+}. Furthermore we found that NaOCl could remarkably reduce the fluorescence caused by Cu^+ without obvious interference to Fe^{2+} (Figure 5.7). Hence Cu^+ wouldn't pose a concern to Fe^{2+} detection. Taken together, this probe displayed excellent selectivity over other biologically concerned species, and could serve as a useful tool for Fe^{2+} detection in living systems.
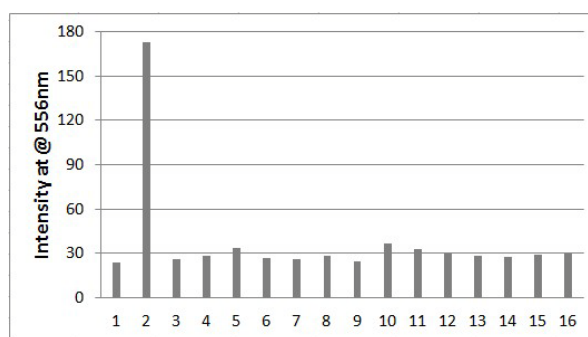

Figure 5.6 (1) Probe-**5** only (2) 50 µM Fe^{2+} (3) 200 µM Cys (4) 200 µM GSH (5) 100 µM Na_2S (6) 200 µM Na_2SO_3 (7) 200 µM $Na_2S_2O_3$ (8) 100 µM NADH (9) 100 µM ascorbate (10) 10 µM Cu^+ (11) 50 µM Cu^{2+} (12) 50 µM Fe^{3+} (13) 50 µM Zn^{2+} (14) 50 µM Ca^{2+} (15) 100 µM H_2O_2 (16) 100 µM NaOCl. The fluorescence was recorded 30 min after incubation.
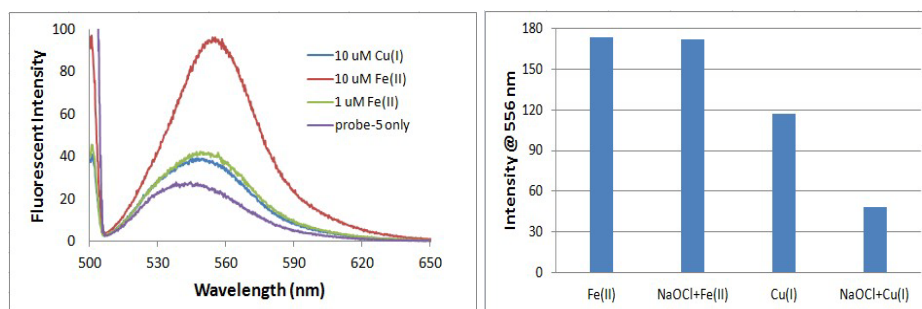
Figure 5.7 Left: the emission spectra of 5 µM probe-**5** in 20 mM HEPES buffer solution when 10 µM Cu^+, 10 µM Fe^{2+} or 1 µM Fe^{2+} was added. Right: the response of 5 µM probe-5 to 50 µM Fe^{2+} or 50 µM Cu^+ with or without the presence of 200 µM NaOCl.

5.2.4 Living Cell Imaging

Finally and importantly, we evaluated the probe in living cellular imaging. HeLa cells were used and incubated with different concentrations of Fe^{2+} followed by incubation with 5 µM probe-**5,** respectively. As shown in Figure 5.8, without Fe^{2+}, the cells displayed a very weak fluorescence. However, with addition of 20 µM Fe^{2+}, fluorescence increase was discernible. When 50 µM Fe^{2+} was used, obvious fluorescence enhancement was obtained.
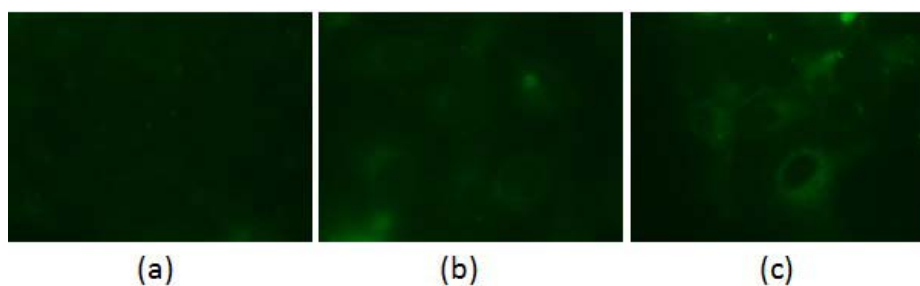

Figure 5.8 Fluorescence images of HeLa cells with Fe^{2+} obtained using an Olympus IX71 fluorescence microscope. HeLa cells were first incubated with (a) 0 µM Fe^{2+}; (b) 20 µM Fe^{2+}; (c) 50 µM Fe^{2+} for 20 min at 37 ^oC, then further incubated with 5 µM probe-**5** for 30 min respectively.

5.2.5 Summary

In conclusion, a novel fluorescent probe for Fe^{2+} has been successfully designed, synthesized and characterized. It displays a desired off-on signaling pattern with naked eye observable color change. It possesses an impressive detection limit as low as 1 µM of Fe^{2+}. Also, the probe exhibits a facile response within 30 min which is superior to the reported ones for off-on imaging of Fe^{2+} in living cells. The proposed detection reaction is proved to be exclusive with a high efficient reaction conversion. Along with the success of the bioimaging experiments, we believe probe-**5** has a potential in application of Fe^{2+} related biological studies.

5.3 A Fluorescent Probe for Real-time Detection of Fe^{2+} in Living Cells

5.3.1 Probe Design

The underdevelopment of Fe^{2+} probe is largely owing to the lack of a suitable detection reaction. In 1988, Novak and coworker reported an interesting Fe^{2+}-induced reduction of N-Aryl-O-pivaloylhydroxylamine with an excellent conversion (95%) at pH 4.6 (Scheme 5.4a).[18] We envisioned that the reaction may serve a base for the design of Fe^{2+} specific probe.

Scheme 5.4 Design of probe-**6** for Fe^{2+}
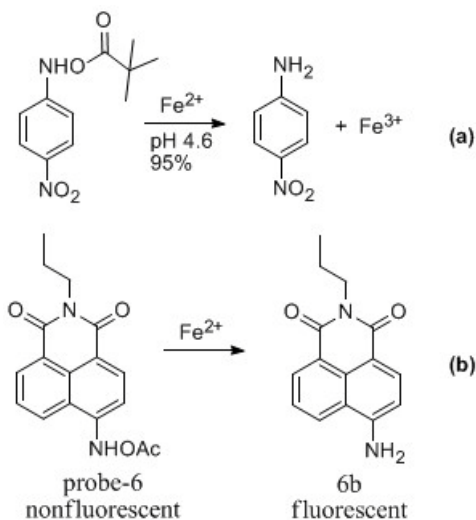
Inspired by our previous work for H_2S probe (Chapter 4), we designed naphthalimide-based probe for Fe^{2+} due to its "push-pull" fluorescence nature (Scheme 5.3b). The "double amide" moiety, serving as a strong EWG in this ICT fluorophore, can also provide an internal force to push forward the N-O cleavage reaction, similar to the function of nitro group in the reported reaction. Due to the electron deficient nature of the

acylated hydroxylamine, it is expected that the probe would be weakly or non-fluorescent. However, after the Fe^{2+}-induced N-O cleavage reaction, a fluorescent naphthalimide-amine (**6b**) could be generated, producing a desired off-on signal.

5.3.2 Synthesis of Probe-6

With the previous developed H_2S probe (**6a**) in hand, the new probe was prepared through an acylation of naphthalimide-hydroxylamine (Scheme 5.5).

Scheme 5.5 Synthesis of probe-**6**

5.3.3 Evaluation of Probe-6 in Buffer Solution

As expected, this probe (λ_{max} = 360 nm, ε = 11400 $M^{-1}cm^{-1}$) was nonfluorescent in aqueous solution. When treated with 1 eq. of Fe^{2+}, notable fluorescence enhancement (more than 27 folds) was observed in 1 min at 544 nm (Figure 5.9). This is the real-time off-on detection of Fe^{2+} was realized for the first time. In addition, an obvious absorption spectra change was observed, which is consistent with the alternation of ICT process (Figure 5.10).
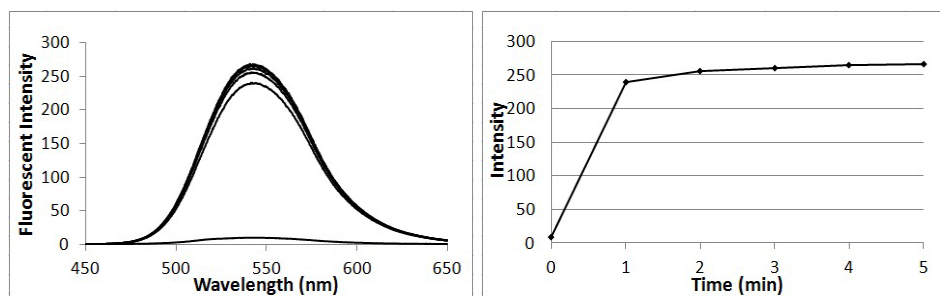
Figure 5.9 To 5 µM probe-**6** in 10 mM pH 7.4 HEPES (containing 0.5% DMSO) was added 5 µM Fe^{2+}. The emission intensity was collected at 544 nm. The excitation was at 440nm, and the slit was set at 5/3.
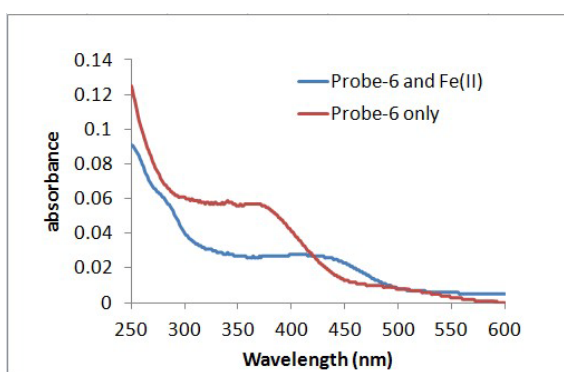

Figure 5.10 The absorption spectra of probe-**6** and probe-**6** with treatment of 10 µM Fe^{2+}.

The formation of naphthalimide-amine (**6b**) (λ_{max} = 435 nm, ε = 14500 $M^{-1}cm^{-1}$, Φ = 0.12) was confirmed by TLC analysis. In addition, the Fe^{2+}-induced emission spectra is matched with that of compound **6b** (Figure 5.11). We also investigated the stability of this probe in buffer solution to reduce the possible false positive signal. When probe-**6** was incubated in 10 mM pH 7.4 HEPES solution for 3 h, only a slight fluorescence change was observed, revealing a negligible influence in the minute's level responsive time (Figure 5.12).
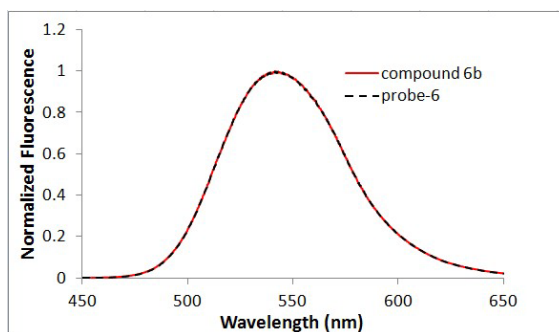
Figure 5.11 The spectra of Fe^{2+}-induced emission vs the emission spectra of naphthalimide amine (compound **6b**).
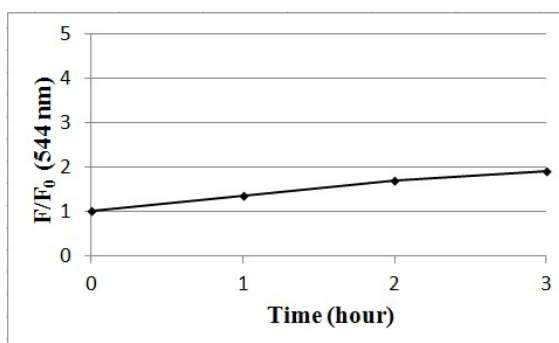
Figure 5.12 5 μM probe-**6** was incubated in 10 mM pH 7.4 HEPES solution; emission at 544nm was recorded every hour.

Next, we investigated the response of this probe to different concentrations of Fe^{2+}. As shown (Figure 5.13), the fluorescence intensity was increased as 1 to 5 μM Fe^{2+} was added. When more than 5 μM Fe^{2+} was added, the fluorescence intensity was leveled off. This implied a 1:1 stoichiometry, and was consistent with the reaction mechanism proposed by Novak.[18] Moreover, the observed detection limit was as low as 0.5 μM with a 3 folds fluorescence enhancement.

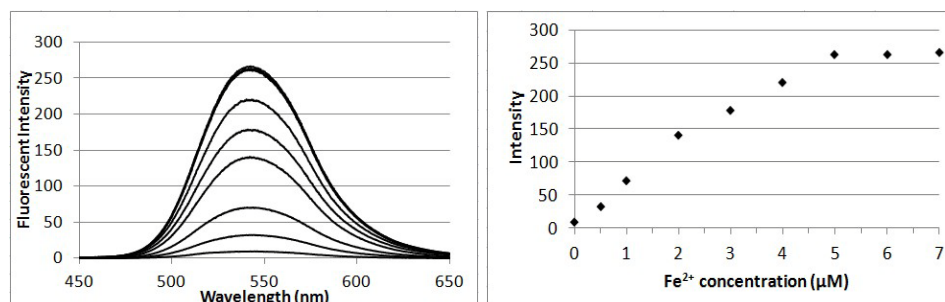**Figure 5.13** To 5 µM probe-**6** in 10 mM pH 7.4 HEPES (containing 0.5% DMSO) was added Fe^{2+} at 0, 0.5, 1, 2, 3, 4, 5, 6, 7 µM. The emission intensity was collected at 544 nm.

Then, we tested the selectivity of the probe over other biologically related species. Firstly, we screened a series of reductive species such as Na_2S, $Na_2S_2O_3$, Na_2SO_3, Cys, GSH, and NADH, even at a longer detection time (10 min) and in an excessive amount, no obvious fluorescence was observed. Only ascorbate led to a marginal fluorescence increase (Figure 5.14).
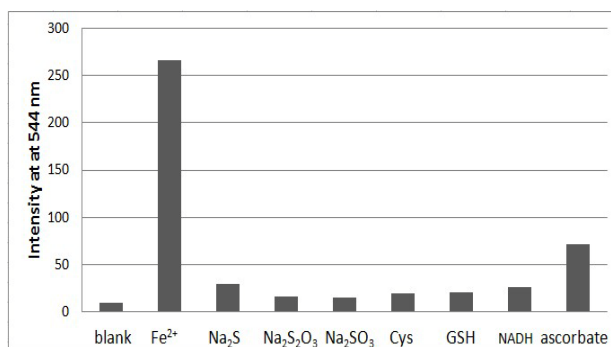
Figure 5.14 To 5 µM probe-**6** in 10 mM pH 7.4 HEPES (containing 0.5% DMSO) was added 1 eq. Fe^{2+}, 2 eq. Na_2S, 10eq. $Na_2S_2O_3$, 10eq. Na_2SO_3, 20eq. Cys, 20eq. GSH, 4eq. NADH, 4eq. ascorbate. The emission intensity was collected 10 min after addition of different reductive species.

Secondly, we carried out a competition assay in the presence of other metal ions (Figure 5.15). Each metal cation with 10 eq, such as Na^+, K^+, Ca^{2+}, Mg^{2+}, Cd^{2+}, Co^{2+},

95

Ni^{2+}, Zn^{2+}, Mn^{2+}, Fe^{3+}, cannot produce noticeable fluorescence increase or interfere the fluorescence triggered by Fe^{2+}. Therefore this probe can be used to differentiate Fe^{2+} from Fe^{3+}. However, Cu^{2+} can elicit a moderate fluorescence, and Cu^{+} behaved very similarly to Fe^{2+} in triggering probe fluorescence (Figure 5.16 and 5.17). So, this probe can be used to sense Fe^{2+} and Cu^{+}.
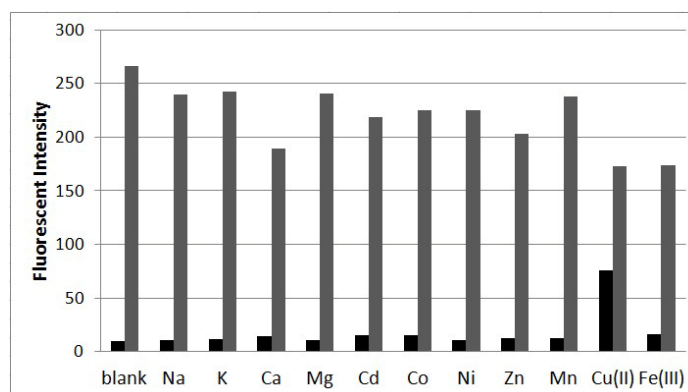

Figure 5.15 The bar on the left was 5 µM probe-**6** or 5 µM probe-6 with 50 µM different cations; the left bar was 5 µM Fe^{2+} in the presence of different cations at 50 µM; The emission was recorded in 10 min at 544 nm.
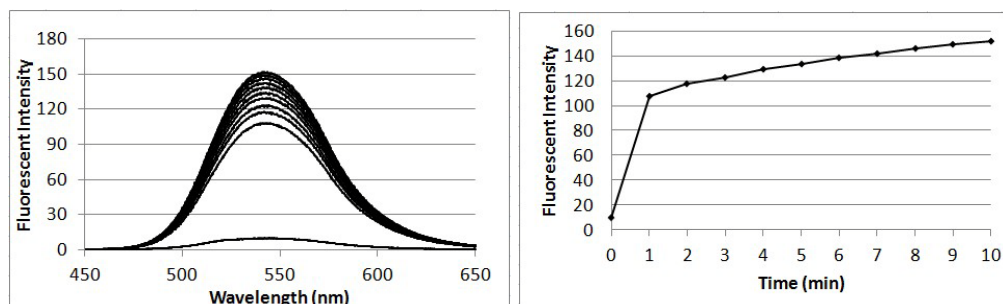

Figure 5.16 To 5 µM probe-**6** in 10 mM pH 7.4 HEPES was added 5 µM Cu^{+}. The emission was recorded in 10 min at 544 nm.
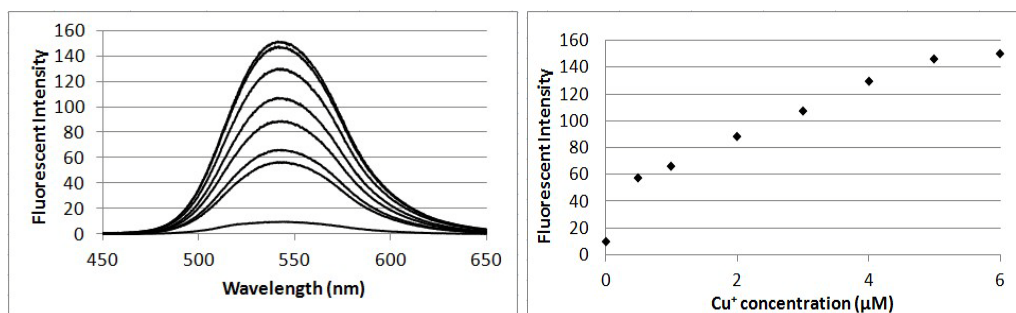
Figure 5.17 To 5 µM probe-**6** in 10 mM pH 7.4 HEPES was added different concentration of Cu$^+$

Despite unexpected exciting results, it is still necessary to discriminate Fe^{2+} from Cu$^+$. It's reported that Cu$^+$ can be oxidized to Cu^{2+} by NaOCl,[19] so we examined the response of probe-**6** to Fe^{2+}, Cu^{2+} and Cu$^+$ in the presence of NaOCl. It was found that Fe^{2+} could still elicit the fluorescence without severe interference in the presence of 50 µM NaOCl, but Cu$^+$ failed to entice fluorescence enhancement (Figure 5.18). In addition, 100 µM NaOCl can suppress a large part of the 50 µM Cu^{2+} induced fluorescence (Figure 5.19). So, NaOCl provided an effective method to specifically monitor Fe^{2+} even in the presence of Cu$^{2+/+}$. It seemed that Cu^{2+}-induced fluorescence was due to the conversion of Cu^{2+} to Cu$^+$ in aqueous redox environment. This hypothesis can also be supported by the observation that the Cu^{2+}-induced fluorescence was time dependant while Fe^{2+}/Cu$^+$-induced fluorescence can be finished in 1 minute. With this discrimination method by NaOCl, well-developed Cu$^+$ probes,[20-24] significant concentration difference,[25] and selective iron chelating agent, we believe Cu$^+$ won't be a significant concern for Fe^{2+} detection in biological study. Taken together, this probe should be able to detect Fe^{2+} without severe encumbrance from other biological species.
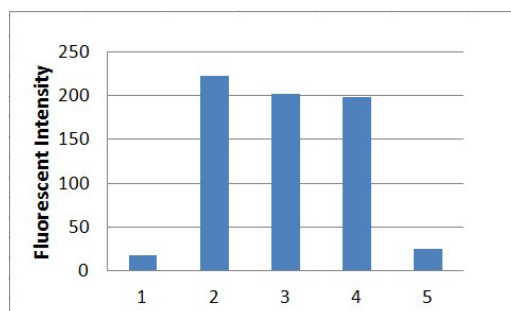
Figure 5.18 1. 5 µM probe-**6**; 2. 5 µM probe-**6** treated with 5 µM Fe^{2+}; 3. 5 µM probe-**6** treated with 5 µM Fe^{2+} in the presence of 50 µM NaOCl; 4. 5 µM probe-**6** treated with 5 µM Cu^+; 5. 5 µM probe-**6** treated with 5 µM Cu^+ in the presence of 50 µM NaOCl.
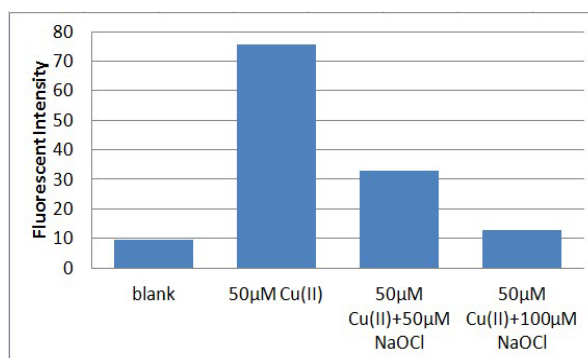
Figure 5.19 The Cu^{2+}-induced fluorescence in the presence of different concentration of NaOCl in 10min.

5.3.4 Biological Evaluation of Probe-6

Firstly, we evaluated this probe in the detection of Fe^{2+} in living cells. Astrocyte cells were firstly treated with 0 or 20 µM Fe^{2+} followed by further incubation with 5 µM probe-**6**. As shown in Figure 5.20, significant fluorescence was observed for cells treated with Fe^{2+} compared to that without Fe^{2+}. In this imaging study, no obvious cytotoxicity was noticed. This experiment y proved that this probe displayed an excellent detection ability for Fe^{2+} in living cells.

Figure 5.20 Fluorescence images of astrocyte cells (a mouse astrocyte cell line) with Fe^{2+} using Olympus IX71 fluorescence microscopy. Astrocyte cells were first incubated with (b) 0 µM Fe^{2+}, (c) 20.0 µM Fe^{2+} for 15 min, then incubated with 5 µM probe-**6** for another 15 min. (a) is the bright field image of (b). 200 ms exposure time was used for this experiment.

Next, we tested if this probe can respond to endogenous Fe^{2+} in astrocyte cells. In the study, the exposure time was increased to 500 ms, and a bright image of astrocyte cells was obtained after incubation with 5 µM probe-**6** for 15 min (Figure 5.21a, e). However, when the cells were pre-treated with desferoxamine (DFO, a selective chelating agent for iron), the obtained fluorescence image was obviously dimmed (Figure 5.21b, e). This experiment indicated that this probe can respond to endogenous Fe^{2+} in living cells.

Finally and importantly, we investigated if this probe can respond to Fe^{2+} flux in living cells. The existence of labile iron pool (LIP) which contains exchangeable iron was supposed to be important for iron homeostasis, but it remains putative.[26,27] We thought the presence of large amount of other transition metals such as Zn^{2+}, some of the chelated Fe^{2+}/Fe^{3+} should be released. With this in mind, the astrocyte cells were incubated with different concentraton of Zn^{2+}, and it was found that 150 µM Zn^{2+} could lead to obvious fluorescence increase (Figure 5.21 c, e). To confirm the fluorescence enhancment was due to the increased concentraton of Fe^{2+}, the cells were incubated with both Zn^{2+} and

DFO. No fluorescence increase was observed (Figure 5.21d, e) compared with Fig.5a/e, but the brightness was still stronger than cells treated only with DFO (Figure 5.21b, e). The study of Zn^{2+}-induced Fe^{2+} flux demonstrated the existence of LIP at least partially. Taken together, this probe may find a place for the bilogically application in study of Fe^{2+} flux in living cells.
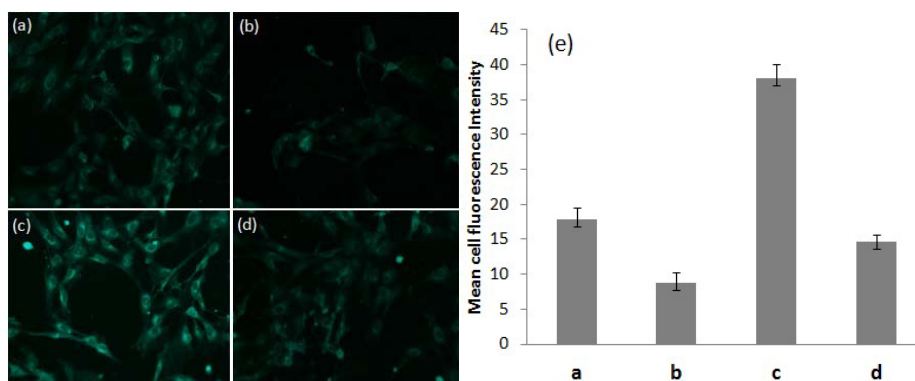

Figure 5.21 Fluorescence images of endogenous Fe^{2+} in astrocyte cells. Astrocyte cells were incubated with (a) 5 µM probe-**6** for 15 min, (b) 20.0 µM DFO for 15 min then 5 µM probe-**6** for another 15 min, (c) 150 µM Zn^{2+} for 15 min then 5 µM probe-**6** for another 15 min, (d) 150 µM Zn^{2+} and 20.0 µM DFO for 15 min then 5 µM probe-**6** for another 15 min. 500 ms exposure time was used for this experiment. (e) Mean fluorescence intensities of cell fluorescence in representative images.

5.3.5 Summary

In summary, an off-on fluorescent probe for Fe^{2+} was developed based on Fe^{2+}-induced N-O cleavage in acylated hydroxylamine. It displayed fast kinetics, which would allow for real-time detection of Fe^{2+} for the first time. It exhibited a good selectivity for a Fe^{2+}. The probe enabled to detect endogenous Fe^{2+}, and respond to Zn^{2+}-induced iron flux.

5.4 Experimental Section

5.4.1 Experimental Data for Probe-5

General Information: Commercial reagents were used as received, unless otherwise stated. Merck 60 silica gel was used for chromatography, and Whatman silica gel plates with fluorescence F_{254} were used for thin-layer chromatography (TLC) analysis. ^1H and ^{13}C NMR spectra were recorded on Bruker tardis (sb300). Data for ^1H are reported as follows: chemical shift (ppm), and multiplicity (s = singlet, d = doublet, t = triplet, q = quartet, m = multiplet). Data for ^{13}C NMR are reported as ppm.

Spectroscopic materials and methods: Millipore water was used to prepare all aqueous solutions. The pH was recorded by a Beckman Φ^{TM} 240 pH meter. Fluorescence emission spectra were obtained on a SHIMADZU spectrofluorophotometer RF-5301pc. UV absorption spectra were obtained on a SHIMADZU UV-1800. Cell imaging experiments were carried out by Olympus IX71 fluorescence microscopy.

**Material used for analysis:** $FeSO_4{\cdot}7H_2O$, $CaCl_2$, $Zn(NO_3)_2{\cdot}6H_2O$, $CuCl_2$, CuI, $FeCl_3$. For each experiment, Fe^{2+} solution was freshly prepared.

Synthesis of probe-5
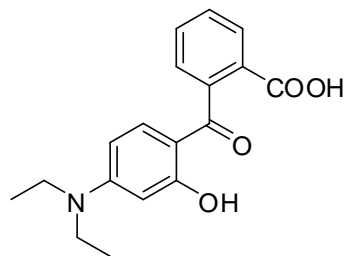
2-(4-(Diethylamino)-2-hydroxybenzoyl)benzoic acid (5a)

To 3-(diethylamino)phenol (3g, 18.16 mM) in 30 mL toluene was added phthalic anhydride (2.82g, 19.04 mM), then the mixture was heated to reflux and stirred for 12 h. After cooled to room temperature, the solvent was removed by rotavapor. The left solid was washed with large amount of ethyl acetate, and dried with oil pump. Without further purification, the product was obtained as a white solid (4g, 70%). ^{1}H NMR (300 MHz, CDCl$_3$): δ 8.11 (d, J = 7.5Hz, 1H), 7.64 (t, J = 6.9Hz, 1H), 7.54 (t, J = 7.8Hz, 1H), 7.38 (d, J = 7.5Hz, 1H), 6.89 (d, J = 9Hz, 1H), 6.15 (d, J = 2.4Hz, 1H), 6.05 (dd, J = 2.3Hz, 9.2Hz, 1H), 3.38 (q, J = 7.1Hz, 4H), 1.19 (t, J = 7.1Hz, 6H).
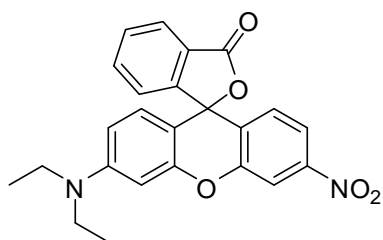
3'-(Diethylamino)-6'-nitro-3H-spiro[isobenzofuran-1,9'-xanthen]-3-one (5b)

To compound 5a (420 mg, 1.34 mM) in 20 mL MeSO$_3$H was added 3-nitrophenol (280 mg, 2.01 mM), then heated to 130 $^{\circ}$C and stirred for 48 h. The mixture was cooled to room temperature, then 40 mL H$_2$O was added. The crude product was extracted with CH$_2$Cl$_2$ (40 mL × 3), and dried over Na$_2$SO$_4$. The product was purified through column chromatograph and obtained as a yellow solid (240 mg, 43%). ^{1}H NMR (300 MHz, CDCl$_3$): δ 8.13 (d, J = 2.1Hz, 1H), 8.06-8.03 (m, 1H), 7.81 (dd, J = 2.4Hz, 8.7Hz, 1H), 7.72-7.62 (m, 2H), 7.18 (dd, J = 1.2Hz, 6.3Hz, 1H), 6.96 (d, J = 8.7Hz, 1H), 6.60 (d, J = 9Hz, 1H), 6.49 (d, J = 2.4Hz, 1H), 6.41 (dd, J = 2.7Hz, 9Hz, 1H), 3.38 (q, J = 7.10Hz, 4H), 1.18 (t, J = 7.05Hz, 6H). ^{13}C NMR (300 MHz, CDCl$_3$): 169.11, 152.56, 152.45, 151.88, 149.95, 148.72, 135.25, 130.08, 129.32, 128.80, 126.63, 126.04, 125.29, 123.89, 117.54, 112.88, 109.18, 103.86, 97.49, 82.44, 44.55, 12.46.
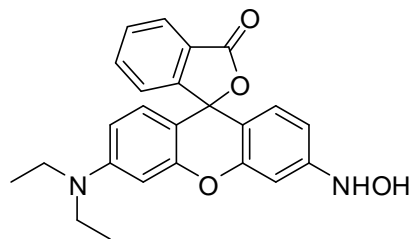
3'-(Diethylamino)-6'-(hydroxyamino)-3H-spiro[isobenzofuran-1,9'-xanthen]-3-one (Probe-5)

To compound 5b (230 mg, 0.55 mM) in 20 mL MeOH was added Zinc powder (722 mg, 11.04 mM) and NH$_4$Cl (590 mg, 11.03 mM), then the mixture was heated to reflux and stirred for 1.5 h. After cooling to room temperature, the solid in solution was removed by filtration, and the solvent was removed by rotavapor. The product was purified through column chromatograph and obtained as pink solid (180 mg, 81%). ^{1}H NMR (300 MHz, MeOD): δ 7.72 (dd, J = 1.5Hz, 7.8Hz, 1H), 7.25-7.19 (m, 1H), 7.14-7.08 (m, 1H), 6.96 (dd, J = 1.05Hz, 8.1Hz, 1H), 6.85-6.77 (m, 2H), 6.45 (d, J = 2.4Hz, 1H), 6.38 (d, J = 2.4Hz, 1H), 6.35-6.30 (m, 2H), 6.11 (s, 1H), 3.30 (q, J = 7.00Hz, 4H), 1.09 (t, J = 6.9Hz, 6H). ^{13}C NMR (300 MHz, MeOD): 172.57, 153.15, 153.03, 150.36, 148.38, 148.07, 132.66, 132.32, 131.96, 131.55, 129.97, 126.56, 116.54, 114.53, 112.41, 109.68, 103.70, 100.76, 45.94, 38.42, 12.75. HRMS (ESI): calcd. for C$_{24}$H$_{22}$N$_2$O$_4$ [M+H]$^+$: 403.1658, found, 403.1715.
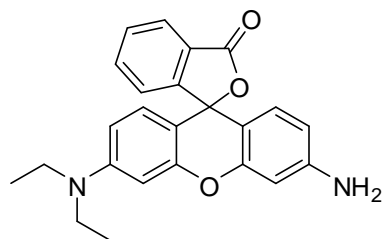
3'-Amino-6'-(diethylamino)-3H-spiro[isobenzofuran-1,9'-xanthen]-3-one(5c)

To compound 5a (217 mg, 0.69 mM) in 8 mL MeSO$_3$H was added 3-aminophenol (80 mg, 0.73 mM), then heated to 130°C and stirred for 20 h. The mixture was cooled room temperature, and 40 mL H$_2$O was poured followed by excessive TEA. The solution was extracted by CH$_2$Cl$_2$ (40 mL × 2), and dried over Na$_2$SO$_4$. The product was purified through column chromatograph, and the obtained product was dissolved in 30 mL CH$_2$Cl$_2$, and washed with dilute aqueous NaOH, dried over Na$_2$SO$_4$. Finally, the product was obtained as a red solid (150 mg, 56%). ^{1}H NMR (300 MHz, CDCl$_3$): δ 7.99 (dd, J = 1.2Hz, 6.6Hz, 1H), 7.62-7.54 (m, 2H), 7.17 (dd, J = 1.2Hz, 6.9Hz, 1H), 6.58-6.42 (m, 4H), 6.35-6.25 (m, 2H), 3.33 (q, J = 7.10Hz, 4H), 1.15 (t, J = 7.05Hz, 6H). ^{13}C NMR (300 MHz, CDCl$_3$): 169.94, 153.23, 153.14, 152.53, 149.66, 149.10, 134.45, 129.31, 129.23, 129.00, 128.02, 124.89, 124.29, 111.43, 109.21, 108.28, 105.82, 101.21, 97.55, 77.35, 44.50, 12.55. HRMS (ESI): calcd. for C$_{24}$H$_{22}$N$_2$O$_3$ [M+H]$^+$: 387.1709, found, 387.1711.

The determination of quantum yield

Fluorescence quantum yields were calculated according to the equation below by reference to rhodamine 6G (Φ = 0.95).[28]

$$\Phi_X = \Phi_S * [A_S / A_X] * [F_X / F_S] * [n_X / n_S]^2$$

where, Φ_S is the reported quantum yield of the standard rhodamine 6G. A_S is the absorbance at the excitation wavelength of the standard. A_X is the absorbance at the excitation wavelength of the measured compound. F_X is the area under the emission spectra of the measured compound. F_S is the area under the emission spectra of the

srandard. n_X is the refractive index of the solvent used. n_S is the refractive index of the solvent of the standard.

Imaging experiment

a. Culture of human HeLa cells

Human HeLa cells were maintained in Dulbecco's modified Eagle's medium (DMEM; Gibco) supplemented with 10% foetal bovine serum (FBS), 100 U/ml penicillin and 100 µg/ml streptomycin at 37°C under a 5% CO_2 atmosphere. For fluorescence image, cells were seeded at a density of $3–5\times10^4$ cells/cm^2 on uncoated coverslips.

b. Intracellular ferrous ion detection by probe

Intracellular ferrous was measured by adding specific probe. HeLa cells were plated onto polylysine-coated glass coverslips. Cells were washed with Dulbecco's Modified Eagle medium (DMEM) and incubated with growth medium containing different concentration of Fe^{2+} (0, 20 and 50 µM) for 20 min at 37$^{\text{o}}$C. After washing the cells with DMEM, 5 µM probe was added into the growth media of the cells and incubated for 30 min at 37$^{\text{o}}$C. Following a through wash, the coverslips were placed onto Olympus IX71 fluorescence microscopy and ferrous was imaged with a GFP dichroic mirror.

5.4.2 Experimental Data for Probe-6

General Information: Commercial reagents were used as received, unless otherwise stated. Merck 60 silica gel was used for chromatography, and Whatman silica gel plates with fluorescence F_{254} were used for thin-layer chromatography (TLC) analysis.

^{1}H and ^{13}C NMR spectra were recorded on Bruker tardis (sb300). Data for ^{1}H are reported as follows: chemical shift (ppm), and multiplicity (s = singlet, d = doublet, t = triplet, q = quartet, m = multiplet). Data for ^{13}C NMR are reported as ppm.

Spectroscopic materials and methods: Millipore water was used to prepare all aqueous solutions. The pH was recorded by a Beckman Φ^{TM} 240 pH meter. Fluorescence emission spectra were obtained on a SHIMADZU spectrofluorophotometer RF-5301pc. UV absorption spectra were obtained on a SHIMADZU UV-1800. Cell imaging experiments were carried out by Olympus IX71 fluorescence microscopy.

Material used for analysis: $FeSO_4{\cdot}7H_2O$, NaCl, K_2CO_3, $CaCl_2$, $MgSO_4$, $Cd(NO_3)_2{\cdot}4H_2O$, $Co(NO_3)_2{\cdot}6H_2O$, $NiCl_2{\cdot}6H_2O$, $Zn(NO_3)_2{\cdot}6H_2O$, $MnSO_4.H_2O$, $CuCl_2$, CuI, $FeCl_3$. For each experiment, Fe^{2+} solution was freshly prepared.

Synthesis of probe-6

The compound 6a and 6b was synthesized according to our reported method.[17]
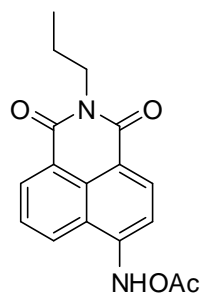
Synthesis of probe-6

To compound 6a (26 mg, 0.096 mM) in 10 mL DCM in ice both was added acetyl chloride (7 µL, 0.098 mM) and TEA (14 µL, 0.100 mM), then stirred for 5 min. The solvent was removed by rotavapor, and the product was purified through column chromatograph, and obtained as a yellow solid (24 mg, 80%).^{1}H NMR (CDCl$_3$): δ 9.65(s, 1H), 8.61(dd, J = 7.2Hz, 0.6Hz, 1H), 8.52(d, J = 8.1Hz, 1H), 8.26(d, J = 8.4Hz, 1H),

7.41(dd, J = 8.4Hz,7.5Hz, 1H), 7.32(d, J = 8.1Hz, 1H), 4.15-4.10(m, 2H), 2.35(s, 3H), 1.82-1.69(m, 2H), 1.00(t, J = 7.5 Hz, 3H). ^{13}C NMR (300MHz, CDCl$_3$): δ169.95, 164.16, 163.73, 147.05, 132.43, 131.39, 128.81, 126.74, 126.53, 123.20, 121.07, 117.71, 110.71, 41.89, 21.40, 18.89, 11,51.

Imaging experiments

a. Primary culture of rat cortical astrocytes

Primary cortical astrocytes were isolated from the cortices of postnatal day 1 rat brains. The cells were harvested from tissue under sterile conditions, placed through one round of enzymatic dissociation and expansion in astrocyte growth medium (85 % Dulbecco's Modified Eagle medium containing 4.5 g/L glucose, and 15 % Fetal Bovine Serum).

b. Intracellular Fe^{2+} detection

Astrocyte cells were plated onto polylysine-coated glass coverslips. Cells were washed with Dulbecco's Modified Eagle medium (DMEM) and incubated with growth medium containing Fe^{2+}, DFO, Zn^{2+} or Zn^{2+}/DFO for 15min at 37°C. After washing the cells with DMEM, 5 μM probe was added into the growth media of the cells and incubated for 15 min at 37°C. Following a through wash, the coverslips were placed onto Olympus IX71 fluorescence microscopy and imaged with a GFP dichroic mirror.

5.5 References

(1) Fiedler, A.; Reinert, T.; Morawski, M.; Bruckner, G.; Arendt, T.; Butz, T. N. I. *Methods Phys. Res., Sect. B* **2007**, *260*, 153.

(2) Liu, X.; Theil, E. C. *Acc. Chem. Res.* **2005**, *38*, 167.

(3) Wingert, R. A.; Galloway, J. L.; Barut, B.; Foott, H.; Fraenkel, P.; Axe, J. L.; Weber, G. J.; Dooley, K.; Davidson, A. J.; Schmidt, B.; Paw, B. H.; Shaw, G. C.; Kingsley, P.; Palis, J.; Schubert, H.; Chen, O.; Kaplan, J.; The Tubingen Screen, C.; Zon, L. I. *Nature* **2005**, *436*, 1035.

(4) Goss, D. J.; Theil, E. C. *Acc. Chem. Res.* **2011**, *44*, 1320.

(5) Stehling, O.; Vashisht, A. A.; Mascarenhas, J.; Jonsson, Z. O.; Sharma, T.; Netz, D. J. A.; Pierik, A. J.; Wohlschlegel, J. A.; Lill, R. *Science* **2012**, *337*, 195.

(6) Que, E. L.; Domaille, D. W.; Chang, C. J. *Chem. Rev.* **2008**, *108*, 1517.

(7) Lee, T. W.; Kolber, M. R.; Fedorak, R. N.; van Zanten, S. V. *J CROHNS COLITIS* **2012**, *6*, 267.

(8) Rajapurkar, M. M.; Shah, S. V.; Lele, S. S.; Hegde, U. N.; Lensing, S. Y.; Gohel, K.; Mukhopadhyay, B.; Gang, S.; Eigenbrodt, M. L. *Am. J. Cardiol.* **2012**, *109*, 438.

(9) Fishbane, S.; Singh, A. K. *Kidney Int* **2008**, *75*, 752.

(10) Crichton, R. R.; Dexter, D. T.; Ward, R. J. *J. Neural Transm.* **2011**, *118*, 301.

(11) Pantopoulos, K.; Porwal, S. K.; Tartakoff, A.; Devireddy, L. *Biochemistry* **2012**, *51*, 5705.

(12) Sahoo, S. K.; Sharma, D.; Bera, R. K.; Crisponi, G.; Callan, J. F. *Chem. Soc. Rev.* **2012,** *41* (21), 7195.

(13) Yang, Y.; Zhao, Q.; Feng, W.; Li, F. *Chem. Rev.* **2012**, *113*, 192.

(14) Li, P.; Fang, L. B.; Zhou, H.; Zhang, W.; Wang, X.; Li, N.; Zhong, H. B.; Tang, B. *Chem.-Eur. J.* **2011**, *17*, 10519.

(15) Chen, J. L.; Zhuo, S. J.; Wu, Y. Q.; Fang, F.; Li, L.; Zhu, C. Q. *Spectroc. Acta Pt. A-Molec. Biomolec. Spectr.* **2006**, *63*, 438.

(16) Hirayama, T.; Okuda, K.; Nagasawa, H. *Chem. Sci.* **2013**, *4*, 1250.

(17) Xuan, W. M.; Pan, R.; Cao, Y. T.; Liu, K. J.; Wang, W. *Chem. Commun.* **2012**, *48*, 10669.

(18) Novak, M.; Lagerman, R. K. *J. Org. Chem.* **1988**, *53*, 4762.

(19) Lou, X. D.; Zhang, Y.; Qin, J. G.; Li, Z. *Sens. Actuator B-Chem.* **2012**, *161*, 229.

(20) Zeng, L.; Miller, E. W.; Pralle, A.; Isacoff, E. Y.; Chang, C. J. *J. Am. Chem. Soc* **2005**, *128*, 10.

(21) Domaille, D. W.; Zeng, L.; Chang, C. J. *J. Am. Chem. Soc* **2010**, *132*, 1194.

(22) Dodani, S. C.; Leary, S. C.; Cobine, P. A.; Winge, D. R.; Chang, C. J. *J. Am. Chem. Soc* **2011**, *133*, 8606.

(23) Taki, M.; Iyoshi, S.; Ojida, A.; Hamachi, I.; Yamamoto, Y. *J. Am. Chem. Soc* **2010**, *132*, 5938.

(24) Dodani, S. C.; Domaille, D. W.; Nam, C. I.; Miller, E. W.; Finney, L. A.; Vogt, S.; Chang, C. J. *Proc. Natl. Acad. Sci. U. S. A.* **2011**, *108*, 5980.

(25) the adult human body contains ~ 3-5 g iron and 100-150 mg copper.

(26) Greenberg, G. R.; Wintrobe, M. M. *J. Biol. Chem.* **1946**, *165*, 397.

(27) Cabantchik, Z. I.; Kakhlon, O.; Epsztejn, S.; Zanninelli, G.; Breuer, W. *Adv.Exp.Med.Biol.* **2002**, *509*, 55.

(28) Kubin, R. F.; Fletcher, A. N. *J. Lumines.* **1982**, *27*, 455.